Aus dem

Institut für Pathologie und Neuropathologie Tübingen

Allgemeine und Molekulare Pathologie

und Pathologische Anatomie

Utility of Mutational Analysis in the Diagnosis of Nodal Marginal Zone Lymphoma and its Differential Diagnosis from other Small B-cell Lymphomas

Inaugural-Dissertation

zur Erlangung des Doktorgrades

der Medizin

der Medizinischen Fakultät

der Eberhard Karls Universität

zu Tübingen

vorgelegt von

Gierer, Hannah Sophie

2026

Dekan:	Professor Dr. B. Pichler
1. Berichterstatter:	Professorin Dr. L. Quintanilla Martinez de Fend
2. Berichterstatter:	Professor Dr. L. Flatz

Tag der Disputation: 27.08.2025

Für meine Großeltern

Table of contents

I. Figures 1

II. Tables 2

III. Abbreviations 2

1 Introduction 1

1.1 General Classification of hematopoietic and lymphatic Malignancies .. 1

1.2 Marginal Zone Lymphoma 3

1.3 Nodal Marginal Zone Lymphoma 3

1.3.1 Epidemiology and Cofactors 3

1.3.2 Pediatric Nodal Marginal Zone Lymphoma 4

1.3.3 Clinical Features 5

1.3.3.1 Symptoms and Diagnosis 5

1.3.3.2 Therapy and Prognosis 6

1.3.4 Pathology and Immunophenotype 7

1.3.4.1 Cell of Origin and Pathological Features 7

1.3.4.2 Immunophenotype 8

1.3.5 Genetic Landscape 9

1.3.6 Relevant Differential Diagnosis 12

1.3.6.1 Follicular Lymphoma 12

1.3.6.2 Chronic Lymphocytic Leukemia 13

1.4 Mutational Analysis using Next Generation Sequencing 14

1.5 Aim of this Thesis 16

2 Material and Methods 17

2.1 Material 17

2.1.1 Patient samples 17

2.1.2 Chemicals and Reagents 17

2.1.3 Kits for Genetic Analysis 18

2.1.4 Oligonucleotide Sequences 18

2.1.5 Devices 20

2.1.6 Software 20
2.1.7 Consumable supplies 21
2.1.8 Companies 21
2.2 Study Design 22
2.3 Microscopy 24
2.4 Immunohistochemical Staining 24
2.5 DNA extraction 25
2.5.1 Preparation of the samples for the following DNA extraction 25
2.5.2 Extraction of the DNA 25
2.5.3 Determination of nucleic acid concentration 26
2.5.4 PCR to analyze integrity of the DNA 26
2.6 Ion Torrent Next-Generation Sequencing 28
2.6.1 Oncomine Lymphoma III Panel 28
2.6.2 PMZL Panel 29
2.6.3 Generation of Amplicon Libraries 30
2.6.3.1 AmpliSeq PCR 30
2.6.3.2 Primer Digestion and Barcode ligation 31
2.6.3.3 AMPure Purification 32
2.6.4 Quantification of Amplicon Libraries 32
2.6.5 Pooling and Sequencing the libraries 33
2.7 Genetic Analysis 34
2.8 Validation of low frequent Mutations 34
2.8.1 Generation of Single Amplicons 35
2.8.2 Quantification and Dilution of Single Amplicons 36
3 Results 37
3.1 Sample Selection 37
3.2 Patient Characteristics 39
3.3 Immunohistochemistry 40
3.4 DNA Integrity 42
3.5 Genetic Analysis 43
3.6 Integrative Results of Immunohistochemistry and Genetic Findings 47

3.6.1 Immunohistochemical and Genetic findings in the NMZL Group 47
3.6.2 Genetic and immunohistochemical findings in the FL Group 53
3.6.3 Genetic and immunohistochemical findings in the CLL Group.... 56
3.6.4 Remaining cases 58
3.7 Examination of normal tissue 59
4 Discussion 60
4.1 Summary of Results 60
4.2 Patient Collective 61
4.2.1 Patient Characteristics 61
4.2.2 Sample Quality 62
4.3 Mutated genes in NMZL and their function 62
4.3.1 KLF2 62
4.3.2 Chromatin remodeling and transcriptional regulation mutated genes and their function 65
4.3.3 NOTCH pathway mutated genes and their function 72
4.3.4 NF-KB pathway mutated genes and their function 76
4.4 Genetic landscape of t(14;18) negative FL compared to NMZL 79
4.5 Genetic landscape of CLL compared to NMZL 82
4.6 Conclusions and Outlook 85
5 Summary (English) 88
6 Zusammenfassung (Deutsch) 90
7 References 92
8 Declaration of Authorship 118
9 Acknoledgements 119

I. Figures

Figure 1 Systematic of hematolymphoid tumors 2
Figure 2 Recurrently mutated pathways in NMZL 11
Figure 3 Next-Generation Sequencing Workflow 15
Figure 4 Flowchart of approach to the study and sample selection 23
Figure 5 Selection process of NMZL cases for NGS analysis and reevaluation 38
Figure 6 Tumor biopsy sites 39
Figure 7 Representative picture of product sizes visualized by QIAxcel ScreenGel 1.4.0 42
Figure 8 Representative mutational finding in the Integrative Genomics Viewer (IGV) 44
Figure 9 Representative histology and immunohistochemical stainings of NMZL (NM11) 49
Figure 10 Representative histology and immunohistochemical stainings of splenic type NMZL (NM56) 50
Figure 11 Representative histology and immunohistochemical stainings of CD5 positive NMZL (NM10) 51
Figure 12 Mutated Genes in the NMZL samples sorted into the 3 subgroups .. 52
Figure 13 Representative histology and immunohistochemical stainings of FL (NM20) 54
Figure 14 Mutated genes in the FL and CLL group and of the remaining cases 55
Figure 15 Representative histology and immunohistochemical stainings of CLL (NM39). 57
Figure 16 Summary of the main affected pathways in NMZL 61

II. Tables

Table 1 Oncomine Lymphoma III Panel 28
Table 2 PMZL Panel 30
Table 3 Immunohistochemical profile and key data of the final collective 41
Table 4 Genetic variants 45
Table 5 Evaluation of germline variants 59

III. Abbreviations

A	Adenine
BAP	Break apark probes
BCL2	B-cell lymphoma 2
BCL6	B-cell lymphoma 6
BCR	B cell receptor
bp	base pairs
C	Cytosine
CD	Cluster of differentiation
CDS	Coding sequence
cFL	Classic follicular lymphoma
chr	Chromosome
CLL	Chronic lymphatic leukemia
DAB	Diaminobenzidine
ddH2O	Double-distilled water
ddNTP	Dideoxynucleotide
DLBCL	Diffuse large B-cell lymphoma
DNA	Deoxyribonucleic acid
dNTP	Deoxynucleotide
E.coli	Escherichia coli
EDTA	Ethylenediaminetetraacetic acid
EMZL	Extranodal marginal zone lymphoma
FDC	Follicular dendritic cells
FFPE	Formalin-fixed paraffin-embedded tissue
FL	Follicular lymphoma
FLIPI	Folicular lymphoma international prognostic index
GI	Gastrointestinal
G	Guanine
H&E	Haematoxylin & Eosine

HCL	Hairy cell leukemia
HCV	Hepatitis C virus
HRP	Horeseradish peroxidase
HS	high sensitivity
ICC	International concensus classification
IGV	Integrative variant caller
LDH	Lactate dehydrogenase
LN	Lymph node
LPL	Lymphoplasmocytic lymphoma
MAF	Minor Allelic Frequency
MALT	Mucosa-associated lymphoid tissue
min	Minute
MZL	Marginal zone lymphomy
NGS	Next generation sequencing
NHL	Non-Hodgkin lymphoma
NM	Case number
NMZL	Nodal marginal zone lymphoma
NTC	Negative control
NTP	Nucleoside triphosphate
OS	Overall survival
PCR	Polymerase chain reaction
PET	Positron emission tomography
PET-CT	Positron emission tomography - computed tomography
PTFL	Pediatric-type folliular lymphoma
QPCR	Quantitative polymerase chain reaction
RNA	Ribonucleic acid
s	second
SBCL	small B-cell lymphoma
SMZL	Splenic marginal zone lymphoma
SNP	Single-nucleotide polymorphism
T	Thyrosine
TE	Tris-EDTA
TRIS	Tris(hydroxymethyl)aminomethane
UV	Ultraviolet
VAF	Variant allele frequency
WHO	World health organisation

1 Introduction

1.1 General Classification of hematopoietic and lymphatic Malignancies

Lymphomas, together with leukemias and myelomas, belong to the group of hematological malignancies. They can occur anywhere in the human body and show very different symptoms, making them a very heterogeneous group. Lymphomas arise from lymphocytes at different stages of maturation that originate at some point of their differentiation (Alaggio et al., 2022, Campo et al., 2022). Circa 85% of all lymphomas derive from B-cells (Mugnaini and Ghosh, 2016).

As the first attempt to classify lymphomas, Hodgkin lymphomas, named after Dr. Thomas Hodgkin (Stone, 2005), and non-Hodgkin lymphomas are distinguished.

Classic Hodgkin lymphomas account for approximately 10% of all lymphomas, and according to the Cancer statistics, there were approximately 9000 new cases and 960 deaths in 2021 in the US (Siegel et al., 2021). The age distribution is bimodal, with one peak in young adults and another one in people 55 years of age or older (Glaser and Jarrett, 1996).

While little has changed in recent years in the classification of classic Hodgkin lymphoma, the group of non-Hodgkin lymphomas has continued to evolve over the past decades, with more and more subgroups forming based on morphological, immunophenotypic and genetic features. Although the classification into Hodgkin and non-Hodgkin lymphomas is outdated, it is still used as a general categorization. According to the current International Consensus Classification (ICC), mature lymphoid and histiocytic/dendritic cell neoplasms are divided into 5 supergroups: mature B-cell neoplasms, classic Hodgkin lymphoma, mature T- and NK-cell neoplasms, immunodeficiency-associated lymphoproliferative disorders and histiocytic and dendritic cell neoplasms (Campo et al., 2022).

Generally, the latest WHO classification of 2022 divides hematolymphoid tumors in 6 major supergroups: myeloid proliferations and neoplasms, histiocytic/dentritic

cell neoplasms, T-cell and NK-cell lymphoid proliferations and lymphomas, stroma-derived neoplasms of lymphoid tissues, genetic tumor syndromes and B-cell lymphoid proliferations and lymphomas, the latter being the most important supergroup for this thesis. This group includes, among others, the mature B-cell neoplasms. Follicular lymphomas and large B-cell lymphomas make up the majority of cases in this group. In addition, the different types of marginal zone lymphomas represent another part of the mature B-cell neoplasms (Alaggio et al., 2022). The exact distribution of the frequencies of the different disease entities varies and is depending on genetics, ethnicity, geographic and economical factors (Perry et al., 2016).

An overview of the classification is shown in **Figure 1**.

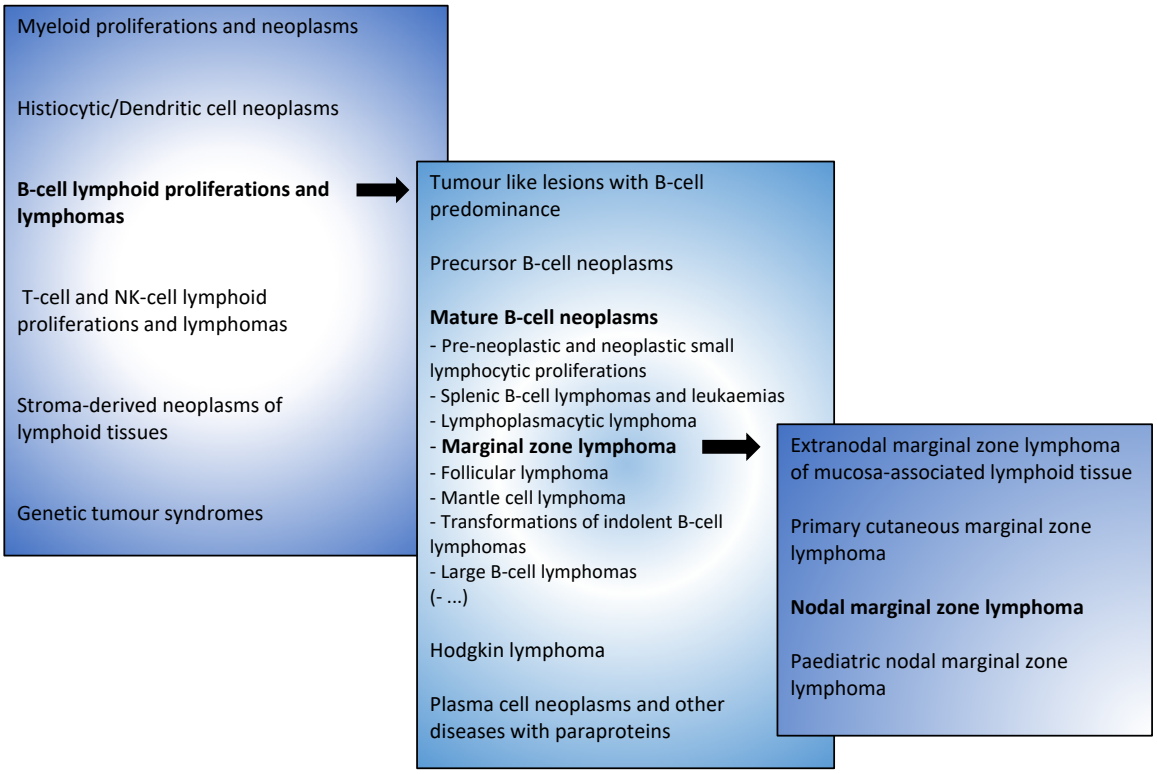

Figure 1 Systematic of hematolymphoid tumors. Shown above on the left are the 6 supergroups of hematolymphoid tumors according to the latest WHO classification of 2022. In the middle, the 4 groups of B-cell lymphoid proliferations and lymphomas with examples of important entities of mature B-cell neoplasms are illustrated. Listed on the right are all lymphomas classifying as marginal zone lymphoma, including Nodal marginal one lymphoma (NMZL) (Alaggio et al., 2022).

1.2 Marginal Zone Lymphoma

Until 2017, NMZL together with Extranodal Marginal Zone Lymphoma (EMZL), also called MALT Lymphoma (mucosa-associated lymphoid tissue lymphoma), and Splenic Marginal Zone Lymphoma (SMZL) formed the group of Marginal Zone Lymphoma (Swerdlow et al., 2017), comprising 7% of all non-Hodgkin lymphomas (Cerhan and Habermann, 2021). However, there have been some changes in the latest editions of the WHO classification and the ICC. The pediatric type nodal marginal zone lymphoma, which has been listed as a subgroup of NMZL before, is now considered as a separate entity in the group of MZL in the WHO classification, while the ICC based on the similar clinical, morphological and molecular features to pediatric-type follicular lymphoma suggested to merge these two entities under the name of pediatric-type follicular lymphoma with and without marginal zone differentiation. Moreover, the primary cutaneous marginal zone lymphoma, which was previously considered part of the EMZL, is listed as a separate entity of MZL in the WHO classification, while in the ICC, it is assigned to the lymphoproliferative disorders (Alaggio et al., 2022, Campo et al., 2022).

The entities show some immunophenotypic and histologic overlap. However, they differ significantly in their clinical presentation, etiology and some genetic features (Ferry, 2022).

Particularly, the nodal marginal zone lymphoma (NMZL) will be discussed in more detail below.

1.3 Nodal Marginal Zone Lymphoma

1.3.1 Epidemiology and Cofactors

As NMZL is a rare lymphoma, it only represents approximately 2% of all mature non-Hodgkin lymphomas (Cerhan and Habermann, 2021). The median age of patients at the time of diagnosis is 50 to 60 years (Berger et al., 2000), an exponential increase with age can be observed. The age-adjusted incidence rate is reported as 6 per 1,000,000 person-years (Cerhan and Habermann, 2021, Natkunam et al., 2022). However, there is also a pediatric-type of the disease

which is now considered a discrete entity (Salmeron-Villalobos et al., 2022, Di Napoli et al., 2022). Among males and non-Hispanic whites, a slightly increased incidence was found (Cerhan and Habermann, 2021).

It has been discussed whether Hepatitis C virus (HCV), could be a cofactor in the pathogenesis of MZL (Armand et al., 2017). In general, HCV is considered a group 1 carcinogen and is commonly associated with B-cell lymphomas (Bouvard et al., 2009). An association of HCV with MZL has been noted in several studies (Anderson et al., 2008, Dal Maso and Franceschi, 2006). Particularly with respect to EMZL and NMZL, an association with HCV seropositivity has been noted (Bracci et al., 2014).

In some studies, an association between NMZL and autoimmune diseases has been found, among these chronic thyroiditis, rheumatoid arthritis, Sjogren's syndrome, hemolytic anemia, systemic lupus erythematosus and rheumatoid arthritis (Arcaini et al., 2007, Kojima et al., 2007). Especially in females with autoimmune diseases, a higher incidence has been observed. Moreover, it has been shown that a family history of NHL is associated with the genesis of NMZL whereas lower consumption of alcohol, especially wine, reduces it´s risk (Bracci et al., 2014).

1.3.2 Pediatric Nodal Marginal Zone Lymphoma

Pediatric Nodal Marginal Zone Lymphoma is listed as a separate lymphoma for the first time in the new ICC and WHO classification while the ICC also considers its relation to the pediatric-type follicular lymphoma.

Although it shares some aspects with adult NMZL, it differs significantly in some histological and clinical features (Di Napoli et al., 2022). Age range for this diagnosis is 2-27 years with a median age of 16 years (Taddesse-Heath et al., 2003, Rizzo et al., 2010, Quintanilla-Martinez et al., 2016). Nevertheless, the pediatric type of NMZL was rarely diagnosed in adults as well (Gitelson et al., 2010, Quintanilla-Martinez et al., 2016). In contrast to adults NMZL, a clear predominance of male patients has been reported for this variant. The most common regions for this lymphoma are cervical lymph nodes, followed by inguinal

and submental regions (Taddesse-Heath et al., 2003, Rizzo et al., 2010). In general, the prognosis is favorable, and the rate of recurrence is very low. It is considered a localized disease and does not require systemic treatment (Salmeron-Villalobos et al., 2022). Concerning the immunophenotype, co-expression of CD43 is quite common, also, IgD is co-expressed in up to 25% of the cases (Rizzo et al., 2010).

1.3.3 Clinical Features

1.3.3.1 Symptoms and Diagnosis

Since it is a rare entity, clinical data on NMZL is lacking and mostly retrieved from a few rather small clinical trials. However, it´s clinical presentation is similar to other indolent nodal lymphomas such as FL, and therefore, some aspects such as risk assessment can be adopted.

Patients with NMZL often present with non-bulky peripheral adenopathy, most commonly affecting lymph nodes in the head/neck region (Angelopoulou et al., 2014, Tadmor and Polliack, 2017), but also involving intra-abdominal and thoracic lymph nodes in approximately 50% and 26% of patients studied, respectively (Arcaini et al., 2007, Berger et al., 2000). In Arcaini´s et al. study from 2007, some patients showed a history of autoimmune disease and as many as 24% had an HCV positive serology (Arcaini et al., 2007). The details of these cofactors have been discussed above. Bone marrow involvement can be observed in about 30-45% of patients, while blood involvement is relatively rare and occurs in only about one in 10 patients. Moreover, it was shown that under 15% present with B- symptoms (Angelopoulou et al., 2014, Tadmor and Polliack, 2017).

Diagnosing NMZL can be challenging. On the one hand, many differential diagnoses have to be considered whereas, on the other hand, it is difficult to determine whether it is primarily a nodal MZL or just a nodal manifestation of one of the other two MZLs. Therefore, an accurate histopathological, immunophenotypic and genetic analysis is of great importance.

In over 50%, patients are diagnosed at an advanced disease stage. The laboratory parameters are rather unspecific. LDH elevation can be observed in about 35-45% of the patients (Angelopoulou et al., 2014). In some cases, an IgM spike is demonstrated that raises the differential diagnosis with Lymphoplasmacytic Lymphoma (LPL) (Berger et al., 2005).

In order to evaluate the lymphoma stage, a total body imaging, as well as bone marrow biopsy must be performed. PET/PET-CT as an imaging modality can be helpful for staging and treatment response assessment (Cheson et al., 2014, Hoffmann et al., 2003).

1.3.3.2 Therapy and Prognosis

There is no specific treatment for NMZL and therapies are adapted from more common indolent B-cell lymphomas. For 20-30 years, therapy was very heterogeneous, as NMZL was rarely diagnosed (Berger et al., 2000).

In localized stages, lymph node resection with or without radiotherapy is the favored option, although Ling et al. found that radiotherapy is underutilized in early stages of MZLs, which has a poor effect on further progression and should be considered more often (Ling et al., 2016, Tadmor and Polliack, 2017). In advanced stages, therapy depends on several factors. If patients are asymptomatic, the “watch and wait” approach may be sufficient. Otherwise, chemo-immunotherapy is the option of choice. Which agents are optimal for treatment is currently still tested but studies concerning new agents such as Bortezomib (de Vos et al., 2009) show promising results. For elderly and unfit patients, a monotherapy with Rituximab can be considered (Angelopoulou et al., 2014, Tadmor and Polliack, 2017). Treatment of relapses and progression depend on many factors such as stage, comorbidities and patient´s age. For example, Bendamustine plus Rituximab (Rummel et al., 2016) or radioimmunotherapy (Witzig et al., 2003) can be a therapy of choice.

NMZL is indolent, mostly uncurable and characterized by relapses but it´s outcome is still rather favorable. A 5 years overall survival (OS) has been calculated in 62-90% (Tadmor and Polliack, 2017) and a median OS of 8.3 years (Olszewski and Castillo, 2013). Age above 60 years, elevated LDH levels and

Cyclin E expression are factors that lead to poorer OS (Arcaini et al., 2007, Oh et al., 2006). A progression to large B-cell lymphoma can be observed in 15% of cases and is rather uncommon (Oh et al., 2006). Since there is no NMZL risk stratification score, the Follicular Lymphoma International Index (FLIPI) is often used and appears to have strong prognostic value for NMZL (Heilgeist et al., 2013).

1.3.4 Pathology and Immunophenotype

1.3.4.1 Cell of Origin and Pathological Features

As the name implies, NMZL refers to the marginal zone of lymph nodes. The marginal zone surrounds the mantle zone of germinal centers and is usually not recognized in lymph nodes (van Krieken and Lennert, 1990). It is suggested that the cell of origin is a marginal zone memory B-cell with post germinal origin. However, the exact origin is unclear and MZL can arise from different subsets of mature B-cells (Thieblemont et al., 2011, van den Brand and van Krieken, 2013). Both the growth pattern and cellular morphology can be very heterogeneous, which is why diagnosis is so challenging and often makes NMZL a diagnosis of exclusion. Nevertheless, some typical morphological patterns in NMZL have been described in the past. It appears that the nodular and diffuse patterns are the most common ones. Other observed patterns include the interfollicular as well as the perifollicular pattern. The diffuse pattern is characterized by small residual reactive germinal centers, which can be visualized by immunohistochemical stains for follicular dendritic cells and germinal center markers. Follicular colonization may be present and raises FL as a differential diagnosis (Camacho et al., 2003, Salama et al., 2009, Traverse-Glehen et al., 2006, van den Brand and van Krieken, 2013). Concerning cytology, various cell types are observed in different distributions, including centrocyte-like cells, plasmacytoid cells, and monocytoid cells, the latter being rather rare (Traverse-Glehen et al., 2006, van den Brand and van Krieken, 2013). Plasmocytic differentiation is observed in several cases and ranges between 22% and 47% of the cases (van den Brand and van Krieken, 2013).

A number of NMZL are characterized by morphological similarities with SMZL. These cases typically show small to medium sized lymphocytes with pale cytoplasm in proximity to residual small regressive germinal centers. Often, these cells express IgD, which is unusual in NMZL (Campo et al., 1999).

1.3.4.2 Immunophenotype

In general, the immunophenotype of NMZLs is not very specific and is similar to the other MZL subsets. The neoplastic cells are positive for pan B-cell markers such as CD19, CD20, CD22, and CD79a. BCL2 is positive in the vast majority of cases, but still varies from 43% to 100% of cases in different studies. CD23, which is a marker for follicular dendritic cells (FDC) is negative in the tumour cells and can be helpful to reveal remaining atrophic germinal centers (Traverse-Glehen et al., 2006, van den Brand and van Krieken, 2013). Immunoglobulins IgM or IgD are expressed in about 30% of cases, with IgD expression more commonly in cases with SMZL-like morphology as mentioned above (Campo et al., 1999, Traverse-Glehen et al., 2006). To distinguish NMZL from mantle cell lymphoma, cyclin D1 staining is performed, which should be negative in NMZL, in contrast to its typical positivity in mantle cell lymphoma (van den Brand and van Krieken, 2013). Co-expression of CD43 is observed in 5-75% of cases, whereas CD5 is aberrantly expressed in up to 17% of cases (Jaso et al., 2013, van den Brand and van Krieken, 2013). In addition, staining for the germinal center markers CD10, BCL6, HGAL, and LMO2 should always be performed when NMZL is suspected to rule out FL. In general, if more than one of these markers is co-expressed, FL as a differential diagnosis must be considered (Dyhdalo et al., 2013). If plasma cell differentiation is present, co-expression of plasma cell markers CD138 and MUM1 can often be observed, sometimes even without evidence of plasma cell differentiation (Camacho et al., 2003, Molina et al., 2011, Traverse-Glehen et al., 2006). Furthermore, a kappa or lambda light chain restriction can be observed in some cases (Camacho et al., 2003).

1.3.5 Genetic Landscape

Data on the genetic landscape of NMZL are mostly from studies with rather small numbers of cases, which could explain the partly contradictory results. However, the genetics of NMZL have been better studied in recent years and some results have been established. An overview of NMZLs genetic landscape out of a review by Pillonel et al. is shown below (**Figure 2**) (Pillonel et al., 2018).

In some aspects the results of all studies agree including that *KMT2D*, a histone methyltransferase, is one of the most frequently mutated genes in NMZL. It is important to note that the *KMT2D* mutation is significantly more common in NMZL compared to SMZL (34% in NMZL vs. 8% in SMZL). This might help to distinguish these two entities which otherwise show similar mutational patterns (Pillonel et al., 2018, Spina et al., 2016, van den Brand et al., 2017). In NMZL collectives, mutations were also found in other epigenetic regulators such as the acetyltransferases *CREBBP* and *TBL1XR1* in up to 20% of cases. However, *KMT2D, CREBBP* and *EZH2* mutations also occur frequently in FL (Nann et al., 2020). The majority of studies found that *KLF2* mutations are present in up to 17% of NMZL cases. Note that this mutation also commonly occurs in SMZL (Pillonel et al., 2018, Spina et al., 2016).

Another genetic characteristic of NMZL is the absence of the *MYD88* L265P (now referred to as *L252P*) mutation, which is important for its differentiation to LPL (Pillonel et al., 2018). Nevertheless, the presence of the latter mutation should not directly lead to the exclusion of diagnosing NMZL since Cheah et al. demonstrated that few cases can actually show presence of those mutations in NMZL (Cheah et al., 2022, Knauf et al., 2021). However, that continues to be a topic of discussion.

Furthermore, oncogenic mutations in genes involved in NOTCH and NFκB pathways are frequently found in NMZL, which is significant because it represents potential sites of therapeutical intervention. These include recurrent lesions in *NOTCH1, SPEN, DTX1, BCL10*, and *TNFAIP3* (Pillonel et al., 2018, Spina et al., 2016, van den Brand et al., 2017). However, the latter occurs more frequently in EMZL, specifically in ocular adne3xal MZL (Moody et al., 2017).

There are different opinions about the presence of lesions in the *PTPRD* gene, a tumor suppressor: In the work of Spina et al. mutations were found in 14.3% of NMZL. This could be an important discovery as this gene mutation is rarely found in other mature B-cell lymphomas, specifically in any other MZL subgroup, implying that *PTPRD* mutations could be specific for NMZL (Spina et al., 2016). However, this could not be confirmed in the genetic analyses of Pillonel et al., where this mutation was not identified. Instead, in this second study *TET2, EZH2* and *BRAF* mutations were found, which was novel, as these were not detected in previous studies. Especially the latter is an important discovery, as it is one of the most frequently mutated genes in cancer (Davies et al., 2002). Moreover, it is a therapeutic target of BRAF kinase inhibitors (Sosman et al., 2012, Tiacci et al., 2015), and is known to be typical for hairy cell leukemia (HCL) (Pillonel et al., 2018, Tiacci et al., 2017). Mutations were found in 16% of the NMZL cases, mostly those strongly expressing IgD (Pillonel et al., 2018). Results regarding the presence of mutations in the *FAS* gene encoding for a receptor of the TNF family (Wajant, 2002) were divergent. While one study postulated its absence (Bertoni et al., 2000), mutations have, in fact, been detected in more recent studies (Pillonel et al., 2018, Spina et al., 2016).

In summary, no specific mutation has been identified for this entity. However, the mutational profile is characteristic and might be helpful for the differential diagnosis with other small B-cell lymphomas in difficult cases.

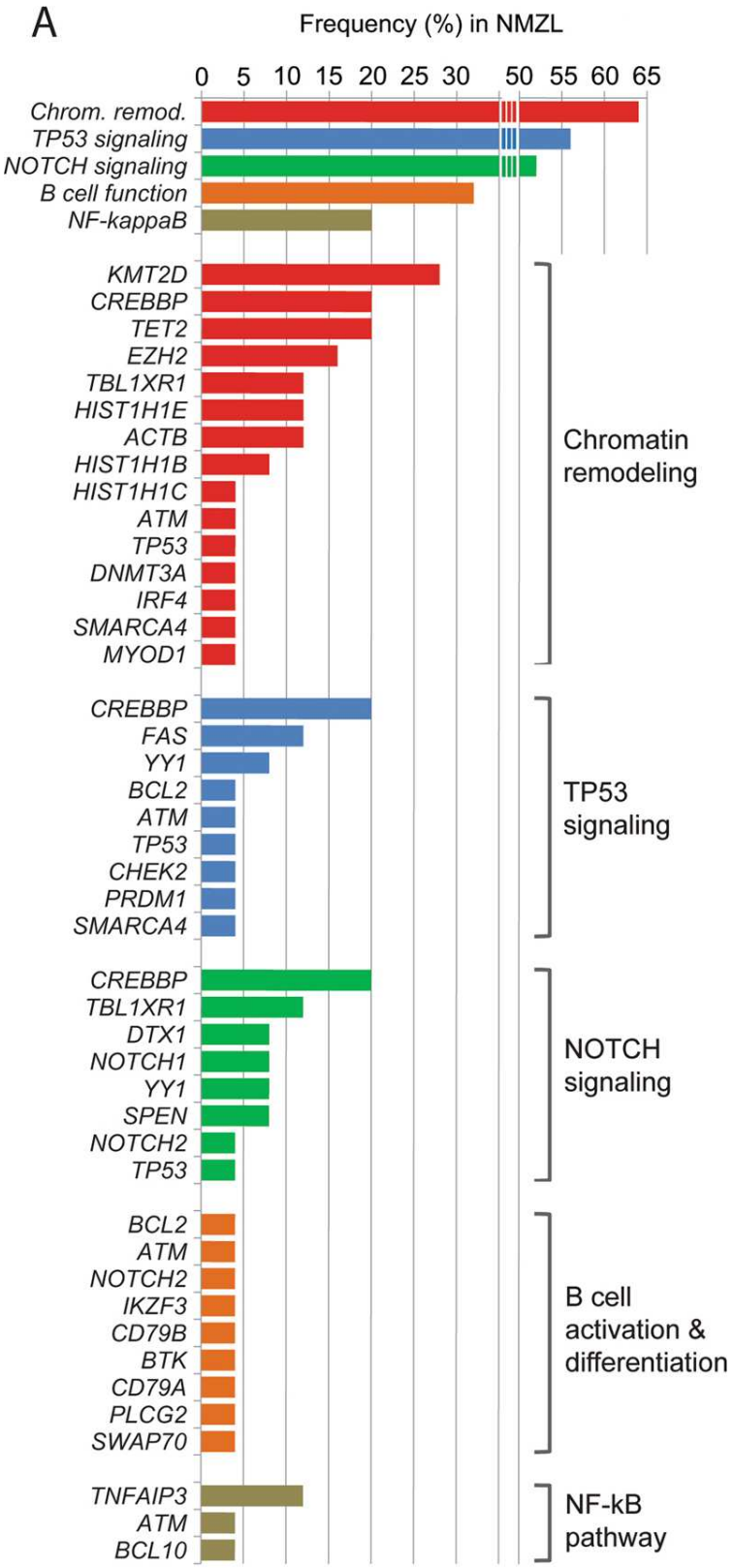

Figure 2 Recurrently mutated pathways in NMZL. The colored bars indicate frequency of mutations in the respective gene. Genes are grouped by pathway affiliation. On top, frequencies of all mutated genes of each pathway are cumulated. Source: (Pillonel et al., 2018).

1.3.6 Relevant Differential Diagnosis

1.3.6.1 Follicular Lymphoma

Follicular Lymphoma (FL) is one of the most important differential diagnoses of NMZL. It is one of the most common mature NHLs and accounts for about 10-20% of all lymphomas (Teras et al., 2016). It is mostly found in lymph nodes but can also occur in other sites such as the GI tract or spleen. Recently, FLs can be subdivided into conventional FLs (cFL) and less common subtypes. The conventional FLs are quite unequivocal to be diagnosed in most cases. Histologically, they show a follicular growth pattern and mostly present with the classic t(14;18)(q32;q21) translocation (Xerri et al., 2022). Especially in grade 1 and 2 FLs this translocation is observed in 90% (Rowley, 1988), whereas it is less common in grade 3B FLs (Ott et al., 2002). This translocation leads to constitutive BCL2 expression, which can be immunohistochemically demonstrated (Leich et al., 2016). However, of particular importance for this work are the translocation negative FLs, which account for approximately 10-15% of all FLs (Xerri et al., 2016). Some of these *BCL2* negative FLs express CD23, which has been shown to correlate with the presence of *STAT6* mutations in over 85% of cases. In fact, the expression of CD23 is a good surrogate marker for *STAT6* mutations (Nann et al., 2020). Because of this, the ICC recognizes *BCL2* negative CD23+ FL as a provisional entity. This entity is not recognized in the new WHO classification (Laurent et al., 2023).

Histologically, a number of FLs show monocytoid B-cell differentiation with monocytes in the marginal and perifollicular zone (Nathwani et al., 1999). These are the cases that predominantly raise MZL as a differential diagnosis. In MZL on the other hand, follicular colonization can be observed occasionally, which is typical for FL (Camacho et al., 2003). Immunohistochemically, FL is positive for pan B-cell markers such as CD19, CD20, CD22, and CD79a. It is also habitually BCL2, BCL6, and CD10 positive and CD5 and CD43 negative. Germinal center markers such as LM02 and HGAL are not routinely stained but are helpful in differentiating it from NMZL (Menter et al., 2015, Natkunam et al., 2007). Other important markers for distinguishing these two entities are IRTA1 and MNDA,

which are usually positive in NMZL and negative in FL (Falini et al., 2012, Kanellis et al., 2009).

Concerning the common genetic profile of FL, frequently mutated genes include *KMT2D, TNFRSF14, EZH2*, and *CREBBP* (Carbone et al., 2019).

1.3.6.2 Chronic Lymphocytic Leukemia

CLL is the most common form of chronic leukemia in western countries, accounting for about 7% of all NHLs. It is characterized by the expansion of mature monoclonal cells in blood, bone marrow, spleen and lymph nodes. CLL occurs more frequently in elderly patients and to date is not curable. As an indolent lymphoma, it initially progresses insidiously. Many cases are detected by chance in a peripheral blood routine examination. Most cases are preceded by monoclonal B-cell proliferation without symptoms. Sometimes, however, affected patients primarily present with lymphadenopathy or splenomegaly (Swerdlow et al., 2017, Naresh et al., 2022)

Microscopically, the histologic picture in lymph nodes is defined by small lymphocytes with round nuclei, prolymphocytes, and scattered paraimmunoblasts. Proliferation centers appear paler and are also referred to as pseudofollicles (Lennert, 1978, Swerdlow et al., 2017). Some cases also show plasmacytoid differentiation (Bonato et al., 1998, Lennert, 1978).

Immunohistochemically, the cells are weakly positive for typical B-cell markers such as CD19 and CD20. Commonly, they are positive for CD23, CD5, and CD200 and negative for CD10 (Swerdlow et al., 2017). Rarely, however, CD23 or CD5 negative cases can be observed. Especially in cases with an atypical immunophenotype, other B-cell neoplasms such as NMZL should be considered as differential diagnosis (Criel et al., 1999, Matutes et al., 1996).

Concerning genetic alterations, the most prevalently mutated gene in CLL is *NOTCH1* in 4-20% of all cases. Other frequently found genetic alterations concern the genes *FBXW7, TP53, ATM, POT1, BIRC3* and *MYD88* (Bosch and Dalla-Favera, 2019), which are all included in the customized panel for analyzing NMZL in this thesis.

1.4 Mutational Analysis using Next Generation Sequencing

Sequencing technologies can be divided into 3 generations. First generation sequencing, known as the Sanger method, is replaced steadily by more advanced and high-efficiency technologies. Nevertheless, Sanger Sequencing marks the beginning of decoding the human genome and is still applied in some domains. The principle of this method is the incorporation of dideoxy nucleotides which lack a 3´OH group into a DNA chain. However, this chemical group is indispensable for the DNA polymerase to bind the next nucleotide to the growing chain. Thus, in Sanger sequencing, chain terminates when a ddNTP is bonded to the DNA chain. Since these modified NTPs are labeled, they can be detected and the sequence subsequently decoded (Sanger et al., 1977). A major disadvantage of this method is that only one reaction can be analyzed at a time and the allelic frequency should be >15% in order to be detected. That problem was mastered in more advanced technologies of second and third generation sequencing, where millions of reactions run in parallel at the same time (Tucker et al., 2009). While the second generation still requires amplified DNA for sequencing, this is no longer necessary with the third generation, which means that individual molecules may be sequenced with these technologies (Heather and Chain, 2016). Next generation sequencing, which was the method of choice in this thesis, is a second-generation technology and will be explained in more detail below. In NGS, many short clonally amplified DNA or RNA molecules are sequenced in parallel. The best-known technologies here were developed by IonTorrent and Illumina, the former being used in this work and visualized in **Figure 3**. In several steps, sample libraries are created from extracted DNA. First core step is a physical, chemical or enzymatic DNA fragmentation to reach optimal size. The ends of those fragments are then repaired to enable adapter ligation. These are used for recognition of fragments in the instrument and contain an individual barcode sequence for each sample that serves for identification when samples are brought together later. For higher quality sequencing, the pools are then purified and concentrated which is essential for optimizing the process. In the subsequent clonal amplification, the DNA fragments are captured in numerous micelles, each with adapters, dNTPs, primers and DNA polymerase,

creating a micro PCR reactor in each individual micelle. On a semiconductor chip, each micelle is dropped into a microwell. This chip is then flooded with the bases, adenine, cytosine, guanine and thymine one after the other. As soon as one of these bases is incorporated into the growing chain of a fragment, a hydrogen ion is chemically released, which is detected by a pH sensor and finally translated into digital data (Hu et al., 2021a, van Dijk et al., 2014, Liu et al., 2012). Since this takes place in many reaction chambers simultaneously, a very large amount of data is generated, which must be analyzed in a multilevel system. In primary and secondary analysis, the quality of the data is analyzed by the instrument itself and the coverage is assessed. Moreover, the data is aligned to a human reference genome and upon those differences, variants are called. In tertiary analysis, the variants are categorized and interpreted using different tools to evaluate its significance (Hu et al., 2021a).

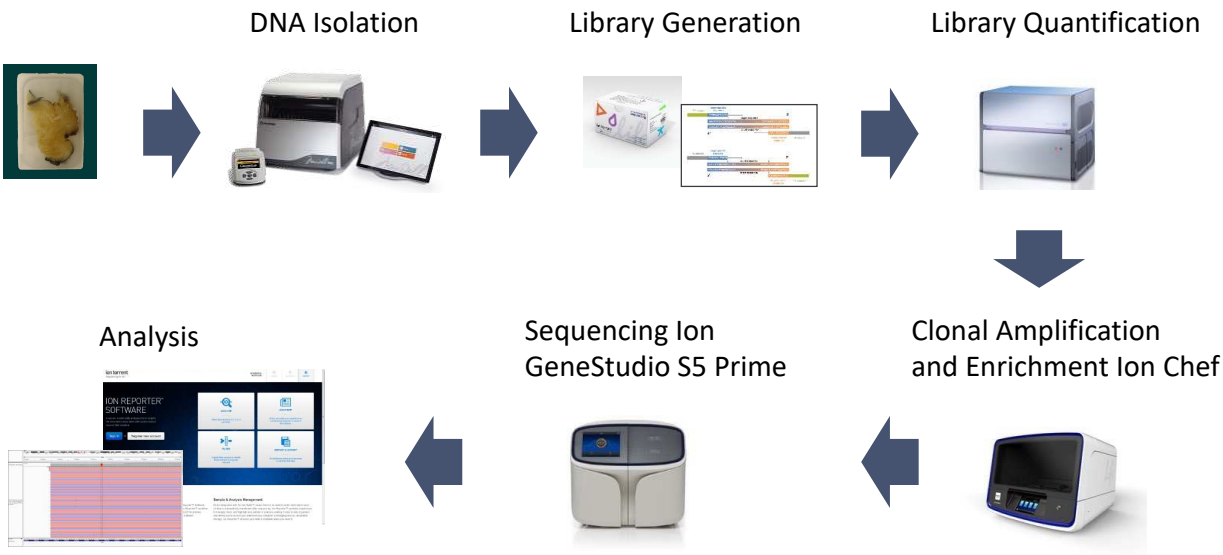

Figure 3 Next-Generation Sequencing Workflow. The process of NGS using the IonTorrent technology is shown in the diagram above. Starting with isolating DNA from desired material, generating and then quantification libraries prepared from extracted DNA, clonally amplifying and sequencing them and finally analyzing the digital data (exemplary workflow Institute of pathology Tübingen).

1.5 Aim of this Thesis

Many hematologic neoplasms have been investigated precisely in the past by numerous studies with large patient collectives using different methods. This allowed to collect data concerning genotype, pathology and clinical presentation, which led to better and more targeted therapy. This is not the case for NMZL, as it is considered a rare entity, and therefore, few studies have been published due to the small patient numbers. Even the existing studies usually have a very small number of patients, which makes it difficult to attain statistically significant results. Especially with respect to genetic information, there is a lack of sufficient data. NMZL is considered in the group of small B-cell lymphomas. While FL and CLL have a characteristic phenotype, which facilitates their diagnosis in routine practice, NMZL lacks specific markers, and therefore, is considered a diagnosis of exclusion. There is currently a great interest in researching the genetics of this entity in more detail and compare the results with other disease entities to facilitate the diagnosis in difficult cases.

The aims of this study were:

1. To identify all cases with the diagnosis or differential diagnosis of NMZL in the last ten years from the archives of the Institute of Pathology, University Hospital Tübingen
2. To review all cases morphologically and phenotypically to confirm the diagnosis of NMZL. Those cases where a differential diagnosis with other small B-cell lymphoma was still entertained were included in the study.
3. All cases with available material will be analyzed using Next Generation Sequencing with a custom panel containing 78 genes. The results will be compared to the mutational landscape reported in other entities.
4. To compare the genetic characteristics with the morphology and phenotype of the tumors in order to recognize possible subgroups.

The final aim of the study is to facilitate the diagnosis of this disease, ease its distinction to other similar small B-cell lymphomas and help to discover novel therapeutic strategies.

2 Material and Methods

2.1 Material

2.1.1 Patient samples

For the selection of the patient collective for this study, a search was performed using the current digital program in the Institute of Pathology -Nexus. The search was performed from 2010 to June 2021 looking for cases with the diagnosis or differential diagnosis of nodal marginal zone lymphoma. All existing sections of these cases were then retrieved from the archive. Most of them could be found in the archives of the Institute for Pathology and Neuropathology at the University Hospital Tübingen. For some of the consult cases, material was requested from the archives of the University Institute of Pathology Salzburg or Stuttgart. For the following DNA extraction, rolls and slides of 5µm were cut by experienced technicians. In some cases, DNA was already available and extracted for previous diagnostic analysis. The study was approved by the Ethics Committee of the Medical Faculty of the University of Tübingen (211/2021BO2).

2.1.2 Chemicals and Reagents

Chemicals and Reagents	*Company*
Agencourt AMPure XP	Beckman Coulter
dNTP	Thermo Fisher Scientific
Ethanol absolute	AppliChem
HighPrep	Biozym
Invitrogen™ UltraPure™ Distilled Water	Thermo Scientific
Hämatoxilin II	Roche
Blueing reagent	Roche
TRIS/Borat/EDTA Puffer (Cell Conditioning I, CCB1)	Roche
Protease 1	Roche

Antibodies for Immunohistochemical Staining:

Antibody (clone)	*Company*	*Dilution*
CD20 (L26)	Agilent Dako	1:1000
CD5 (SP19)	Medac	1:100
CD10 (SP67)	Roche	Ready to use
BCL6(GI191E/A8)	Roche	Ready to use
BCL2 (100D5)	DCS	1:20
IgD (poly rabbit)	Agilent Dako	1:1000
Ki67 (MIB-1)	Agilent Dako	1:400
Cyclin D1 (SP4)	Roche	Ready to use
CD3 (2GV6)	Roche	Ready to use
CD23 (SP23)	Roche	Ready to use
Kappa (poly rabbit)	Agilent Dako	1:25.000
Lambda (poly rabbit)	Agilent Dako	1:25.000

2.1.3 Kits for Genetic Analysis

Kit	*Company*
AmpliTaq Gold® DNA Polymerase	Thermo Fisher Scientific
Ion 530™ & Ion 540™ Kit – Chef	Thermo Fisher Scientific
Ion 530™ Chip & Ion 540TM Chip – Kit	Thermo Fisher Scientific
Ion AmpliSeq™ Library Kit 2.0 - 96LV	Thermo Fisher Scientific
Ion Library TaqMan™ Quantitation Kit	Thermo Fisher Scientific
OptiView Amplification Kit	Roche
Maxwell® RSC FFPE Plus DNA Purification KIT	Promega Corporation
QIAxcel DNA Kit	QIAGEN
Qubit™ dsDNA HS Assay Kit	Thermo Fisher Scientific
Qubit™ dsDNA BR Assay Kit	Thermo Fisher Scientific

2.1.4 Oligonucleotide Sequences

PCR Primer to assess DNA integrity (van Dongen et al., 2003):

Primer	*Sequence (5´-3´orientation)*
AF4/X3U	GGAGCAGCATTCCATCCAGC
AF4/X3L	CATCCATGGGCCGGACATAA
AF4/X11U	CCGCAGCAAGCAACGAACC
AF4/X11L	GCTTTCCTCTGGCGGCTCC
PLZF/X1U	TGCGATGTGGTCATCATGGTG
PLZF/X1L	CGTGTCATTGTCGTCTGAGGC
RAG1/X2U	TGTTGACTCGATCCACCCCA
RAG1/X2L	TGAGCTGCAAGTTTGGCTGAA
TBXAS1/X9U	GCCCGACATTCTGCAAGTCC
TBXAS1/X9L	GGTGTTGCCGGGAAGGGTT

Ion Xpress™ Barcoding Adapters (example):

IonXpress_030: CGAGGTTATC

Single Amplicon Primer (example):

These primers were used to validate mutations with low allelic frequency.

Red sequence is the adapter, green the barcode, black marks sequence for distinguishing barcode from sequence specific part, blue part genome sequence for PCR amplification.

Primer	*Sequence (5´-3´orientation)*
KLF2_E318_BC70_A_F	CCATCTCATCCCTGCGTGTCTCCGACTCAGCCTACT GGTCGATGAGAAGCCCTACCACTGCAA
KLF2_E318_BC70_A_R	CCATCTCATCCCTGCGTGTCTCCGACTCAGCCTACT GGTCGATATGTGCCGTTTCATGTGCA
KLF2_E318_trP1_F	CCTCTCTATGGGCAGTCGGTGATGAGAAGCCCTAC CACTGCAA
KLF2_E318_trP1_R	CCTCTCTATGGGCAGTCGGTGATATGTGCCGTTTCA TGTGCA

2.1.5 Devices

Utilization	*Device*	*Company*
Staining	BenchMarkULTRA staining automate	Roche
Centrifuge	Combi-Spin FVL-2400N	Peqlab
	Heraeus Multifuge 1L-R	Thermo Fisher Scientific
	PerfectSpin Mini centrifuge	Peqlab
DNA Extraction	Maxwell® RSC Instrument	Promega Corporation
Electrophoresis	QIAxcel Advanced Instrument	QIAGEN
Fluorometer	Qubit® Fluorometer	Thermo Fisher Scientific
NGS system	Ion Torrent Ion Chef™ System	Thermo Fisher Scientific
	Ion Torrent Ion S5™ System	Thermo Fisher Scientific
Microscope	Axiostar 2	Carl Zeiss
Pipettes	PIPETMAN® Classic	Gilson
	Research® plus	Eppendorf
Spectrophotometer	NanoDrop™ 2000	Thermo Fisher Scientific
Thermal Cycler	GeneTouch Thermal Cycler	Biozym
	Mastercycler® nexus	Eppendorf
	X2/GX2e LightCycler® 480 II	Roche
Thermoshaker	Thriller®	Peqlab
Vortexer	Vortex-Genie™ 2	Scientific Industries SI™
Workstations	HERAsafe™ biological safety cabinet	Thermo Fisher Scientific
	UV Sterilizing PCR workstation	Peqlab

2.1.6 Software

Utilization	*Software*	*Company*
Citation/Reference management	EndNote™ 20.4	Clarivate Analytics

Electrophoresis analysis	QIAxcel ScreenGel Software	QIAGEN
Genomics Viewer	Integrative Genomics Viewer (v.2.8.0)	Broad Institute
Patient/Sample management	PAS.net	Nexus
Primer Design	Primer3 (v.4.1.0)	Whitehead Institute for Biomedical Research
Data analysis	Ion Torrent Suite Software (v.5.12 and v.5.16.1)	Thermo Fisher Scientific
	Ion Reporter (v.5.16.0.2 and v.5.18.2.0)	Thermo Fisher Scientific
Writing	Word 2021 (v.16.48)	Microsoft

2.1.7 Consumable supplies

Supplies for laboratory routine such as pipette tips, reaction tubes and medical examination gloves were provided by the following companies: Abena, Biozym, Eppendorf, Falcon, Greiner, Neolab and Sarstedt.

2.1.8 Companies

Company	*Headquarter*
Abena	Aabenraa, Denmark
Agilent Dako	Santa Clara, United States of America
AppliChem	Darmstadt, Germany
Beckman Coulter	Brea, CA, United States of America
Biozym	Oldendorf, Germany
Carl Zeiss	Oberkochen, Germany
Clarivate Analytics	Philadelphia, PA, United States of America

DCS	Hamburg, Germany
Eppendorf	Hamburg, Germany
Falcon	Corning, NY, United States of America
Gilson	Middleton, WI, United States of America
Greiner	Kremsmünster, Austria
Microsoft	Redmond, WA, United States of America
Medac	Wedel, Germany
Neolab	Heidelberg, Germany
Nexus	Villingen-Schwenningen
Peqlab	Erlangen, Germany
Promega Corporation	Fitchburg, WI, United States of America
Qiagen	Venlo, Netherlands
Roche	Basel, Switzerland
Sarstedt	Nümbrecht, Germany
Scientific Industries SI™	Bohemia, NY, United States of America
Thermo Fisher Scientific	Waltham, MA, United States of America

2.2 Study Design

Firstly, cases with diagnosis or differential diagnosis of NMZL mentioned in any of the documents found in the program Nexus/Pathologie (PAS.net) were preselected and evaluated if suitable for the study. People under the age of 18 and cases where a different diagnosis has been established have been excluded. Cases in which enough material was available, were morphologically evaluated and if considered suitable, were further analyzed using NGS. Finally, a morphological reevaluation took place (**Figure 4**).

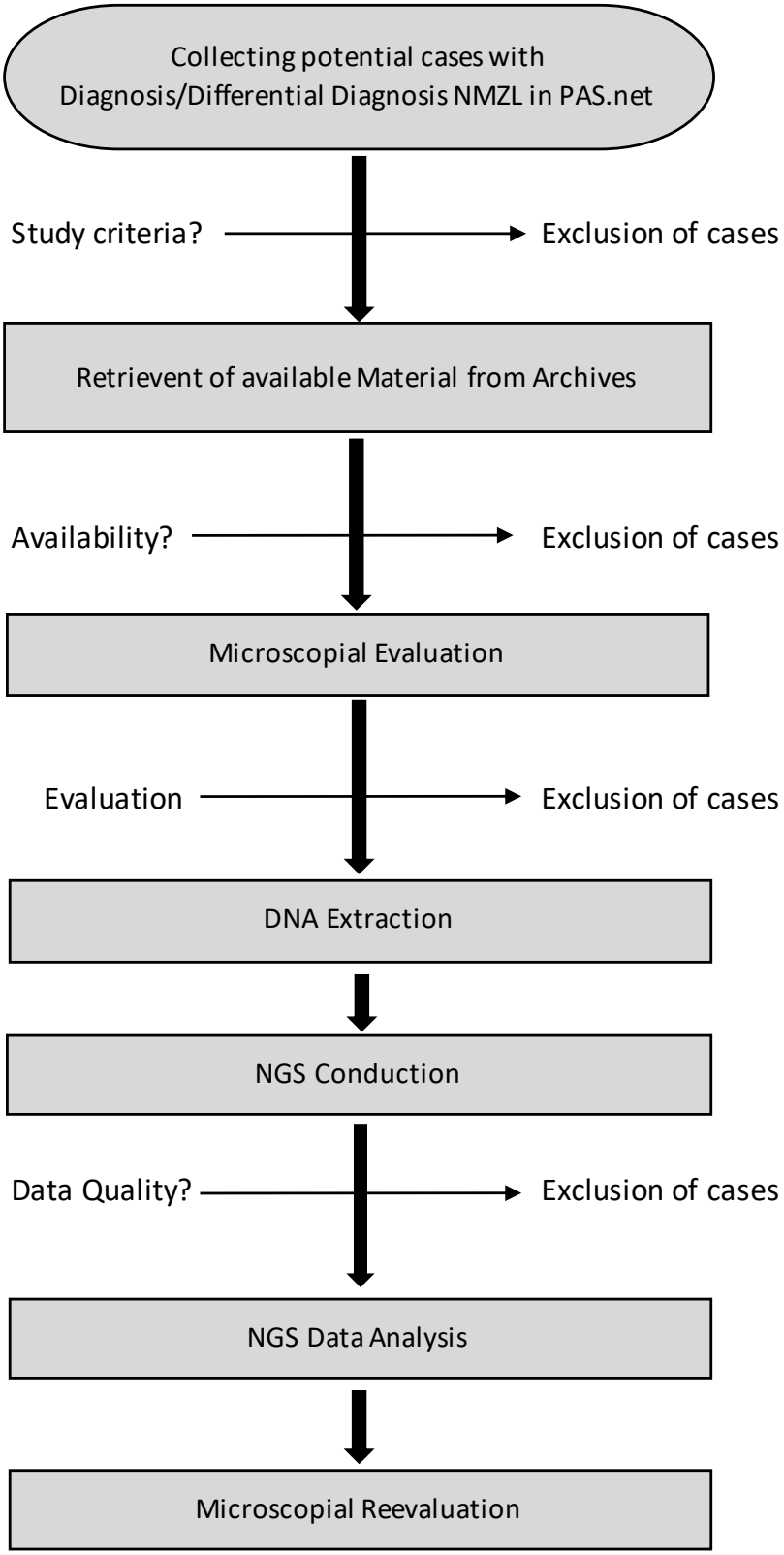

Figure 4 Flowchart of approach to the study and sample selection. After collecting a preselection of all cases in which NMZL was mentioned in any of the documents, available material of suitable remaining cases was retrieved. After microscopical evaluation, DNA extraction and NGS conduction took place. Samples with sufficient quality were analyzed and reevaluated under the microscope.

2.3 Microscopy

To assess all cases morphologically prior to genetic analysis, all available retrieved slides from the archives were evaluated together with Prof. Dr. Leticia Quintanilla Fend and Dr. Dominik Nann. Slides included HE and a range of immunohistochemical stainings for each case. In most cases, more immunohistochemical markers were necessary for better evaluation, and therefore, stained by technicians from the Institute upon request. Samples were only approved to subsequent analysis if after histological assessment, NMZL was still considered as a probable differential diagnosis. if they were still suitable for the study after histological assessment.

2.4 Immunohistochemical Staining

The BenchMark ULTRA fully automatic stainer was used for all the immunohistochemical staining. The following steps were performed automatically in the machine according to the manufacturer's protocols.

First, the slides were deparaffinized.

Next, the slides were pretreated with different reagents for antigen retrieval. For the stains CD20, CD5, CD10, BCL6, BCL2, IgD, Ki67 (MIB-1) and Cyclin D1, the slides were boiled in a TRIS/Borate/EDTA buffer (Cell Conditioner 1; CC1) for 64 minutes, for CD3 and CD23 for 32 minutes. For kappa and lambda staining Protease 1 was used as pretreatment; for kappa for 8min, for lambda for 4min. The next steps were conducted using the OptiView Amplification Kit. First, H_2O_2 was applied to all slides to block background staining. The next step was the staining with the respective primary antibody, again using different incubation times and temperatures:

Antibody	**Temperature**	**Duration**
CD20, CD5, CD10, BCL6, BCL2, IgD, Ki67 (MIB-1), Cyclin D1, CD23, kappa	37°C	32min
CD3	Room temperature	20min
Lambda	Room temperature	16min

The bridging antibody (hydroxyquinoline xylene) was then added, followed by the secondary antibody (HRP (Horseradish peroxidase) multimer). Finally, H_2O_2, copper and the DAB (Diaminobenzidine) were added. The treatment with the OptiView kit was then completed. For counterstaining, hematoxylin II was incubated for 20 minutes and a bluing reagent for 8 minutes. The slides could then be removed from the machine. Finally, the sections were washed, dehydrated and covered for airtight sealing.

2.5 DNA extraction

2.5.1 Preparation of the samples for the following DNA extraction

To perform a mutation analysis of paraffin embedded samples, one first must extract the DNA from the samples for further experiments. At first, the selected FFPE samples (rolls) were centrifugated briefly. Then, 180µl incubation buffer was added to each sample, followed by 20µl proteinase K. After that, the samples were transferred to a thermocycler to be incubated overnight at 70°C to let proteinase K digest the proteins. The preparation of the samples was performed in several runs.

2.5.2 Extraction of the DNA

For the automated extraction of DNA from FFPE samples, the Maxwell RSC Instrument was used. One cartridge and one 0,5mL elution tube per sample were placed in the Maxwell RSC Cartridge Rack. As the next step, 60µL nuclease-free water was added into each elution tube. The overnight incubated samples were now transferred from the thermocycler to a centrifuge and centrifuged for 10s to get all contents to the bottom of the tube and avoid losing any DNA when opening the lids. 400µl lysis buffer was added to each sample. Each sample was transferred individually into the first well of the cartridge. Then, the loaded rack was placed into the Maxwell instrument. The following automated process of extracting the DNA took 24min. After that, the elution tubes were centrifugated briefly and placed on a magnetic stand to isolate the magnetic beads from the

eluate. The eluate without magnetic beads was transferred into the new labeled 1,5mL tubes. To extract DNA from all samples, all steps above were performed in several runs.

2.5.3 Determination of nucleic acid concentration

To determine the concentration of DNA in the samples, two methods were used. Firstly, all DNA (single and double strand) in the samples was measured using NanoDrop 2000, then only intact double stranded DNA was measured using the Qubit Fluorometre 3.0.

To calibrate the NanoDrop 2000 instrument, 1 µL of distilled water was added to the lower pedestal and measured. To measure the nucleic acid concentration of the samples, 1µL of the respective sample was added to the lower pedestral and measured.

For the double strand DNA quantification using Qubit 3.0, a working solution was prepared at first. Therefore, Qubit dsDNA HS reagent had to be thawed protected from light. To dilute the Qubit dsDNA HS reagent, 199µL Qubit dsDNA HS buffer per sample and 1µL reagent per sample were combined. Into new tubes, 199µL of the working solution and 1µL of the respective sample were added, resulting in a total of 200µL per tube. To measure the samples, the program “dsDNA High Sensitivity” was selected. One by one, each tube was inserted into the Qubit fluorometer and the concentration measured.

2.5.4 PCR to analyze integrity of the DNA

Extracted DNA from paraffin embedded tissue can be quite fragmented. For further experiments, it is important to determine the length of fragments of the extracted DNA to estimate it´s integrity. Therefore, a multiplex PCR with amplification of gene products of different lengths was performed with all samples. When performing PCR it is very important to respect a strict separation of rooms for preparing the PCR mix and adding the extracted DNA to avoid any contamination of PCR materials. To ensure that all equipment was free of DNA,

PCR tubes, water, buffer, tube for PCR mix and $MgCl_2$ was UV-irradiated for 30min. While material was being irradiated, dNTPs and primermix was thawed protected from light. After irradiation was done, the PCR master mix was prepared:

Tabular protocol for PCR mix per sample:

Reagent	**Volume**
ddH_2O	16,8µL
10x Buffer II	2,5µL
25mM $MgCl_2$	2µL
AmpliTaq Gold DNA Polymerase (5U/µL)	0,2µL
dNTPs (10mM)	0,5µL
Primer mix (Primer AF4/X3 2,5µM, all others 1,25µM)	2µL
Total	**24µL**

One PCR master mix was prepared for all samples combining the contents listed above. Before adding the DNA Polymerase, it is important to centrifugate only briefly to avoid destroying the enzymes. 24µL of the PCR master mix was added to each PCR tube. Then, 50ng of the extracted DNA was added to the respective PCR tube. The tubes were then inserted into the Thermocycler.

Tabular PCR program:

Temperature (°C)	**Duration**
95°C	7min
35 cycles: 95°C 60°C 72°C	 45s 45s 1min
72°C	4min
16°C	Until removal

To perform gel electrophoresis to assess length of the DNA fragments, QIAxel Advanced was used. Therefore, 15µL of each sample was transferred into new PCR tubes and put into the QIAxel Advanced, where the automated gel electrophoresis was performed.

2.6 Ion Torrent Next-Generation Sequencing

2.6.1 Oncomine Lymphoma III Panel

On all cases, NGS was conducted using the Oncomine Lymphoma III Panel which is an Oncomine tumor specific custom panel by Thermo Fisher Scientific. It was designed using the AmpliSeq Designer (v.7.49) and covers 78 which are listed in the table below (**Table 1**).

The former mutation *MYD88* p.L265P under the reference number NM_002468 is now referred to as *MYD88* p.L252P under the reference number NM_002468.5. For clarity, the old nomenclature is used throughout this thesis as this was still the valid one at the time the results were analyzed, and the thesis was written.

Table 1 Oncomine Lymphoma III Panel. Customized panel for the analysis of nodal marginal zone lymphoma. All genes are listed with transcript number and region (Hotspot= only hotspot region is covered; CDS= 95.80% of the complete coding sequences is covered).

Gene	Transcript	Region	Gene	Transcript	Region
ALK	NM_004304.5	Hotspot	***CREBBP***	NM_004380.3	CDS
ARAF	NM_001654.5	Hotspot	***CXCR4***	NM_001008540	CDS
BRAF	NM_004333.6	Hotspot	***EP300***	NM_001429.4	CDS
BTK	NM_000061.3	Hotspot	***ETV6***	NM_001987.5	CDS
CARD11	NM_032415.6	Hotspot	***EZH2***	NM_004456.5	CDS
CBL	NM_005188.4	Hotspot	***FAS***	NM_000043.6	CDS
CCND1	NM_053056.3	Hotspot	***FBXW7***	NM_033632.3	CDS
CD79B	NM_001039933.3	Hotspot	***GNA13***	NM_006572.6	CDS
DDR2	NM_006182.4	Hotspot	***H1-4 (HIST1H1E)***	NM_005321.3	CDS
GATA2	NM_032638.5	Hotspot	***HLA-B***	NM_005514.8	CDS
H3C2 (HIST1H3B)	NM_003537.4	Hotspot	***ID3***	NM_002167.5	CDS
IKBKB	NM_001556.3	Hotspot	***IRF4***	NM_002460.4	CDS
KRAS	NM_033360.4	Hotspot	***JAK2***	NM_004972.4	CDS
MAP2K1	NM_002755.4	Hotspot	***JAK3***	NM_000215.4	CDS

MTOR	NM_004958.4	Hotspot	***KLF2***	NM_016270.4	CDS
MYD88	NM_002468	Hotspot	***KMT2D***	NM_003482.4	CDS
PAX5	NM_016734.3	Hotspot	***MEF2B***	NM_001145785.2	CDS
RHOA	NM_001664.4	Hotspot	***MYC***	NM_002467.6	CDS
SF3B1	NM_012433.4	Hotspot	***NFKBIA***	NM_020529.3	CDS
STAT3	NM_139276.2	Hotspot	***NOTCH1***	NM_017617.5	CDS
STAT5B	NM_012448.4	Hotspot	***NOTCH2***	NM_024408.4	CDS
XPO1	NM_003400.4	Hotspot	***PIM1***	NM_002648.4	CDS
ARID1A	NM_006015.6	CDS	***PLCG2***	NM_002661.5	CDS
ARID1B	NM_001371656.1	CDS	***POT1***	NM_015450.3	CDS
ATM	NM_000051.3	CDS	***PRDM1***	NM_001198.4	CDS
B2M	NM_004048.3	CDS	***REL***	NM_002908.4	CDS
BCL2	NM_000633.2	CDS	***SGK1***	NM_001143676.1	CDS
BCL6	NM_001706.5	CDS	***SMARCA4***	NM_001128849.3	CDS
BCL10	NM_003921.5	CDS	***SOCS1***	NM_003745.1	CDS
BCL11A	NM_022893.4	CDS	***SPEN***	NM_015001.3	CDS
BIRC3	NM_182962.3	CDS	***STAT6***	NM_003153.5	CDS
BTG1	NM_001731.3	CDS	***TCF3***	NM_001136139.4	CDS
BTG2	NM_006763.3	CDS	***TERC***	NR_001566	CDS
CCR4	NM_005508.5	CDS	***TET2***	NM_001127208.2	CDS
CD28	NM_006139.4	CDS	***TMSB4X***	NM_021109.4	CDS
CD70	NM_001252.5	CDS	***TNFAIP3***	NM_001270507.2	CDS
CD79A	NM_001783.4	CDS	***TNFRSF14***	NM_003820.3	CDS
CDKN2A	NM_001195132.1	CDS	***TP53***	NM_000546.5	CDS
CHD2	NM_001271.4	CDS	***TRAF3***	NM_003300.4	CDS

2.6.2 PMZL Panel

In 33 cases we analyzed the *PTPRD* gene in addition to the 78 genes included in the Oncomine Lymphoma III panel. For this purpose, an existing AmpliSeq custom panel by Thermo Fisher Scientific, which was originally designed for PMZL and contains the *PTPRD* gene, was used. The preparation of the samples for this panel was performed by Rebecca Braun and Franziska Mihalik. It covers the 6 genes which are listed in the table below (**Table 2**).

Table 2 PMZL Panel. Panel originally designed for the analysis of PMZL including the PTPRD gene. The 6 genes are listed with transcript number and region (Hotspot= only hotspot region is covered; CDS= 93.53% of the complete coding sequences is covered).

Gene	Transcript	Region
KLF2	NM_016270.4	CDS
NOTCH3	NM_000435.3	CDS
PTPRD	NM_002839.4	CDS
TET2	NM_001127208.3	CDS
TBL1XR1	NM_024665.7	CDS
BRAF	NM_004333.6	Hotspot

2.6.3 Generation of Amplicon Libraries

The AmpliSeq™ Library Kit 2.0 - 96LV was used to generate Amplicon libraries for NGS. All steps were performed following the manufacturer's instructions. Initially, all samples were diluted to a DNA concentration of 5ng/µL with water.

2.6.3.1 AmpliSeq PCR

For decontamination, all tubes and aliquoted water was UV-irradiated for 30min. At first, a PCR MasterMix was prepared for each sample, containing 3,5µL of ddH2O and 5µL HiFi Mix, which had to be thawed on ice. To that mix, 4µL of the respective sample was added, resulting in a total of 12,5µL. Then, one PCR tube with 5µL of primer pool 1 and one PCR tube with 5µL of primer pool 2 of the Oncomine Lymphoma III was filled for each sample. As the next step, 5µL of the PCR mix of the respective sample was added to each of the two PCR tubes with pool 1 and 2, now containing a total of 10µL. Afterwards they were put into a ThermoCycler and the first PCR with the following program was performed:

Temperature (°C)	**Duration**
99°C (Initial Denaturation)	2min
17/18 cycles: 99°C (Denaturation) 60°C (Annealing/Extension)	 15s 8min
10°C (Hold)	Until removal

2.6.3.2 Primer Digestion and Barcode ligation

For Primer digestion, 2µL of FuPa reagent was added to each library and then vortexed carefully. In a ThermoCycler, libraries were incubated for another 40min.

After that, ligation with barcoding sequencing adapters was performed and libraries were incubated again.

Tabular Barcode ligation protocol:

Reagent	**Quantity**
Switch Solution	4µL
DNA Ligase	2µL
Barcode	2µL
Digested Amplicons	22µL
End volume	**30µL**

Incubation protocols are shown below:

Primer Digestion:

Temperature (°C)	**Duration**
50°C	10min
55°C	10min
60°C	20min
10°C	Until 1h

Barcode Ligation:

Temperature (°C)	**Duration**
22°C	30min
68°C	5min
72°C	5min
10°C	Until 1h

2.6.3.3 AMPure Purification

To purify the libraries, AMPure XP magnetic beads were used.

First, 45µL of AMPure reagent was added to each library and incubated for 5min at room temperature. After incubation, tubes were placed on a magnetic rack and incubated for another 2min at room temperature. Then, 70µL of the supernatant was discarded carefully from the tubes without damaging the magnetic beads. In the following, 200µL of 70% Ethanol was added to each tube and they were rearranged on the magnetic plate to let the magnetic beads walk through the alcohol. Beads should not touch Ethanol longer than 30s to avoid destroying the DNA. 200µL of the Ethanol supernatant was then discarded and the last step was repeated again with 200µL Ethanol. After Ethanol was removed again, beads were dried at room temperature. When beads were dry but not cracked already, 35µL of LowTE buffer was added to each tube and incubated for another 5min at room temperature on the normal rack, followed by 2min incubation on the magnetic rack. As the last step, 30µL of the supernatant were then transferred to new tubes. The whole purification was then repeated a second time for all libraries.

2.6.4 Quantification of Amplicon Libraries

To quantify amplicons after purification, a real-time PCR was performed using the Ion Library TaqMan™ Quantification Kit.

For subsequent calculation, standard concentrations are necessary. Therefore, three dilutions of Escherichia coli DH10B with 6,8pM (1:10), 0,68pM (1:100) and 0,068pM (1:1000) were prepared using the E.coli stock solution and ddH2O. Libraries were diluted 1:500 with ddH2O. Hereafter, a PCR MasterMix consisting of 5µL of 2X Ion TaqMan Master Mix and 0,5µL of 2X Ion TaqMan Assay per sample was prepared in a tube. When calculating the volumes of the reagents, it had to be considered that PCR of libraries was always being conducted in duplicates. 5,5µL of the PCR Master Mix was then transferred into each used well of a 98-well-plate. Then, 4,5µL of diluted library, E.Coli dilution or ddH2O as

negative control was added to the respective wells and mixed into the PCR MasterMix using the pipette. Pipetting layout is shown in the table below:

	1	2	3	4	5	6	7	8	9	10	11	12
A	E.coli 6,8	Sample 2										
B	E.coli 6,8	Sample 2										
C	E.coli 0,68	Sample 3										
D	E.coli 0,68	Sample 3										
E	E.coli 0,068	Sample 4										
F	E.coli 0,068	Sample 4										
G	Sample 1	NTC										
H	Sample 1	NTC										

LightCycler real-time PCR program can be seen in the following:

Temperature (°C)	**Duration**
50°C	2min
95°C	20s
40 cycles: 95°C 60°C	 1s 20s

2.6.5 Pooling and Sequencing the libraries

Before chip loading, all libraries were diluted to 30pM, using 4µL of DNA with the calculated quantity of water to reach the desired dilution. 3,3µL of each dilution was then combined in one tube, which resulted in a Librarypool of 29,7µL since nine samples were put on one 540er chip. Subsequently, 22,9µL of the Librarypool was combined with 2,1µL of ddH2O, being the final pool with a volume of 25,0µL. This was then transferred into the cartridge of the Ion Torrent Ion Chef™ System for clonal amplification, where amplicons are being annealed to Ion Sphere™ Particles of the Ion 540™ Kit – Chef, as well as enrichment and loading the Ion 540™ chip. After that, the chip was transferred into the Ion S5 Prime System by Thermo Fisher Scientific, where sequencing was being

conducted. Hereafter, raw files were uploaded onto the Ion Torrent server for further analysis.

2.7 Genetic Analysis

The raw data was genetically analyzed with Ion Torrent Suite Software (versions 5.12. or 5.16.1). To match reads to the human reference sequence built 38 (hg19), the Torrent mapping alignment program was used, which is already integrated in the software. Genetic alterations were analyzed with the Ion Reporter Software (versions 5.16.0.2 or 5.18.2.0) and visualized with the Integrative Genomics Viewer to distinguish artifacts from real mutations. Besides, the open-source online tools VarSome, ClinVar, COSMIC, dbSNP, OncoKB, cbj.jax as well as SIFT PolyPhen-2 and CADD Scores were used to evaluate whether the mutations found were SNPs or known somatic mutations. Depending on the quality of the samples, variants were filtered with a threshold allele frequency between 5% and 10%. In three cases (3, 11, 28) variants were filtered with a threshold allele frequency of 19%. Regarding the coverage threshold, variants > 200 reads were considered, with the exception of a few variants <200 reads but convincing VAF. In general, only variants noted as “pathogenic”, “likely pathogenic” or “uncertain significance” in Varsome were taken into account. Results of the PMZL Panel were analyzed by Vanessa Borgmann.

2.8 Validation of low frequent Mutations

In 9 cases, one or two mutations had to be validated due to a low allelic frequency and/or a low coverage using the Amplicon Library Preparation (Fusion Method) technology by Thermo Fisher Scientific or a different customized panel. Cases are listed below. Therefore, single amplicons of about 200-300bp in size covering the respective gene locus were designed for each mutation using Primer3 Software.

Sample	*Genes with questionable variants*
NM9	*KLF2, POT1*

NM13	*SMARCA4*
NM23	*SMARCA4*
NM31(2)	*CXCR4*
NM35	*KLF2*
NM39	*BRAF, KRAS*
NM41	*BTG1*
NM45	*STAT5B, KLF2*
NM57	*NOTCH1*

2.8.1 Generation of Single Amplicons

First, all PCR tubes which were needed later on were UV-irradiated for 30min. For each single amplicon, 4 primers were needed. Since primers come in lyophilizated form, they must be diluted first. Therefore, the calculated quantity of ddH2O was added to each original tube to achieve a 100µL dilution. After that, primers were diluted again to a concentration of 10µL (1:10). Then, Primer Mix 1 and Primer Mix 2 were being prepared as shown in the following:

Primer Mix	Primer	Total volume
Primer Mix 1	3µL F-Primer with Barcode Adapter + 3µL R-trP1 Primer	6µL
Primer Mix 2	3µL R-Primer with Barcode Adapter + 3µL F-trP1 Primer	6µL

As the next step, 2 pools were prepared for each single amplicon, one with Primer Mix 1, one with Primer Mix 2. Therefore, 22,5µL of the Phusion PCR Super Mix HiFi was mixed with 0,5µL of the respective Primer Mix and 5µL of the respective DNA, which was diluted to a 5ng/µL concentration beforehand. This resulted in a total volume of 28µL for each pool. Pools were then incubated in a ThermoCycler. PCR protocol is shown below:

Temperature (°C)	Duration
94°C	3min
40 cycles:	
94°C	30s
58°C	30s
68°C	1min
16°C	Until removal

After 2h and 10min of Incubation, PCR products were purified using the Magbio HighPrep PCR magnetic beads. First, 54µL of HighPrep was added to each product, then vortexed and centrifugated carefully and incubated at room temperature for 5min on a plastic rack. After 5min, tubes were placed on a magnetic plate and incubated for 2min at room temperature. Then, the supernatant was discarded carefully without damaging the magnetic beads. For purification, 200µL of 80% Ethanol was added into each tube and discarded again after a maximum of 30s. This washing step was repeated one more time. After Ethanol supernatant was removed for the second time, beads were dried at room temperature for about 2min. After that, 35µL of low-TE buffer was added to the dried beads to dissolve the DNA products from the magnetic beads. They were then incubated for 5min at room temperature. As the next step, tubes were placed on the magnetic rack again and incubated for another 2min. Lastly, 30µL of the supernatant, the purified DNA products, was transferred to freshly labeled PCR tubes.

2.8.2 Quantification and Dilution of Single Amplicons

To assess quantity of the purified products, contained double strand DNA was measured using Quibit 3.0 as described above in 2.3.3. Then, products were diluted 1:100 by adding 2µL of libraries to 198µL of H2O. To reach the final dilution of 5pM, the needed quantity of H2O was calculated and 2µL of the 1:100 dilution was added to the respective tube with H2O.

After that, products were sequenced and analyzed as described earlier.

3 Results

3.1 Sample Selection

Initially, a collective of 78 cases was selected. After reviewing all existing documents on these cases with Prof. Dr. Quintanilla Fend, 16 cases were excluded from the study. In these cases, NMZL was only mentioned as one of the differential diagnoses in the report but then were classified as a different entity. From the remainder 62 cases, 13 cases were excluded because either there was not enough material available for the DNA extraction (7 cases) or because after rereviewing the cases, it was considered that a different diagnoses was more likely (6 cases). NGS was performed on these remaining 49 cases. For one patient, 2 different samples from different lymph nodes were available and analyzed separately. The most recent sample was diagnosed as DLBCL most probably a transformation from the pre-existing lymphoma. Five cases needed to be excluded due to poor quality of the DNA and NGS data. This resulted in a final collective of 44 patients with 45 samples that could be fully examined histologically and genetically (**Figure 5**).

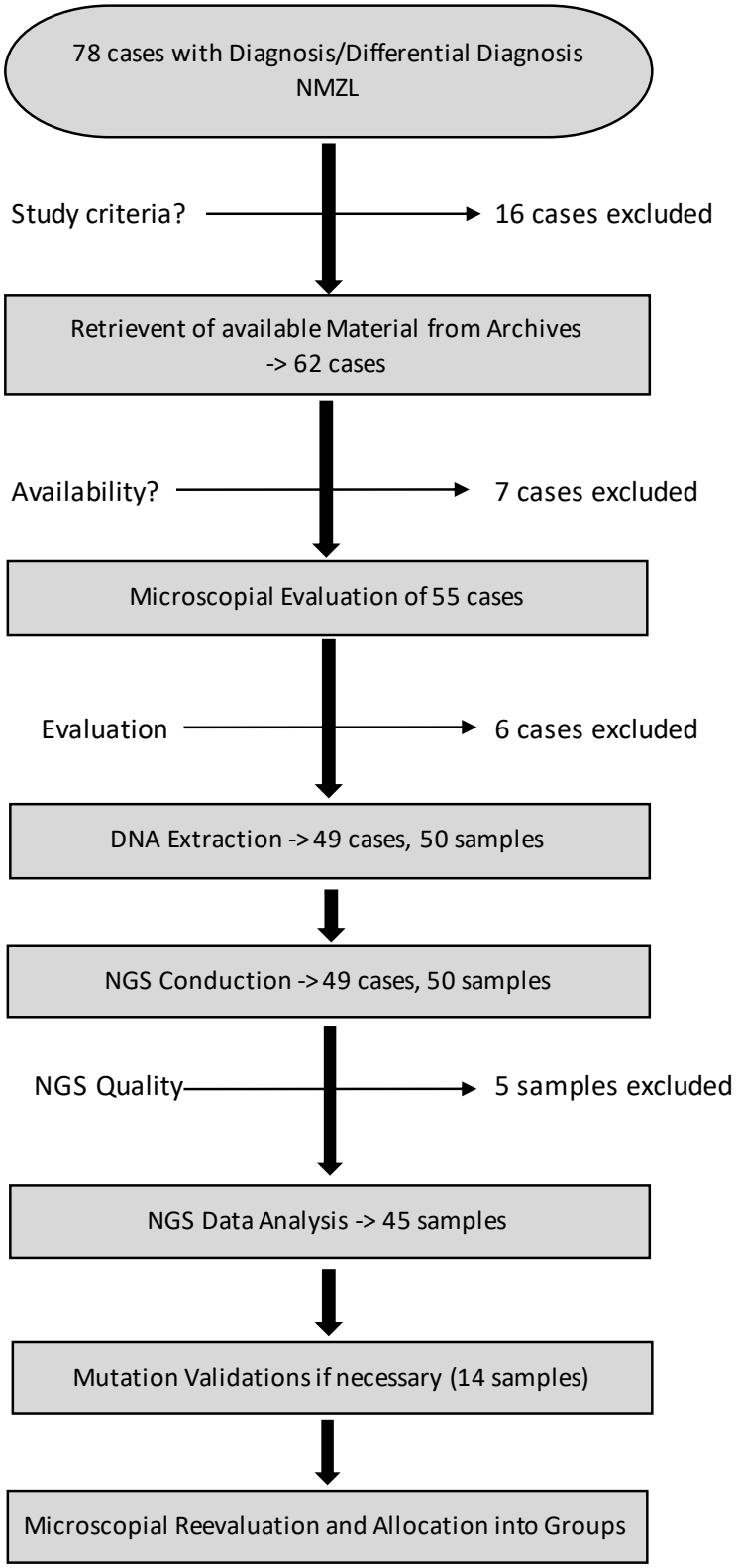

Figure 5 Selection process of NMZL cases for NGS analysis and reevaluation. From a collective of 78 cases, a total of 29 cases had to be sorted out because they were classified as a different or material was not available. On the remaining 50 samples, NGS was conducted. Finally, 45 were analyzed after 5 had to be excluded due to insufficient data quality. Moreover, 10 of these 45 cases had to be validated laboratory before reevaluation took place.

3.2 Patient Characteristics

The collective consisted of 23 females (52%) and 21 males (48%). The mean age of the patients was 66 years (range of 36 – 86 years) at the time of diagnosis. The median age at diagnosis of the 29 cases assigned to the NMZL group was 66 years as well (range of 36 – 85 years) (see **Table 3**).

All samples were lymph node biopsies. The most common were inguinal, axillary and cervical lymph nodes. The exact biopsy sites are listed in **Table 3** and illustrated in **Figure 6**.

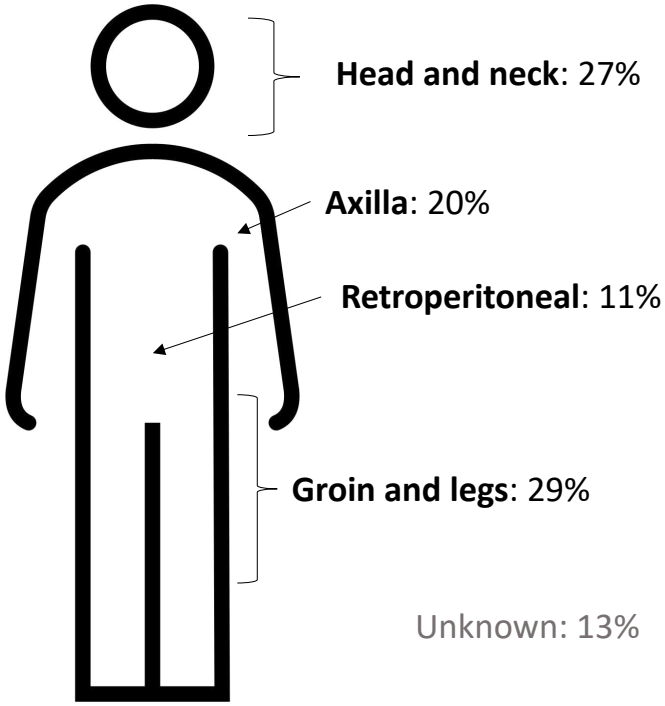

Figure 6 Tumor biopsy sites. The illustration shows the distribution of the biopsy sites of the tumor lymph nodes investigated in this study with respective percentages. Most biopsies were taken from lymph nodes in the groin and legs (29%), followed by the neck and head region (27%). 20% came from the axilla and 11% were retroperitoneal lymph nodes. In 13% of cases, the exact localization was unknown.

3.3 Immunohistochemistry

As part of the diagnostic work-up, all cases have already been immunophenotyped. CD20 staining was performed in all cases. It was strongly positive in 42/45 (93%) of the cases and weakly positive in 3/45 (7%). CD5 staining was performed in 43 cases, of which 6 cases (14%) were positive, one was weakly positive, the rest of the tumor samples (36/43, 84%) were CD5 negative. CD3 was stained in all cases, one showed a slight positivity in the tumor cells. CD23 immunohistochemistry was performed on 43 samples and was positive in 4 cases (9%), weakly positive in 3 (7%) and otherwise negative (84%) in the neoplastic cells. 4 (10%) of the 39 CD10 stained cases were positive, one was weakly positive and 34 (87%) were negative. BCL6 was stained in 37 samples, was negative in 70% (26/37), weakly positive or positive in 8/37 (22%) and could not be clearly assessed in 3 cases. Only 3 of the 35 BCL2 stained samples were negative for this marker, while 3 were difficult to evaluate; the remaining 29 cases were positive. IgD immunohistochemistry was performed on 40/45 samples, 22 showed negativity, 17 weak positivity or positivity and one was challenging to assess. MIB-1 staining to determine the tumor cell proliferation was performed on 40 samples. Overall, the collective revealed a rather low proliferation rate with values between 1% and 40% (mean: 15%). An overview of all the immunohistochemical results is shown in **Table 3**.

Table 3 Immunohistochemical profile and key data of the final collective. All cases are listed with respective age and sex (M= male, F= female) and biopsy site of the sample (LN= lymph node). A plus sign represents an observed positive staining for the respective marker, (+) marks a weak positivity, a minus sign a negativity for the marker and nd means that the staining was not performed on that sample.

Case	Sex	Age, y	Biopsy site	CD20	CD5	CD3	CD23	CD10	BCL6	BCL2	IgD	MIB1, %
3	M	86	Renal hilar LN	+	+	-	-	-	-	+	-	10
5	M	46	Inguinal LN	+	-	-	-	-	nd	nd	-	nd
6	M	64	Obturator LN	+	-	-	-	-	-	+	(+)	<5
7	M	47	Retroperitoneal LN	+	-	-	-	-	-	+	-	<5
8	M	85	Axillary LN	+	+	-	-	nd	nd	nd	(+)	<5
9	F	61	Cervical LN	+	-	-	-	nd	-	(+)/-	-	<5
10	F	60	Inguinal LN	(+)	+	-	-	-	-	(+)	nd	30
11	F	73	Axillary LN	+	-	-	-	-	-	(+)	-	1
12	F	49	Intraparotid LN	+	-	-	-	-	-	(+)	-	<10
13	M	82	Inguinal LN	+	+	-	-	nd	nd	nd	-	5
15	M	83	Cervical LN	+	-	-	-	-	-	+	-	5-10
16	F	62	Cervical LN	(+)	-	-	nd	-	-	(+)	-	50
19	F	83	Axillary LN	+	+	-	-?	-	-	+	nd	1-30
20	F	46	Inguinal LN	+	-	-	+	+	+	-	-	30
22	M	67	Inguinal LN	+	-	-	-	-	?	?	-	30
23	F	72	Retroperitoneal LN	+	-	-	-	-	-	+	+	15
24	M	69	Orbita	+	-	-	-	-	-	nd	-	5
25	M	68	LN	+	-	-	-	nd	nd	nd	+	<5
27	F	55	Pelvis	+	-	-	-	-	-	+	-	10
28	F	60	Flank LN	+	-	-	-	-	-	(+)	+	10-15
30	F	76	Inguinal LN	+	-	-	-	nd	nd	nd	+	nd
31 (1)	F	47	Inguinal LN	+	-	-	(+)	+	?	?	?	15
31 (2)			LN	+	-	-	(+)	+	nd	+	nd	40
32	F	82	LN	+	nd	-	-	-	-	-	+	<5
33	M	66	Axillary LN	+	-	-	+	+	+/-	nd	-	10
35	M	47	Mesenteric LN	+	-	-	nd	-	-	+	-	nd
38	F	36	Submandibular LN	+	-	(+)	-	-	-	+	+	5-10
39	F	73	Paracaval LN	+	-	-	-	-	-	+	+	20
41	M	77	Axillary LN	+	nd	-	-	-	-	+	(+)	nd
44	F	46	Inguinal LN	+	-	-	-	-	-	+	+	<5
45	M	60	Axillary LN	+	-	-	-	-	-	+	-	5-10
46	M	67	Axillary LN	+	-	-	+	(+)	(+)	(+)	-	15-20
47	M	61	LN	+	-	-	-	-	(+)	+	-	30
48	F	84	Axillary LN	+	-	-	-	-	-	+	nd	<5
51	M	38	Perineal LN	+	-	-	-	-	-	+	+	5
52	F	60	Cervical LN	+	-	-	-	-	+	+	-	30-40
53	M	75	Inguinal LN	+	-	-	-	-	-	-	-	5-10
54	M	67	LN	(+)	-	-	-	-	+	nd	+	5
55	F	71	Cervical LN	+	-	-	-	-	(+)	+	(+)	30
56	F	62	Parotid LN	+	-	-	-	-	nd	nd	+	<5
57	M	68	Cervical LN	+	+	-	-	-	-	+	+	5
59	M	71	Supraclavicular LN	+	-	-	+	-	(+)	+	-	10
60	F	91	Cervical LN	+	-	-	-	nd	nd	nd	nd	nd
61	F	64	Axillary LN	+	(+)	-	(+)	-	-	+	+	10-15
62	F	77	LN	+	-	-	-	-	(+)	+	-	10

3.4 DNA Integrity

In all samples (50/50, 100%), adequate concentrations of DNA could be retrieved. In 24/50 cases, DNA was already extracted before for diagnostical reasons. In these cases, DNA was retrieved from the archives and used for further experiments. In that group, the DNA integrity ranged between 300bp to 600bp. Concerning the remaining 26 cases, quantifiable concentrations of DNA were extracted and amplified by PCR. To investigate the DNA quality, gel electrophoresis has been performed (**Figure 7**). Maximum amplicon size in this group ranged between 200bp to 400bp.

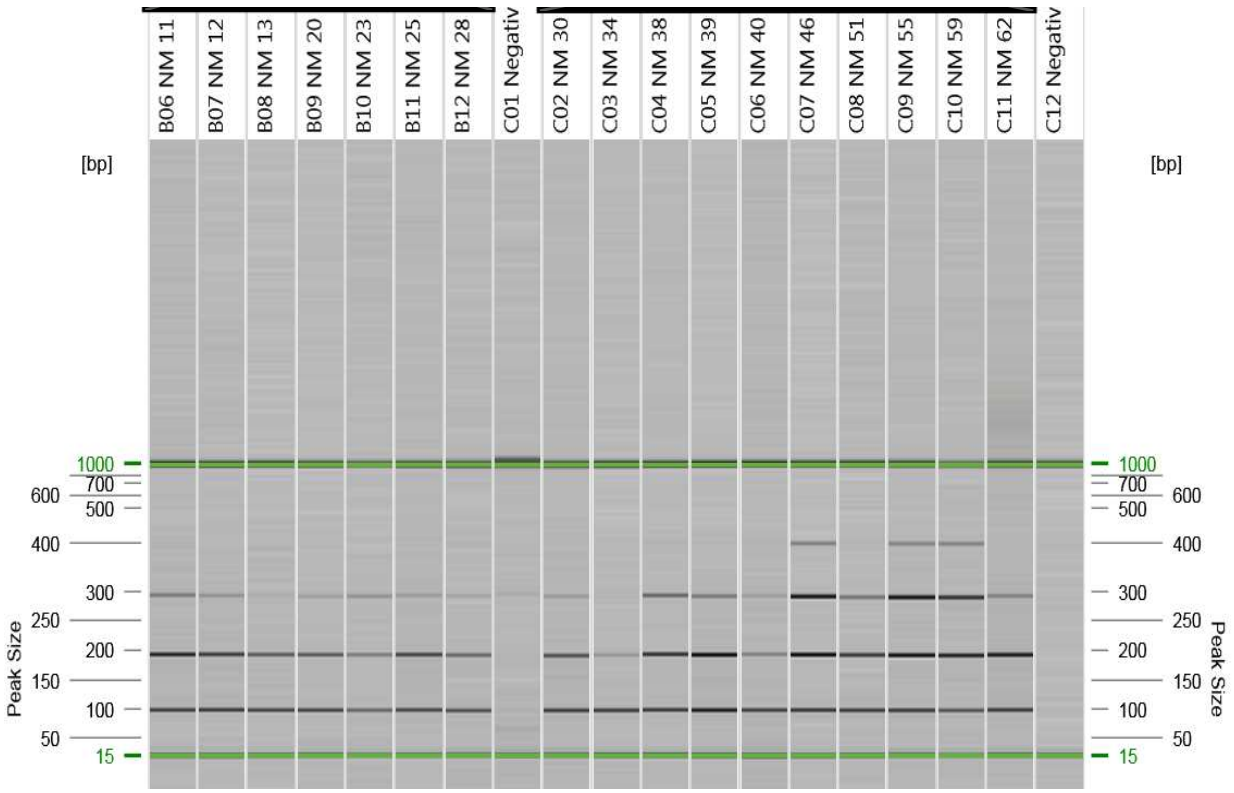

Figure 7 Representative picture of product sizes visualized by QIAxcel ScreenGel 1.4.0. After PCR had been performed on the extracted DNA, products were transferred into QIAxcel where gel electrophoresis took place completely automated. Results could be viewed digitally. As an example, a picture of representative results are shown above. While C01 and C12 are non-template controls with water, the other columns show 17 different samples. Green lines mark maximum (1000) and minimum (15) bp size readable. While some samples show a peak size of 200bp, others are of higher integrity with a peak size of 400bp.

3.5 Genetic Analysis

On 50 samples from a total of 49 patients, NGS was conducted. With the help of the Integrative Variant Caller Software, possible mutations were analyzed from the amplicon library data and displayed with the Integrative Genomics Viewer (IGV). An example is shown in **Figure 8**. 45/50 samples (90%) were analyzed successfully while 5/50 (10%) could not be evaluated due to poor data quality. The remaining 45 cases were separately reviewed concerning all 78 genes listed in **Table 1** above. Since the relevant genes *PTPRD*, *TBL1XR1* and *NLRP14* were not covered in the customized panel, relevant cases were examined with another, already existing panel originally designed for pediatric marginal zone lymphoma containing these genes. It is visualized in **Table 2**. This was pipetted by lab technicians with routine lab work and evaluated by Vanessa Borgmann. The results of both panels are listed in **Table 4**. Since the genes *KLF2*, *BRAF* and *TET2* were part of both panels, some mutations in these genes could be confirmed in 10 cases. The number of mutations per case varied between 0 and 9 with an average of 2.6 mutations per case. Mutations were found in 39 samples (87%). The coverage of the mutations detected varied in a range from 254 to 122577 with an average coverage of 4884 per gene mutation. Concerning allelic frequency, the values varied between 3% and 74% with a mean frequency of 31 per mutation. 6 samples (13%) did not show any mutations in examinated genes and are labeled as wildtypes.

In 42/78 genes, mutations were detected in one or more cases, while 36/78 genes were not mutated in any of the cases. A detailed table with all genetic findings, their locus and DNA integrity values is illustrated in **Table 4**.

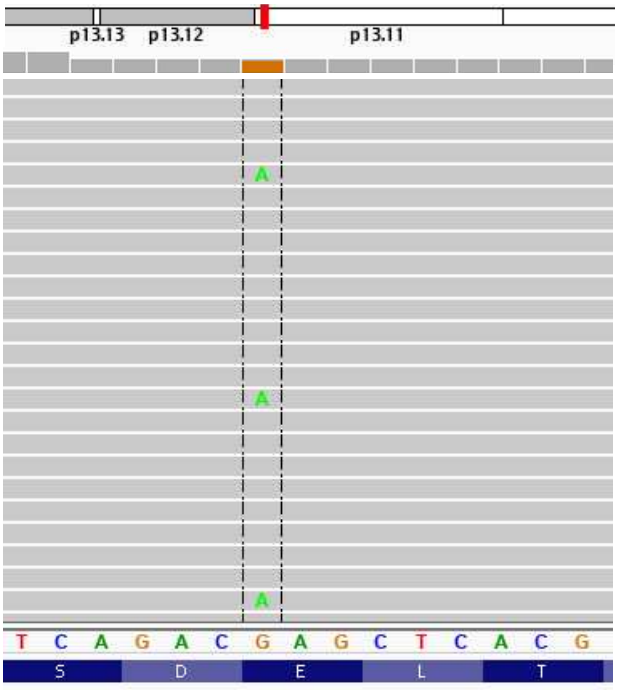

chr19:16.437.726

Total count: 457
A: 37 (8%, 21+, 16-)
C: 0
G: 420 (92%, 207+, 213-)
T: 0
N: 0

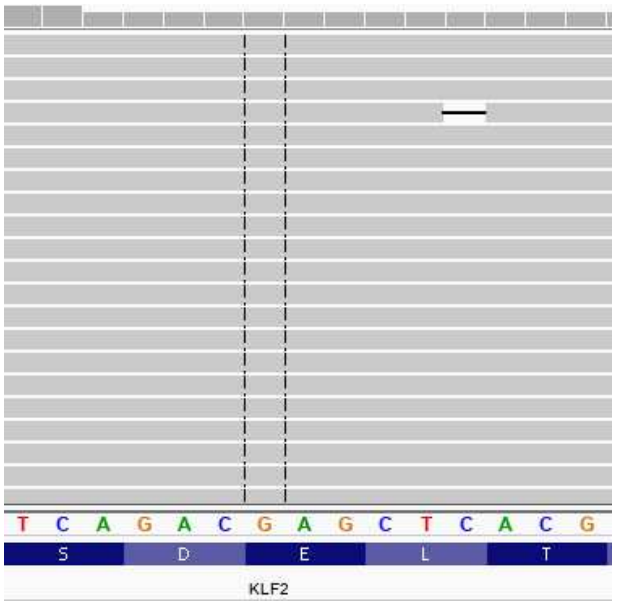

chr19:16.437.726

Total count: 761
A: 0
C: 0
G: 761 (100%, 333+, 428-)
T: 0
N: 0

Figure 8 Representative mutational finding in the Integrative Genomics Viewer (IGV). Shown is a locus of the *KLF2* gene of two different cases. A chromosome map is displayed at the top of the image, the red line marks the current locus. A *KLF2* mutated case is shown at the top, a non-mutated case at the bottom for comparison. The horizontal gray lines each show a sequence read. These are compared with the sequence of the reference genome hg19, which is shown in the colored letters at the bottom of the images. The white letters in the blue bar below the colored letters show which amino acid the 3 bases code for. If a different base is read than the reference genome, the letter of the base can be seen in color in the gray bars, in this example the base is adenine (A). Next to the graphs the exact chromosomal location, the number of amplicon reads and how often the corresponding base was read is listed. The plus and minus signs in the brackets show the distribution of reads in sense (+) and antisense (-) strands. The example above shows a variant with an Adenine (A) bult in instead of Guanine (G) in 8% of the reads, which results in a KLF2 mutation.

Table 4 Genetic variants. For each case, DNA integrity and all mutational findings are with gene name, locus, change on cDNA and protein level, coverage and allelic frequency. If a variant has been verified and how is listed on the very right. The 6 wildtype cases (NM8, 38, 45, 48, 54, 60) are not listed since no mutations were detected.

Sample ID	DNA Integrity	Gene	Chr	Position (hg19)	cDNA change	Protein change	Coverage	Allele frequency	Verification
NM3	200bp	*TP53*	17	7578222-7578223	c.626_627del	p.R209Kfs*6	2447	42	
		TP53	17	7578203	c.646G>A	p.V216M	2461	38	
NM5	400bp	*TBL1XR1*	3	176755901	c.1107C>G	p.D369E	5297	13	
NM6	300bp	*ATM*	11	108183212	c.5993G>T	p.G1998V	3528	58	
		MYD88	3	38182641	c.794T>C	p.L265P	1946	43	
NM7	200bp	*KMT2D*	12	49441774	c.4210T>G	p.Y1404D	2448	33	
		CREBBP	16	3788606	c.4348T>G	p.Y1450D	6506	40	
		KMT2D	12	49427093	c.11395C>T	p.Q3799*	679	55	
		MYC	8	128750938	c.475C>T	p.L159F	4719	55	
		TP53	17	7577115	c.823T>C	p.C275R	6891	70	
NM9	300bp	*POT1*	7	124482912	c.1112C>T	p.P371L	2996	8	single amplicon
		KLF2	19	16437726	c.952G>A	p.Q318K	456	8	single amplicon
NM10	300bp	*KLF2*	19	16436813	c.862C>A	p.H288N	3761	20	pMZL panel
		HLA-B	6	31324576	c.232C>T	p.Q78*	1723	22	
		TBL1XR1	3	176767799	c.688T>C	p.S230P	7882	49	
NM11	300bp	*NOTCH2*	1	120458147	c.7198C>T	p.R2400*	2072	39	
		KMT2D	12	49438241	c.5027del	p.P1676Lfs*46	4523	51	
		KLF2	19	16436711	c.761del	p.E254Gfs*36	1084	73	pMZL panel
		FAS	10	90771831	c.644T>A	p.L215*	802	40	
		TBL1XR1	3	176755899	c.1109A>G	p.D370G	4279	37	
NM12	300bp	*ID3*	1	23885677	c.241C>T	p.Q81*	5878	37	
NM13	300bp	*BCL10*	1	85742008	c.28G>A	p.E10K	3127	31	
		TRAF3	14	103371738	c.1324A>G	p.S442G	2706	12	
NM15	400bp	*NLRP14*	11	7064719	c.1462G>C	p.A488P	3926	22	
NM16	300bp	*CXCR4*	2	136872623-136872624	c.886_887dup	p.F296Sfs*2	3584	22	
		SOCS1	16	11349314	c.22G>C	p.A8P	1467	25	
		SOCS1	16	11348813	c.523C>T	p.Q175*	1032	33	
		SOCS1	16	11349071-11349079	c.257_265del	p.V86_G88del	2985	32	
		ID3	1	23885758	c.160C>G	p.L54V	6723	27	
		ID3	1	23885777	c.141C>A	p.C47*	6701	29	
		ARID1A	1	27023408	c.514C>T	p.Q172*	254	32	
		ARID1B	6	157522485	c.5006C>T	p.T1669M	3506	48	
		TBL1XR1	3	176765158	c.794A>C	p.H265P	1462	48	
NM19	600bp	*TRAF3*	14	103338283-103338284	c.275_276del	p.Q92Rfs*5	1733	12	
		TRAF3	14	103336551-103336560	c.14_23del	p.K5Tfs*12	1043	14	
		TRAF3	14	103342009-103342017	c.346_354delinsA	p.Y116Kfs*2	1420	12	
NM20	300bp	*TNFRSF14*	1	2491271-2491272	c.316_317insCGC	p.L105_R106insP	2270	14	
		STAT6	12	57496661	c.1256A>G	p.D419G	908	14	
		CREBBP	16	3781324-3781326	c.5039_5041del	p.S1680del	2222	33	
NM22	400bp	*KMT2D*	12	49432710	c.8429del	p.L2810Yfs*41	2496	29	
		CREBBP	16	3788633	c.4321del	p.R1441Gfs*18	10241	31	
		KMT2D	12	49434844	c.6709C>T	p.Q2237*	2670	31	
		ARID1A	1	27094367	c.3076del	p.R1026Vfs*13	1727	32	
		FAS	10	90773105-90773106	c.657_658del	p.V220Gfs*6	4295	30	
NM23	300bp	*BCL10*	1	85733594	c.418G>T	p.E140*	9835	19	
NM24	400bp	*TNFAIP3*	6	138196171	c.486del	p.N163Tfs*53?	6184	17	
		NOTCH2	1	120480519	c.3298G>A	p.V1100M	3752	50	
NM25	300bp	*MYD88*	3	38182641	c.794T>C	p.L265P	3995	45	
		SMARCA4	19	11094928	c.101C>T	p.P34L	2375	55	
NM27	400bp	*MYD88*	3	38182641	c.794T>C	p.L265P	2973	37	
		BTG2	1	203274789	c.55T>C	p.F19L	3233	39	
		TP53	17	7578370	c.559+1G>A	p.?	1441	57	
NM28	300bp	*TMSB4X*	X	12994364	c.-16-1G>C	p.?	8395	27	
		ARID1B	6	157527866-157527866	c.5843_5844del	p.S1948*	4212	30	
		CREBBP	16	3799626	c.3836+2T>G	p.?	2322	30	
		CREBBP	16	3794922	c.3955C>T	p.R1319*	3276	36	

		KLF2	19	16435804	c.70C>T	p.Q24*	485	38	pMZL panel
		KMT2D	12	49432409-49432412	c.8727_8730del	p.S2910Rfs*32	3645	39	
		FBXW7	4	153249384	c.1394G>C	p.R465P	5640	34	
NM30	300bp	*SPEN*	1	16258748	c.6013A>T	p.K2005*	2124	34	
		MYD88	3	38182025	c.649G>T	p.V217F	11005	38	
		KLF2	19	16436837	c.886C>T	p.H296Y	5141	41	pMZL panel
NM31(1)	300bp	*STAT6*	12	57496654	c.1263T>A	p.N421K	1050	23	
		JAK3	19	17945385	c.2345C>T	p.S782F	849	46	
		SPEN	1	16259847	c.7112A>G	p.E2371G	3290	74	
NM31(2)	600bp	*CXCR4*	2	136873272	c.238T>G	p.Y80D	6235	7	single amplicon
		MYC	8	128750595	c.132G>C	p.E44D	5774	10	
		MYC	8	128750938	c.475C>G	p.L159V	7734	21	
		SPEN	1	16259847	c.7112A>G	p.E2371G	4579	30	
		STAT6	12	57498345	c.1114G>A	p.E372K	2880	30	
		TNFRSF14	1	2491376-2491385	c.421_430del	p.Y141Pfs*46	2719	46	
		JAK3	19	17945385	c.2345C>T	p.S782F	1432	49	
NM32	400bp	*KMT2D*	12	49423207-49423208	.14051_14052insC	p.H4685Lfs*113	4104	28	
		TET2	4	106180895	c.3923A>C	p.K1308T	3080	51	pMZL panel
		PTPRD	9	8376677	c.4436T>G	p.L1479R	15098	34	
NM33	400bp	*SOCS1*	16	11349329	c.7G>A	p.A3T	1943	10	
		CREBBP	16	3788647	c.4307G>T	p.S1436I	12379	10	
		KMT2D	12	49428071	c.10519C>T	p.Q3507*	3880	11	
		CREBBP	16	3841994	c.1318C>T	p.R440*	5711	11	
		TNFAIP3	6	138192400	c.36G>C	p.L12F	3455	14	
		STAT6	12	57498344	c.1115A>C	p.Q372A	2754	24	
NM35	300bp	*KMT2D*	12	49427555	c.10933C>T	p.Q3645*	1586	18	
		SPEN	1	16262741	c.10006C>T	p.R3336W	1098	51	
		KLF2	19	16436062-16436084	c.111_133del	p.D38Gfs*49	492	16	pMZL panel
NM39	300bp	*KRAS*	12	25398255	c.64C>A	p.Q22K	1940	24	melanoma panel
		ATM	11	108206607	c.8187A>T	p.Q2729H	2045	45	
		ARID1A	1	27023620-27023621	c.735_737dup	p.A247dup	399	45	
		BRAF	7	140481402	c.1406G>C	p.G469A	9925	4	melanoma panel
NM41	400bp	*ETV1*	12	12037427	c.1058G>A	p.R353Q	9159	72	
		BTG1	12	92538139	c.233C>T	p.P78L	2454	7	single amplicon
NM44	400bp	*MYD88*	3	38182641	c.794T>C	p.L265P	3096	18	
NM46	400bp	*BIRC3*	11	102201966-102201967	1318_1319insGATT	p.E440Gfs*9	938	18	
		TNFRSF14	1	2489816	c.215del	p.G72Afs*19	1652	42	
		KMT2D	12	49437653	c.5317C>T	p.Q1773*	848	47	
		STAT6	12	57496662	c.1255G>A	p.D419N	939	48	
		EZH2	7	148508728	c.1936T>A	p.Y646N	12202	25	
NM47	300bp	*KLF2*	19	16437726	c.952G>A	p.E318K	4469	4	pMZL panel
		KLF2	19	16436843	c.892G>A	p.G298S	741	3	pMZL panel
NM51	300bp	*KMT2D*	12	49437439	c.5446G>T	p.E1816*	3500	33	
		H1-4	6	26157108	c.490G>A	p.A164T	5160	15	
		KMT2D	12	49421791	c.14515+1G>A	p.?	1277	30	
NM52	400bp	*CD79B*	17	62006812-62006813	c.575dup	p.E193Gfs*11	5441	39	
NM53	600bp	*MYD88*	3	38182025	c.649G>T	p.V217F	2970	27	
NM55	400bp	*KLF2*	19	16436832-16436850	c.881_892+7del	p.?	122577	11	pMZL panel
		CREBBP	16	3832819	c.1439C>T	p.S480F	3760	12	
		NFKBIA	14	35873653	c.198G>A	p.W66*	5788	15	
		NFKBIA	14	35873646	c.205C>T	p.Q69*	6648	16	
		H1-4	6	26157108	c.490G>A	p.A164T	7780	24	
		H1-4	6	26157106	c.488C>T	p.A163V	7786	25	
		TNFRSF14	1	2494577-2494584	c.727-9_728del	p.?	8163	15	
		TBL1XR1	3	176750787	c.1388A>C	p.D463A	4388	14	
NM56	400bp	*ARID1A*	1	27105676-27105678	c.5299_5301del	p.E1767del	5303	52	
NM57	300bp	*NOTCH1*	9	139438549-139438550	c.66_67delGCinsTT	p.R23*	3238	7	single amplicon
		ATM	11	108201008	c.7375C>G	p.R2459G	4799	34	
		CXCR4	2	136872471	c.1039G>T	p.E347*	2165	18	
		NLRP14	11	7064597	c.1340T>A	p.L447H	5035	49	
NM59	400bp	*EZH2*	7	148508727	c.1937A>T	p.Y646F	7351	18	
		BRAF	7	140453133	c.1799T>A	p.V600E	6316	40	pMZL panel
NM61	400bp	*BIRC3*	11	102201943-102201944	c.1296dup	p.E433Rfs*5	1021	32	
NM62	400bp	*KMT2D*	12	49426285	c.12203C>G	p.S4068*	1816	9	

3.6 Integrative Results of Immunohistochemistry and Genetic Findings

By combining the molecular biological and histological data collected, the cases were assigned into different groups. In 29 cases, the diagnosis of NMZL was confirmed. 11 of the cases were reassigned to either FL (6 cases) or CLL (5 cases), and 5 remained that could not be assigned to any of the 3 aforementioned entities. The 29 cases of NMZL were further subdivided in 3 subtypes: the classic NMZLs (22 cases), the NMZLs with splenic type (3 cases) and the CD5+ NMZLs (4 cases). These groups are described separately below.

3.6.1 Immunohistochemical and Genetic findings in the NMZL Group

The diagnosis of NMZL was confirmed in 29 cases. This group was divided into 3 subgroups: classic type NMZL (22/29, 76%), splenic type NMZL (3/29, 10%) and CD5 positive cases (4/29, 14%).

Immunohistochemical analysis: All cases in this group were CD20 positive. Four of the cases were CD5 positive, corresponding to the subgroup of CD5 positive NMZL. CD3 was negative in the neoplastic cells in almost all (28/29, 97%) samples, only in one case there was a weak aberrant expression in the tumor cells. CD23 was stained in 27/29 cases, only one was positive. The CD23 positive sample showed CD5 negativity. CD10 was negative in all samples performed (25/29). BCL6 was stained in 24 of the cases, showing mild positivity in 4 cases, one was difficult to assess, and 19 cases were BCL6 negative. BCL2, on the other hand, was positive or slightly positive in 88% (21/24) of the cases, while one case was unclear and 2 were negative. IgD was performed on 26 of the 29 tumor samples, and was negative in 15 (58%), and positive in 11 (42%). The proliferation rate, as demonstrated with MIB-1 staining, mostly showed a rate of 5-10%, with an overall range between 1 and 30%. An example of histology and immunohistochemistry, one of each subgroup, is visualized in **Figures 9-11** below.

Genetic analysis: The most frequent mutation identified in this group was *KLF2*, which was present in 8/29 cases (28%) and could not be found in any of the other groups. It was striking that 88% (7/8) of this mutation occurred in women and only

12% (1/8) in men. One of these cases showed two *KLF2* mutations. The allelic frequency varied from 4% to 73% (median: 16%).

The second most frequent mutation in this group was *KMT2D*, which was mutated in 7/29 cases (24%), the allelic frequency varying between 9% and 51% (median: 31%). In two of these 7 cases, 2 mutations were identified per case with similar allelic frequencies. *KMT2D* mutations were also found in 50% (3/6) of the FL cases.

The next most common mutated genes in this group were *TBL1XR1* and *MYD88*, which were found to be mutated in 4/29 (14%) cases each. For *TBL1XR1* the median allelic frequency lied at 42,5% with a range from 14% to 49% while for *MYD88* it was 32% with a range from 18% to 38%.

Genes *ARID1A* and *CREBBP* were mutated in 3 cases (10%) each. Concerning *SPEN, NOTCH2, BCL10* and *HIST1H1E* we found mutations in 2 cases each.

Only 2 cases (7%) carried *TRAF3* mutations, and it was remarkable that these were both CD5 positive. Moreover, *ARID1B, ID3* and *FAS* mutations were demonstrated in 2 cases (7%) each, all being part of the classic-type NMZL subgroup. Concerning the following genes, mutations were found in only one case each: *PTPRD, CXCR4, EZH2, BRAF, STAT6, TNFRSF14, ATM, TP53, BIRC3, NLRP14, SOCS1, TNFAIP, BTG2, BTG1, ETV6, FBXW7, HLA-B, NFKBIA, POT1, TET2, TMSB4X, NOTCH1*. An overview of mutant genes is shown in the matrix below (**Figure 12**).

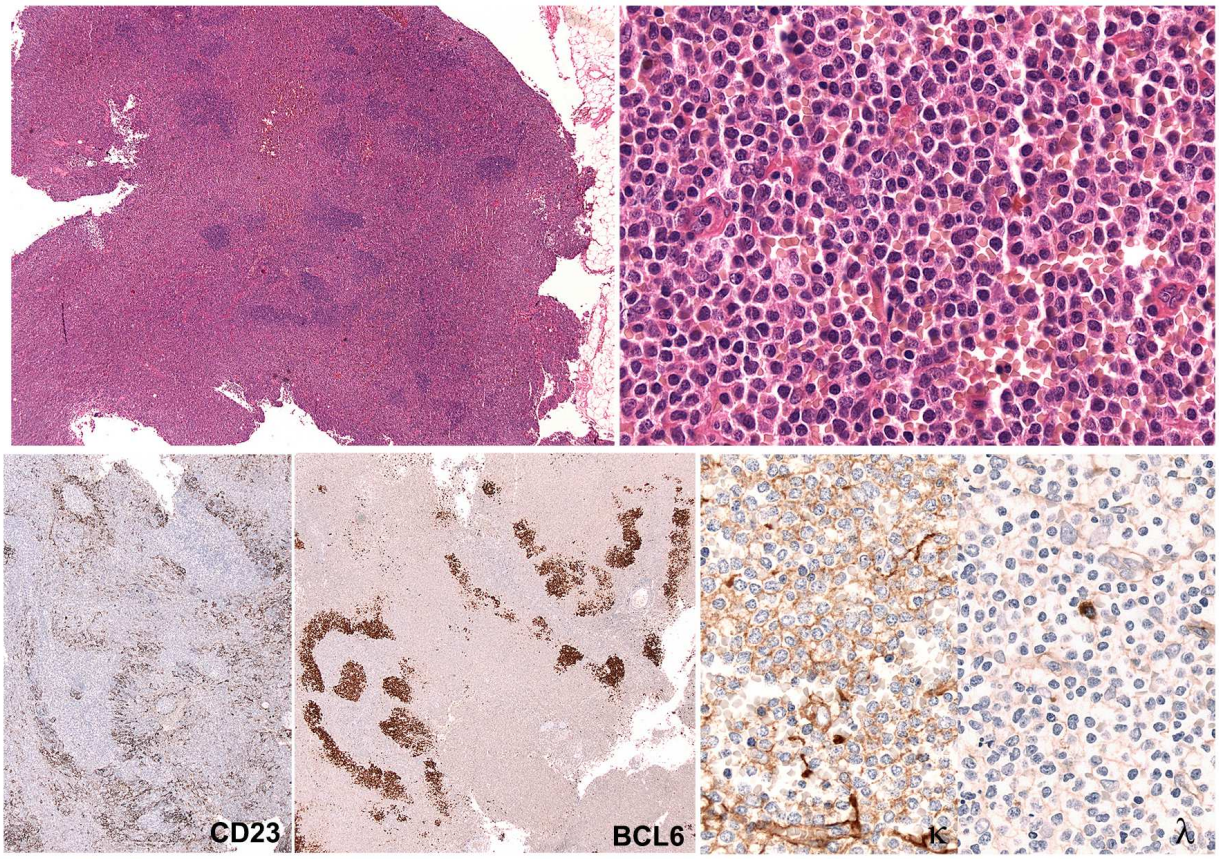

Figure 9 Representative histology and immunohistochemical stainings of NMZL (NM11). The top left picture shows an overview image of the sample. The lymph node architecture is disrupted, showing a predominantly monotonous proliferation with interspersed follicular structures. Top right is a higher magnification showing numerous monotonous cells with relatively dense chromatin and partially plasmacytoid morphology. The CD23 staining is shown at the bottom left; the neoplastic cells are negative, but irregularly configured FDC (follicular dendritic cells) networks can be observed. The BCL6 staining at the bottom center shows the residual germinal centers cells and the colonized germinal centers by BCL6 negative tumor cells. There is kappa light chain restriction.

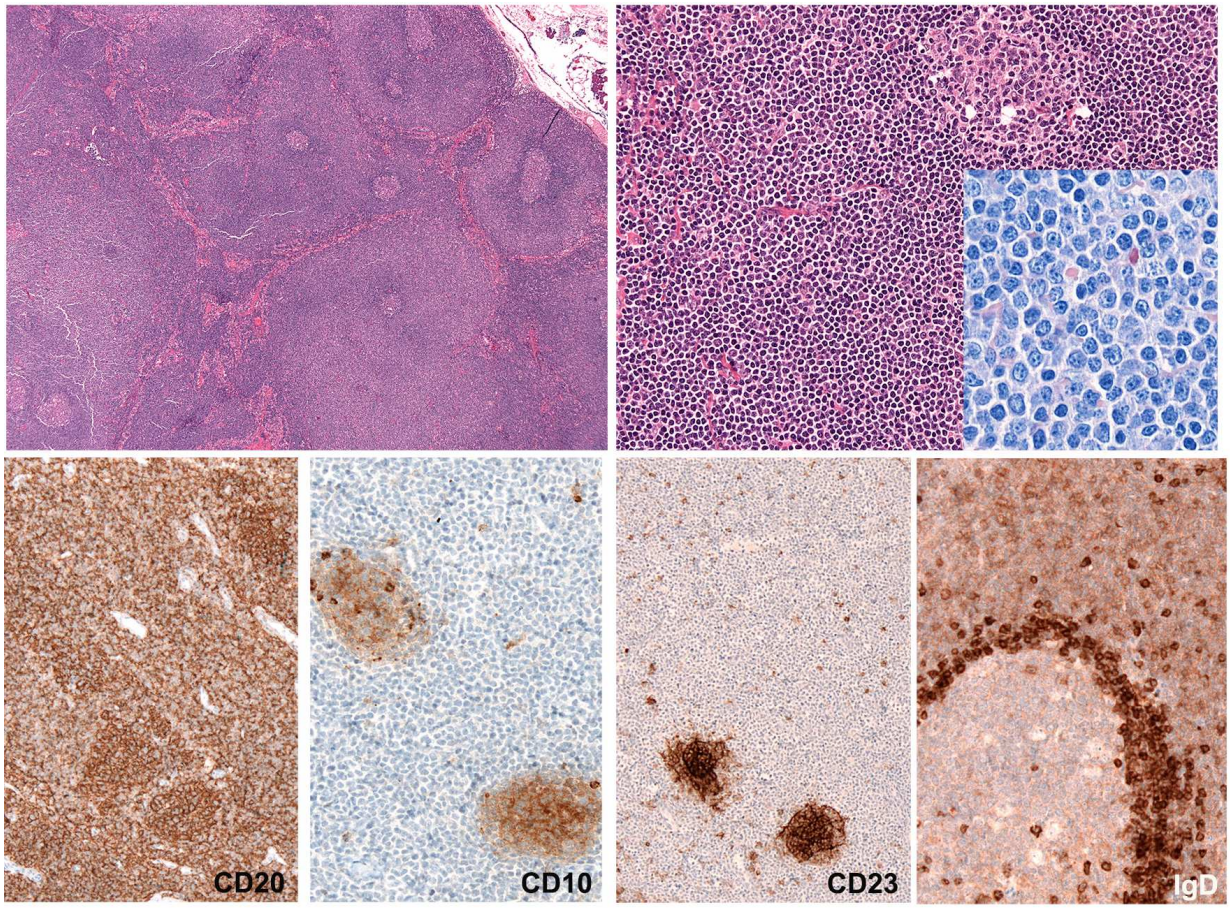

Figure 10 Representative histology and immunohistochemical stainings of splenic type NMZL (NM56). In the overview image at the top left, a lymph node with a nodular pattern can be seen, containing small, regressive-looking germinal centers with an expanded marginal zone. The magnified image to the right shows the expanded marginal zone with monotonous, rather small cells with mature chromatin. In the Giemsa stain, the slightly loosened chromatin and small nucleoli can be observed. In the CD20 staining at the bottom left, the neoplastic cells stain positively. The CD10 staining marks the small germinal center structures, the remaining cells are negative. CD23 reveales the follicular dendritic cell networks in the small regressive germinal centers, the marginal zone remains negative. IgD stains the cells of the mantle zone strongly positive and the neoplastic cells.

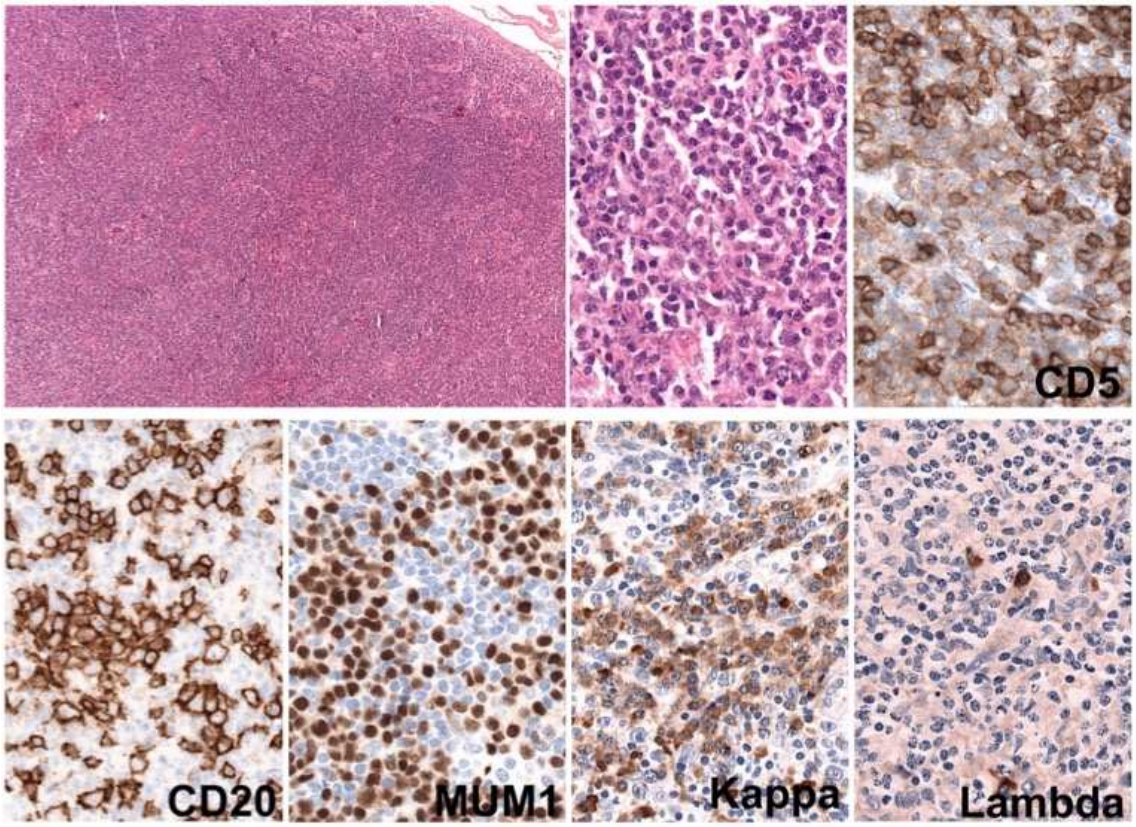

Figure 11 Representative histology and immunohistochemical stainings of CD5 positive NMZL (NM10). The overview at the top left shows a lymph node with an effaced architecture and a relatively diffuse pattern. The higher magnification upper left shows cells with mature, clumped chromatin with small, inconspicuous nucleoli, overall a monotonous image with only some interspersed larger cells. Individual cells show plasmacytoid differentiation. CD5 in the upper right corner shows a strong positive staining of the T cells and a weak positive aberrant co-expression of the B cells. CD20 bottom left shows some B cells; MUM1 shows many positive cells, indicating plasmacytoid differentiation of the cells. The kappa and lambda stainings show kappa light chain restriction.

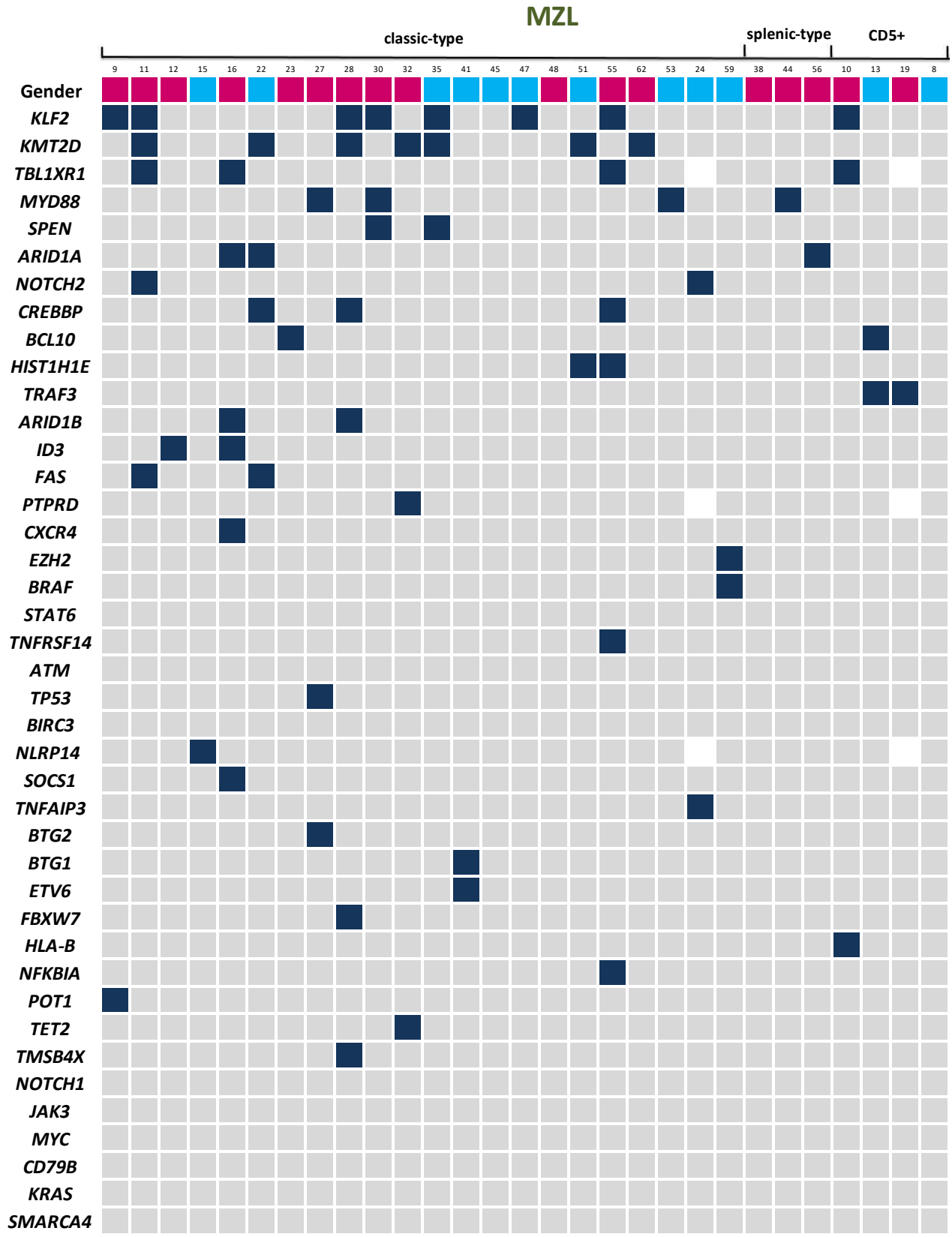

Figure 12 Mutated Genes in the NMZL samples sorted into the 3 subgroups. Each column represents one of the cases, on the left the genes are listed according to the frequency of mutations. A dark blue box means that the case carries a mutation in the respective gene, gray that we detected none and blank boxes indicate that the gene was not analyzed in this case. The cases are divided into their subgroups; at the top the sex of the patient is coded by pink = female and blue = male.

3.6.2 Genetic and immunohistochemical findings in the FL Group

Prior to genetic analysis, FL was entertained as a differential diagnosis in 17 of 45 samples. After immunohistochemical and genetic analysis, 6 cases could be diagnosed as *BCL2* translocation negative FLs.

Immunohistochemically, all 6 cases were CD20 positive and CD3 and CD5 negative. CD23 and CD10 were each positive or slightly positive in 4/6 samples and negative in 2 cases. BCL6 staining was performed on all 6 biopsies, but 2 were difficult to assess while 3 were positive and one negative. One case expressed neither CD10 nor BCL6 but was positive in the BCL2 staining. BCL2 was slightly positive or positive in 3 of the 4 stained cases, one was negative. The IgD staining was negative in all samples. MIB-1 demonstrated a proliferation rate between 5 and 40%. An example of histology and immunohistochemistry is visualized in **Figure 13**.

It was remarkable that none of these cases carried a *KLF2* mutation, which was the most common mutated gene in NMZL. While in the NMZL group, *KMT2D* was the second most mutated gene (24% of all cases), it was also found mutated in 3/6 (50%) cases of FL. One of these cases showed 2 *KMT2D* mutations. The median allelic frequency varied between 11% and 55%, its median frequency being 40%.

However, the most frequent mutated gene was *STAT6*, present in 4/6 (67%) of the cases, allelic frequency varying between 14% and 48% (median: 23,5%). All these cases also expressed CD23. In 50% of the samples (3/6), *CREBBP* was mutated with an allelic frequency ranging between 10% and 40 % (median: 22%). In one case, 2 *CREBBP* mutations were detected. In the group of NMZL, CREBBP mutations were identified in 3/29 of the cases (10%).

In 2/6 FL cases (33%), mutations within *TNFRSF14* could be detected, this only applied to one case of the NMZL group. Concerning the genes *SPEN, EZH2, TP53, BIRC3, SOCS1, TNFAIP3, BTG2, JAK3, MYC and CD79B,* mutations were only found in one or two cases each.

An overview of mutant genes is shown in the matrix below (**Figure 14**).

After diagnosis, the question was raised of whether the FL cases carried the typical t(14;18) chromosomal translocation and could therefore have been identified directly if suspected. Therefore, analysis with break apart probes (BAP) was performed by Barbara Mankel for *BCL2* to detect a possible translocation. In none of the 6 cases a *BCL2* translocation has been found.

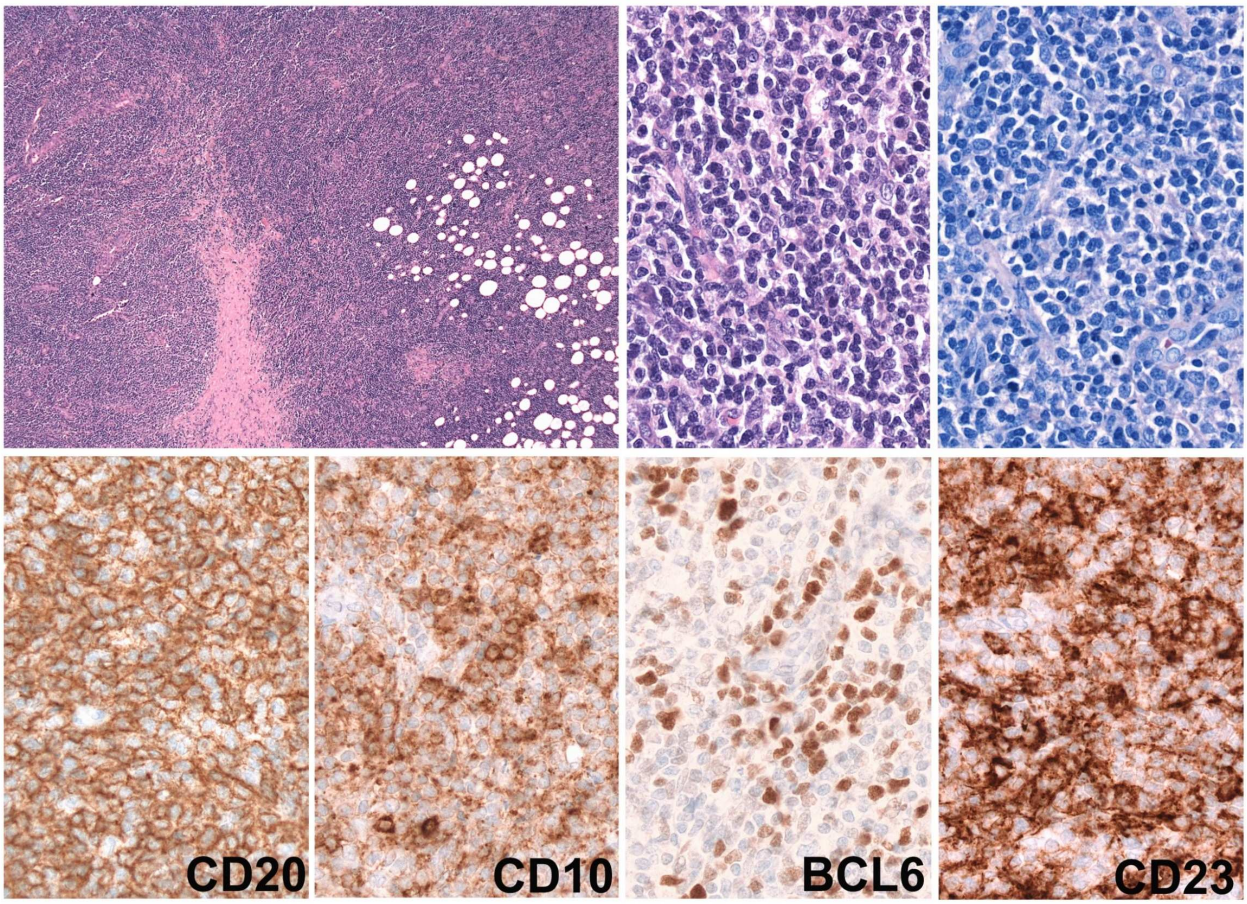

Figure 13 Representative histology and immunohistochemical stainings of FL (NM20). The overview image at the top left shows a diffuse infiltration of a lymphatic population in the lymph node. The two images top right with higher magnification show small to medium sized centrocytoid cells with slightly loosened chromatin with partially irregular nuclei. The CD20 and CD10 staining at the bottom left are positive, BCL6 at the bottom center is heterogeneously positive. The staining at the bottom right reveals aberrant CD23 coexpression of the tumor cells.

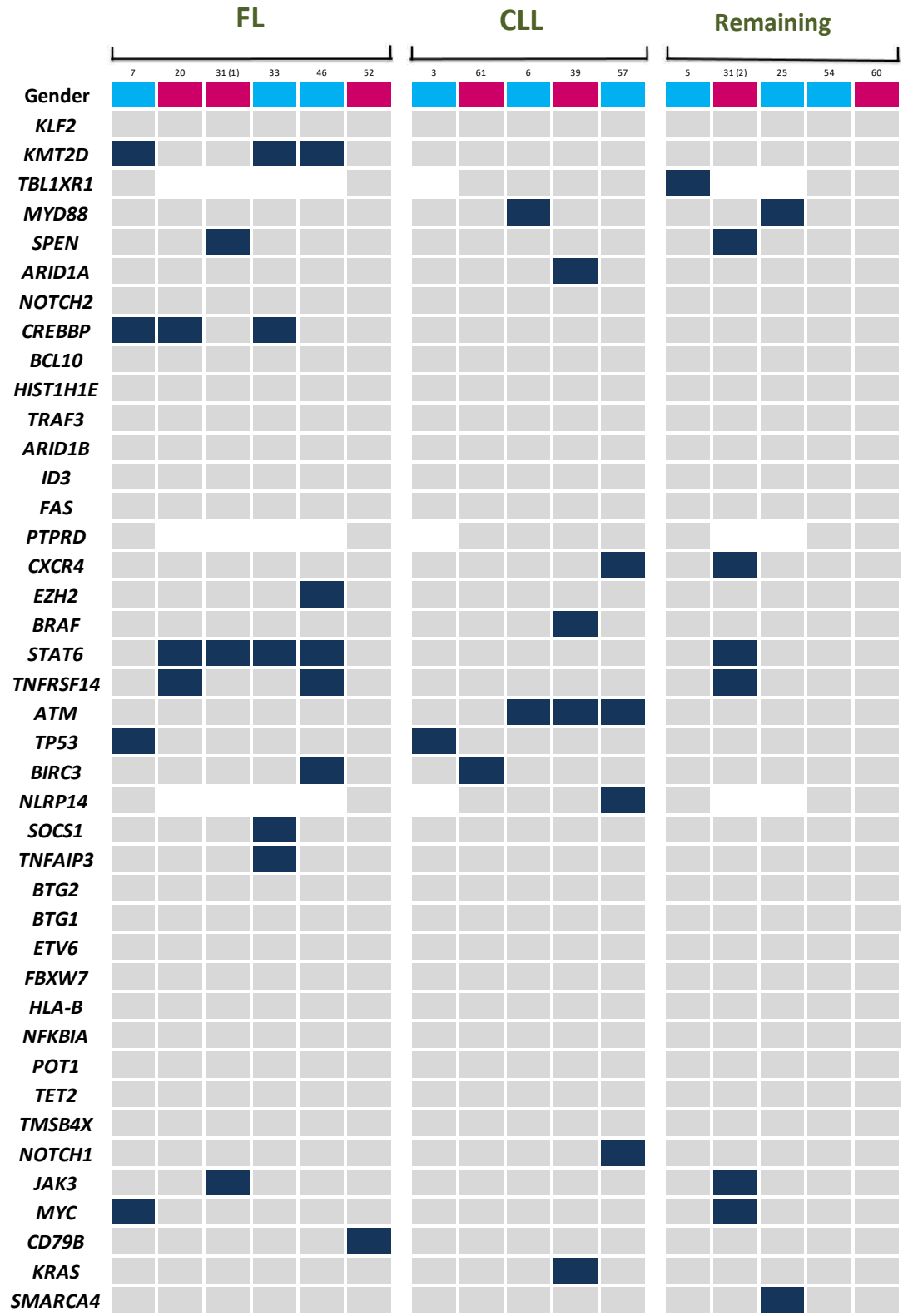

Figure 14 Mutated genes in the FL and CLL group and of the remaining cases. Samples are sorted into their assigned group: FL, CLL and remaining cases. Diagnosis of the remaining cases is explained in detail below. At the top the sex of the patient is coded by pink = female and blue = male. All mutated genes are listed on the left. Dark-blue boxes show that the gene was found mutated in the respective case, gray that we detected none. Blank boxes clarify that these genes were not examined on that sample.

3.6.3 Genetic and immunohistochemical findings in the CLL Group

Before NGS analyses, a differential diagnosis of CLL was considered in 8 cases. After the comprehensive assessment, 5 cases were ultimately classified as a CLL with aberrant immunohistochemical expression pattern.

First of all, the immunohistochemical results. The CD20 and BCL2 staining was positive in all 5 cases while CD3, CD10 and BCL6 were negative in all samples. Furthermore, we observed negative staining for CD23 in 4 of the 5 cases, with only one showing slight positivity. CD5 was slightly positive or positive in 3 of the cases and negative in the two remaining. IgD staining was also performed on all 5 cases, with one IgD negative and 4 slightly positive or positive tumor samples. Using MIB-1, we determined a proliferation rate between 5% and 20%. An example of histology and immunohistochemistry is visualized in **Figure 15**.

Concerning their mutational profile, none of the cases showed mutations in genes *KLF2* and *KMT2D,* which were typical for NMZL. Instead, 60% of the cases (3/5) revealed *ATM* mutations with an allelic frequency ranging between 34% and 58%. Furthermore, mutations in genes *MYD88, ARID1A, CXCR4, BRAF, TP53, BIRC3, NLRP14, NOTCH1* and *KRAS* could be detected in one case each.

An overview of mutant genes is shown in the matrix above (**Figure 14**).

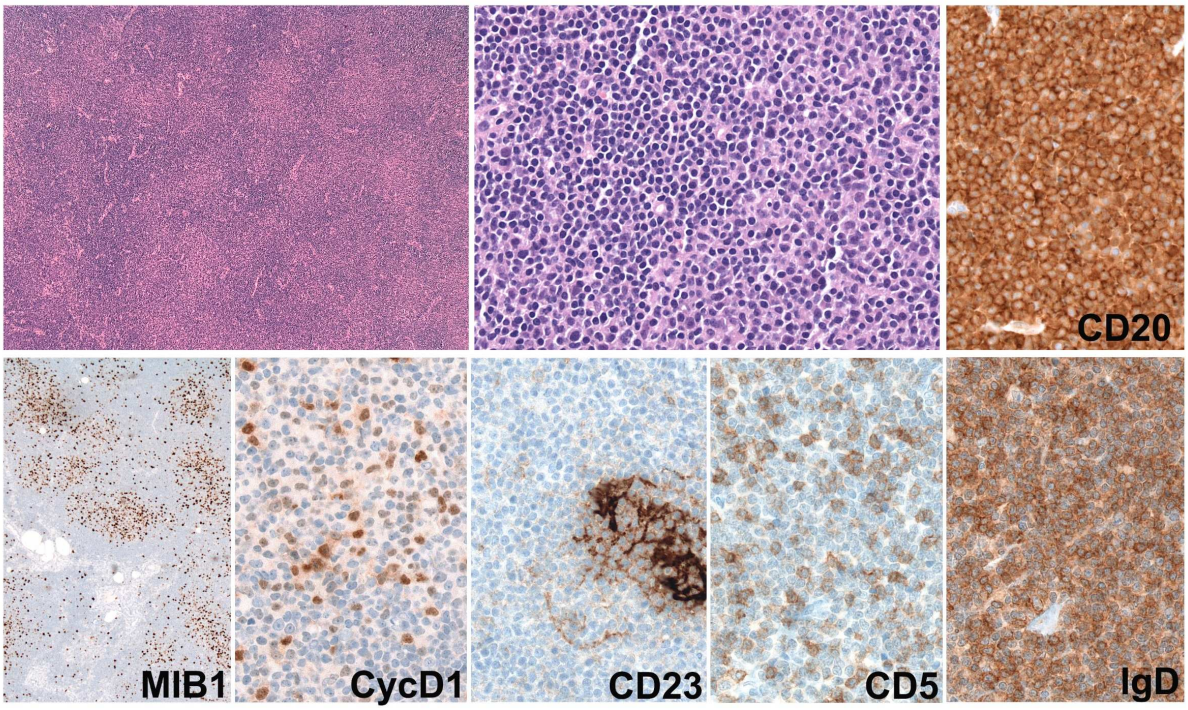

Figure 15 Representative histology and immunohistochemical stainings of CLL (NM39). In the overview image at the top left, a vaguely nodular pattern characteristic of proliferation centers. At a higher magnification in the top center of the figure, a monotonous population of small lymphoid cells (CLL) and some medium-sized cells “paraimmunoblasts and prolymphocytes” can be recognized in the proliferation centers.. The CD20 staining on the top right is positive. The MIB-1 staining on the lower left shows increased proliferative activity in the proliferation centers. CyclinD1 (CycD1) staining shows no aberrant expression of this marker in the tumor cells, however, some cells in the proliferation centers and the endothelial cells are positive. CD23 is also negative in the neoplastic cells. There is no clear co-expression of CD5, only T-cells stain positively. The staining at the bottom right indicates IgD expression of the tumor.

3.6.4 Remaining cases

Five cases were analyzed but could not be further classified into one of the well-recognized discrete entities. Immunohistochemically, all 5 cases were CD20 positive and CD3 and CD5 negative.

NM5 only showed one mutation in total in *TBL1XR1* with an allelic frequency of 13%. Combined with its histological picture, a possible differential diagnosis considered was a pediatric-type –FL.

Case NM25 carried a *MYD88* mutation. Retrospectively the morphology and immunophenotype, together with the molecular results confirmed the diagnosis of lymphoplasmacytic lymphoma. In addition to *MYD88*, *SMARCA4* was found mutated.

NM 31(2) was diagnosed as a DLBCL, and was included in the study since the patient had a questionable NMZL before, which raised the possibility of transformation (31(2). NM31(1) was finally diagnosed as a follicular lymphoma, BCL2-*R* negative transformed to 31(2) DLBCL. The two tumors had three shared mutations including *SPEN*, *STAT6* and *JAK3*. Additionally, the DLBCL acquired 3 private mutations during transformation (*TNFRSF14, CXCR* and *MYC)*.

Cases NM54 and NM60 were wildtype, as no mutations could be detected in any of the exanimated genes. The final diagnosis in these two cases remained elusive.

3.7 Examination of normal tissue

Many variants showed an allelic frequency of around 50%, which makes them suspicious for being germline variants. Non-hematopoietic tissue was available in 3 cases. DNA was extracted from these and NGS conducted using the Oncomine Lymphoma Panel III (**Table 4**). In case NM46, the *TET2* mutation, which was found in the lymphoma tissue with a VAF of 53% was also present in the associated healthy tissue. Suspicious *KMT2D* and *STAT6* variants of NM61 existed in both lymphoma and normal tissue with comparable VAFs. Furthermore, the prediction of Varsome suggested benign moderate, benign supporting or benign strong for these variants. However, the Minor Allelic Frequencies (MAF) are quite low, meaning the variants do not occur frequently in the population. In conclusion, despite the low MAFs, these variants are likely indicative of infrequent SNPs. Concerning the two *H1-4* mutations in NM55, they could not be detected in the patient's normal tissue. These variants could be interpreted as tumor-specific mutations which aligns with their low MAFs. Results are shown in **Table 5** below.

Table 5 Evaluation of germline variants. In 3 cases, DNA of non-hematopoietic tissue was extracted and evaluated using NGS. Samples derived from duodenum in 2 cases and mucosa of the tongue in the third case. Exanimated gene variants with locus, dbSNP rs-number, MAF (Minor Allelic Frequency) and Varsome predicition ("-" means Varsome was not checked) are demonstrated. In the last column, respective variant allelic frequency for both lymphoma and corresponding normal tissue are listed.

Sample ID	Gene	Tissue Type	Mutation	rs-Number dbSNP	MAF	Varsome predicition	Allele frequency
NM46	*TET2*	Lymphoma	p.P985S c.2953C>T	rs1053689215	T=0./0 (ALFA)	Beningn moderate	53
		Duodenum	p.P985S c.2953C>T				50
NM55	*H1-4*	Lymphoma	p.A163V c.488C>T	rs748517682	T=0.000071/1 (ALFA)	-	25
		Mucosa tongue	p.A163V c.488C>T				not found
	H1-4	Lymphoma	p.A164T c.490G>A	rs201935674	A=0.000031/1 (ALFA)	-	24
		Mucosa tongue	p.A164T c.490G>A				not found
NM61	*KMT2D*	Lymphoma	p.R746Q c.2237G>A	rs371911838	T=0.000054/1(ALFA)	Beningn strong	43
		Duodenum	p.R746Q c.2237G>A				31
	STAT6	Lymphoma	p.G397C c.1189G>T	rs372158354	T=0./0 (ALFA)	Bening supporting	64
		Duodenum	p.G397C c.1189G>T				45

4 Discussion

4.1 Summary of Results

In this thesis, a collective of 44 samples with diagnosis or differential diagnosis of NMZL was examined genetically and morphologically to explore NMZLs mutational landscape and distinguish the cases from phenotypically similar entities, mostly being FL and CLL. Additionally, we analyzed one DLBCL to examine whether it developed from a low-grade B-cell lymphoma, potentially NMZL. After analyzing all samples genetically and putting this information together with morphology and immunohistochemical data, cases were sorted into four groups: NMZL (29 cases), FL (6 cases), CLL (5 cases) and remaining cases (5 cases). NMZL has three subgroups being the typical NMZL, the CD5+ NMZL, and splenic type NMZL. Overall, the most commonly mutated gene was *KLF2*, which only occurred in the NMZL group, followed by *KMT2D, TBL1XR1, MYD88, SPEN, ARID1A, NOTCH2* and *CREBBP* for this group. A summarizing illustration of the mutations is shown in **Figure 16** below. Concerning the FL group, the majority of cases showed *STAT6* mutations as well as *KMT2D, CREBBP* and *TNFRSF14*. As for the CLL cases, the only mutation occurring in more than one case was *ATM.* The roles of the genes in the development of tumors as well as their importance for differentiating the entities will be discussed in detail below.

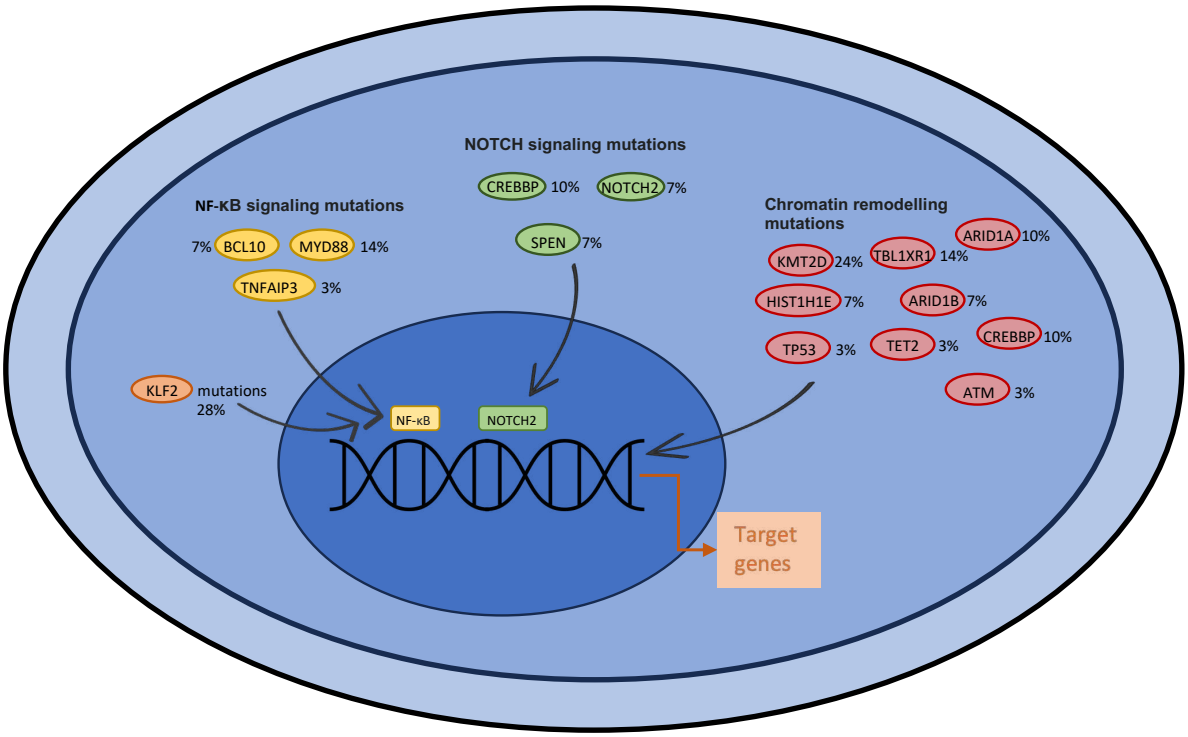

Figure 16 Summary of the main affected pathways in NMZL. The illustration schematically shows all pathways affected from mutations in our group of NMZL. Affected pathways in are displayed with the mutated genes listed underneath. The frequency of the mutation is featured next to each gene.

4.2 Patient Collective

4.2.1 Patient Characteristics

The first question is whether the patient collective of this study is representative concerning age and gender distribution compared to already published data. The median age at diagnosis of the final collective of 44 cases was 66 years. The median age at diagnosis of the 29 cases assigned to the NMZL group was 66 years as well. This seems to be in line with other studies where median age ranges between 50 and 64 (Arcaini et al., 2009, Khalil et al., 2014, Thieblemont et al., 2011). The gender distribution in the NMZL collective showed a female predominance with 17/29 females (59%) and 12/29 male patients (41%). Published data are equivocal since some studies observed a male predominance while others described female predominance. Nevertheless, a very recent review stated a male predominance in NMZL (Rossi et al., 2022), which we could not confirm in our research.

4.2.2 Sample Quality

An amplifiable amount of DNA could be extracted from all samples. However, in 5 samples, NGS did not give informative results. 4 of these 5 samples revealed DNA integrity of 200bp and 1/5 of 300bp, which is normally the lower limit for NGS analyses. The remaining 45 samples were successfully genetically assessed with DNA integrity raging from 200bp to 600bp, although 93% (42/45) showed DNA integrity of 300bp or above. These results indicate that with a DNA integrity of at least 300bp, it is safest to achieve reliable results from NGS analyses.

4.3 Mutated genes in NMZL and their function

The diagnosis of NMZL was confirmed with mutational and morphological evaluation in 29 cases. Four of these were CD5+ whereas 3 were identified as splenic-type NMZL. No correlation between phenotype and mutational spectrum was found, therefore, the whole group will be discussed together. Of note, the 2 subgroups showed particularly low mutational burden with a maximum of 1 mutation per case.

4.3.1 KLF2

Kruppel-like factor 2 *(KLF 2)*, also known as lung Kruppel-like factor (*LKLF*), was the most commonly mutated gene identified in NMZL. Of the 29 cases, 8 cases (28%) showed *KLF2* mutations. *KLF2* could also be detected in other studies, but never as the most frequent mutated gene of this entity. In a study by Spina et al., 15% (5/35) of the NMZL showed *KLF2* mutations (Spina et al., 2016). In another study, *KLF2* mutations were detected in 12% of the cases (3/25), although it should be noted that the collective was slightly smaller (Pillonel et al., 2018). In both studies mentioned above, the mutations discovered in NMZL were compared to mutations in a group of SMZL, that demonstrated that *KLF2* is not an exclusive marker for NMZL but was also present in 21% and 8% of the SMZL

samples, respectively (Pillonel et al., 2018, Spina et al., 2016). It is even considered to be one of the typical mutations of this entity (Bonfiglio et al., 2022, Piva et al., 2015, Rossi et al., 2012b), making it inappropriate as an indicator to distinguish these two entities.

However, we could neither find *KLF2* mutations in the FL nor the CLL sample group, which are important differential diagnoses of NMZL. Thus, this mutation might be relevant to distinguish questionable NMZL from these two lymphoma types.

KLF2 mutations are usually inactivating mutations (Clipson et al., 2015). The protein KLF2 belongs to the mammalian Kruppel-like transcription factor family. These bind to GC-rich DNA domains via 3'terminal zinc fingers (Pearson et al., 2008). It was originally discovered in the lung and is known to be important for cardiac function (Kaczynski et al., 2003). In addition; however, it also controls proliferation and differentiation of various cell types. In lymphocytes, KLF2 plays a role in differentiation, trafficking, functional capacity and is crucial for regulation at especially late maturation stages (Hart et al., 2012).

In T-cells, the transcription factor is firstly upregulated in single positive T-cells, afterwards downregulated once these cells are activated and mature and lastly re-expressed in T memory cells. Thus, they enter a “resting stage” in which no proliferation occurs, and in which the cells are relatively resistant to apoptosis (Buckley et al., 2001, Kuo et al., 1997). Loss of function of *KLF2* would therefore be expected to result in the thymocytes not entering the resting stage and being activated uncontrolled and subsequently resulting in programmed cell death (Di Santo, 2001, Hart et al., 2012, Kuo et al., 1997). A report from the Leiden group showed exactly this: deficiency of KLF2 caused increasing T-cell activity markers and in the following loss of peripheral T-cells (Kuo et al., 1997). However, further studies on this topic discussed this hypothesis and showed that several other factors contribute to this process and that *KLF2* is not always solely responsible (Hart et al., 2012). In conclusion, *KLF2* plays a certain role in establishing the quiescent state of T-cells and ensuring their viability in the periphery.

In general, B-cell development is strongly driven by the expression of transcription factors and signaling molecules and components. The transcription factor KLF2 also plays a certain role in this context. These interactions are crucial to comprehend the effect of loss of function mutations as observed frequently in our study. Therefore, it is important to distinguish between the 3 subgroups of B-cells: follicular, marginal and B1 cells, which possess different functions and phenotypes. It is already known that *KLF2* is a target gene during early B-cell development of pre-BCR signaling (Schuh et al., 2008). Microarray studies examining the expression pattern of *KLF2* found that it is upregulated in resting B-cells, plasma cells and memory cells and downregulated upon mitogenic activity. This suggests that *KLF2* is important for B-cell quiescence, as it is already described in T-cells (Bhattacharya et al., 2007, Glynne et al., 2000, Winkelmann et al., 2011). With this information, Winkelmann et al. hypothesized that Pre-B cells lacking KLF2 would lead to hyperproliferation. However, this could not be confirmed in vivo, as it is likely that other members of the KLF family, especially KLF4, compensate for the loss (Hart et al., 2012, Winkelmann et al., 2011). Thus, for hyperproliferation to occur, other genetic aberrations must be present. In knockout experiments, however, the loss of *KLF2* led to an increase in the marginal zone cell subset, whereas it had little effect on follicular cells (Hart et al., 2011, Hoek et al., 2010, Winkelmann et al., 2011). Furthermore, expression studies using retroviral expression constructs for *KLF2* were performed. These showed that retroviral transduced *KLF2* leads to increased cell cycle inhibitors p21 and p27 and decreased MYC levels. Thus, overexpression of KLF2 blocks Pre-BCR induced proliferation and triggers apoptosis (Winkelmann et al., 2014).

On a molecular level, KLFs are considered master regulators of several pathways controlling proliferation, differentiation and apoptosis (Zhang et al., 2023).

One of the regular functions of KLF2 in lymphocytes is to inhibit the NF-κB signaling pathway, whose overactivation is known to contribute to the development of cancer. It accomplishes so by binding the promoter and inhibiting the recruitment of certain key coactivators of the pathway, regulating their expression. In addition, KLF2 prevents germinal center B-cells from migrating to the marginal zone (Spina and Rossi, 2017). Thus, if the transcription factor is

functionally restricted by a mutation, it cannot translocate to the nucleus where it can inhibit NF-κB and its coactivators. As a result, the pathway is constitutively activated by upstream signaling such as the BCR and TLR pathways (Spina and Rossi, 2016). Furthermore, subsequent gene expression reinforces migration of cells into the marginal zone (Clipson et al., 2015). KLF2 also exerts influence via the NOTCH pathway. Wang et al found that KLF2 normally inhibits oncogenesis by inhibiting the HIF-1α/NOTCH1 signaling axis. A loss-of-function mutation therefore leads to overactivation and thus promotes the development of cancer (Wang et al., 2017, Zhang et al., 2023).

All in all, it can be assumed that a loss of function of *KLF2* together with other cell cycle disorders occurring in parallel disturbs B and T cell homeostasis and leads to activation of several pathways involved in oncogenesis and therefore support the occurrence of certain types of lymphoma such as NMZL.

4.3.2 Chromatin remodeling and transcriptional regulation mutated genes and their function

Overall, we found the highest number of mutations in genes involved in chromatin remodeling and transcriptional regulation in the 29 cases examined. Among these, *KMT2D* mutations were found as the second most frequent mutation of all (in 24%), followed by *TBL1XR1* in 14% and *ARID1A* and *CREBBP* in 10% each. Mutations in *HIST1H1E* and *ARID1B* were found in 2 cases each, while those in *TP53, TET2*, and *ATM* were identified in 1 case each. This clustering of mutations in chromatin remodeling and transcriptional regulation genes could also be confirmed in other studies. In the research by Spina et. al. and Pillonel et. al., *KMT2D* was even the most frequent mutation of all, found in 34% and 28% of the cases, respectively. In both studies, this was further compared with a cohort of SMZL. In both, *KMT2D* mutations were found markedly less frequently in the SMZL group, namely in only 8% each (Pillonel et al., 2018, Spina et al., 2016). This suggests that when deciding between NMZL and SMZL for diagnosis, *KMT2D* mutations should rather lead one to think in the direction of NMZL. However, this mutation is less suitable for the differentiation from other differential

diagnostic entities: in our group of FL, we could detect the mutation in 3/6, i.e. in 50%. Pillonel et al. also examined a group of LPL and EMZL for comparison, where *KMT2D* mutations were detected in 27% and 13% of cases, respectively (Pillonel et al., 2018).

TBL1XR1 mutations have been identified in 12-14% of the cases of comparable research (Pillonel et al., 2018, Spina et al., 2016), which aligns with our results. They could not be detected at all in the SMZL comparison group (Pillonel et al., 2018). In a study by Ganapathi et. al., a group of dural marginal zone lymphomas, a recognized but rather rare primary site of occurrence of marginal zone lymphoma, was investigated. Here, *TBL1XR1* mutations could even be indexed in 29%, while *KMT2D* mutations were much rarer with 14% (Ganapathi et al., 2016). Striking in the studies of Pillonel et. al. was that *TET2* and *CREBBP* mutations with 20% each were considerably more frequent than in our study (Pillonel et al., 2018). However, the *TET2* is a typical mutation of thyroidal MZL (Rossi et al., 2022, Vela et al., 2022). Overall, the results in recent publications are comparable to ours.

The role of some of the gene mutations found involved in epigenetic modification will be discussed below.

Chromatin remodeling protein complexes reorganize chromatin and thus play an essential role in the regulation of a variety of cellular processes in the human body. Especially important in this context are histone enzymes. These modify a part of the histone structure post-translational, which causes an alteration of the nucleosome structure, leading to increased or decreased recruitment of proteins. These processes play an important role in the development of diseases, especially in the development of cancer. If components of these complexes are abnormally altered, oncogenesis-promoting genomic reprogramming and altered protein expression can occur (Zhang and Li, 2022). Thus, sequencing studies have shown that somatic mutations in epigenetic modifiers such as methyl-, acetyltransferases or histone proteins are crucial for the development of various lymphomas. Hereby, early driver mutations in chromatin remodeling genes are of

particular interest (Morin et al., 2011, Okosun et al., 2014, Pasqualucci et al., 2011, Zhang et al., 2015).

A key group of enzymes in this regard are histone lysin methyltransferases, abbreviated KMTs (Martin and Zhang, 2005, Sims et al., 2003). Among others, these include KMT2D (previously known as MLL2), which was the second most frequently mutated gene in NMZL in our study and even the most frequently mutated gene in comparable studies (Pillonel et al., 2018, Spina et al., 2016). KMT2D is the major methyltransferase of H3K4, whose methylation is particularly important for epigenetic regulation (Shilatifard, 2012, Strahl et al., 1999). This enzyme is mutated in various types of cancers, including lymphomas. Mutations in the gene encoding KMT2D most often result in loss of function, arguing for *KMT2D* as a tumor suppressor gene. However, the exact events on a molecular level are not entirely understood and require further research (Dhar and Lee, 2021). In lymphomas, the role of *KMT2D* has particularly been investigated in DLBCL and FL as it a common early mutation in these two entities (Ortega-Molina et al., 2015, Zhang et al., 2015, Morin et al., 2011). It has been shown that early mutations cause decreased enzyme activity, leading to decreased methylation of H3K4 in germinal center B-cells. This in turn results in proliferation of germinal center B-cells and increased B-cell development in general (Zhang et al., 2015). That process is enhanced through KMT2D mediated activation of BCL2. Nevertheless, it has been shown that deficient KMT2D is able to trigger B-cell malignancy even in the absence of BCL2 (Ortega-Molina et al., 2015). In addition, KMT2D regulates the expression of other key regulators of signaling pathways such as the CD40, Toll-like, and B-cell receptor pathway. Other target genes are *TNFAIP3, SOCS3, SGK1, TRAF3, TNFRSF14* and *ARID1A*, which are less expressed when *KMT2D* is mutated and thus their product can no longer fulfill their function as a tumor suppressor (Ortega-Molina et al., 2015). Recapitulating, functioning KMT2D suppresses the development of lymphomas by inhibiting survival and proliferation genes and activating pro apoptotic genes, whereas mutation in the gene encoding this enzyme promotes the development of B-cell lymphomas (Dhar and Lee, 2021).

Another histone modifying enzyme is CREBBP. This gene was found mutated in 10% (3/29) in our group of NMZL and is particularly known to be mutated in FL and DLBCL (Zhu et al., 2023). In fact, 50% (3/6) of the FLs we identified carried *CREBBP* mutations. CREBBP stands for CREB binding protein which is an acetyltransferase and transcriptional cofactor that affects gene expression by regulating the acetylation levels of histones. It is closely related to EP300. CREBBP has various DNA and protein binding domains. In the context of this study, the HAT domain, which is responsible for the interaction with histones, is of particular interest (Zhu et al., 2023). By modifying histones, CREBBP regulates critical cellular functions such as DNA repair mechanisms (Ding et al., 2019, Dutto et al., 2018), apoptosis (Ogiwara et al., 2016), and proliferation and differentiation (Dutta et al., 2016, Garcia-Carpizo et al., 2018). It is essential for normal hematopoiesis, where it acts as a tumor suppressor. Moreover, it plays a role in the homeostasis of hematopoietic microenvironment. Especially in GC B-cells, CREBBP/EP300 regulates key mechanisms of differentiation. Thus, mutations in one of these acetyltransferases can lead to the development of tumors (Zhu et al., 2023). As a matter of fact, in a mouse model, it was found that CREBBP deactivation leads to an increased incidence of hematologic malignancies later in life (Kung et al., 2000). In FL and DLBCL, mutations mostly affect the HAT domain and inactivate it, which has generally been linked to development of lymphomas (Pasqualucci et al., 2011). The exact mechanisms behind this are being investigated, particularly in germinal center derived lymphomas such as FL and DLBCL.

The so called BCL6/SMRT/HDAC repression complex is of special interest in this context since it acts as a CREBBP counterpart. The complex and CREBBP both influence histone H3K27. While CREBBP acetylates it, the HDAC repression complex is responsible for its deacetylation. Physiologically, there exists a balance in which H3K27 remains largely acetylated. This leads to the activation of important enhancers that promote terminal differentiation of GC cells into plasma cells and control immune signaling programs in mature B cells. In the case of *CREBBP/EP300* being mutated and inactivated, the balance is disturbed and the BCL6/SMRT/HDAC complex deacetylates the corresponding enhancers.

As a result, the differentiation of GC B-cells is disrupted, this cell line expands, malignant transformation can occur and eventually HDAC-dependent lymphomas develop (Höpken, 2017, Jiang et al., 2017, Zhu et al., 2023). In FL and DLBCL, it has also been observed that *CREBBP* mutations frequently occur together with *KMT2D* mutations (Jiang et al., 2017). In our NMZL cohort, 2 of the 3 *CREBBP* mutated cases additionally carried a *KMT2D* mutation. KMT2D affects CD40 signaling, which normally terminates the activity of the BCL6/SMRT/HDAC3 complex. On the other hand, if *KMT2D* is mutated, the corresponding enhancers respond to KMT2D in a reduced manner and the activity of the repression complex cannot be terminated (Ortega-Molina et al., 2015). It is still necessary to conduct further research to determine if these processes described in DLBCL and FL, also have a similar influence on the development of NMZL.

TBL1XR1, which belongs to the *TBL1* gene family (Yan et al., 2005), was found mutated in 14% of our study. Like KMT2D and CREBBP, it is involved in transcriptional regulation. Its overexpression has been associated with poor prognosis in various cancers (Pray et al., 2022). In aggressive DLBCL, where it is frequently mutated, it has been associated with extranodal manifestations, contributing to a poorer prognosis (Chapuy et al., 2018, Schmitz et al., 2018). Knowledge of the exact role of TBL1XR1 is limited, but it is known to be part of the SMRT/NCOR1 transcriptional repression complex which has already be mentioned above regarding CREBBP (Yoon et al., 2003). This complex includes enzymes that bind chromatin and thereby modify histones and DNA (Li et al., 2000, Yoon et al., 2003). A key component is HDAC, which enables transcriptional repression of the SMRT/NCOR1 complex (Hatzi et al., 2013). In GC B-cells, the complex is bound and recruited by BCL6, which is important for GC formation while inhibiting differentiation to plasma cells (Hatzi et al., 2013, Venturutti et al., 2020). Venturutti et al. investigated a collective of DLBCL and found that mutations in *TBL1XR1* lead to a switch from BCL6 to BACH2, another transcriptional regulator gene, in the SMRT/NCOR1 complex. This results in an expansion of pre-malignant B cells, which in turn promotes lymphomagenesis (Venturutti et al., 2020). Furthermore, mutations in *TBL1XR1* have been related to activating mutations in BCR and TLR pathway genes (Chapuy et al., 2018,

Schmitz et al., 2018). Analogous to DLBCL, these changes could also play a role in NMZL. It is also known that the wild-type NCoR complex represses important pathways via interaction with transcriptional factors like NF-KB (Ghisletti et al., 2009, Li et al., 2015). In a study by Jung et. al., the localization and effects of *TBL1XR1* mutations in ocular marginal zone lymphomas have been studied in detail. They are often localized in the WD40 domain of the gene, where alterations led to simplified binding of TBL1XR1 to the NCoR protein. This in turn resulted in increased degradation of said complex and by that in overactivation of the NF-KB and c-Jun pathways (Jung et al., 2017). This demonstrates that *TBL1XR1* mutations could also contribute to lymphomagenesis by effecting pathways like NF-KB which are known to be altered in lymphoma.

ARID1A and *ARID1B*, which were mutated in 17% of our studied cases, belong to the ARID family, which stands for AT-rich interaction domain (Wilsker et al., 2004). They are part of the SWI/SNF chromatin remodeling complex (Mathur, 2018). This complex plays a part in various types of cancer since genes encoding for subunits are mutated in 20% of all human malignancies (Helming et al., 2014). Hereby, *ARID1A* mutations are particularly relevant, as they are present in 6% of all cancers (Jiang et al., 2020), for example in DLBCL and SMZL (Spina et al., 2016, Zhang et al., 2013)

The SWT/SNF complex regulates the accessibility of the respective DNA to transcription factors and the transcription apparatus. This is achieved via ARID1A and ARID1B, the DNA-binding subunits (Mathur, 2018, Tang et al., 2010). Hence, the two proteins participate in various pathways and signaling cascades, including various DNA damage repair pathways such as the nonhomologous end joining repair pathway, the PI3K/Akt/mTOR and KRAS pathway and immune function (Mullen et al., 2021, Shen et al., 2015, Watanabe et al., 2014). In addition, they regulate the expression of important cell cycle control genes (Nagl et al., 2005, Nagl et al., 2007). Moreover, ARID1A is involved in homologous recombination, an important repair mechanism in proliferating cells (Shen et al., 2015, Watanabe et al., 2014). Another interesting function of ARID1A in the context of cancer is it´s regulation of TERT (telomerase reverse transcriptase) since maintenance of telomere length is essential for tumor survival in the human

body (Suryo Rahmanto et al., 2016). Overall, ARID1A and ARID1B are involved in numerous different cascades and their loss of function can support tumor formation.

HIST1H1E is another gene that affects chromatin remodeling and influences lymphomagenesis (Yusufova et al., 2021). In our study, it was mutated in about 7% (2/29) of cases, comparable to results of other studies (6%-12%) (Pillonel et al., 2018, Spina et al., 2016). *HIST1H1E* encodes for H1.4, a linker histone protein of the H1 family. Linker histones restrict access to chromatin and thus influence gene expression (Wolffe, 1997). H1, as one of these linker histones, acts as a transcriptional repressor, achieving this repressive activity through a variety of molecular mechanisms. On the one hand, it binds the nucleosome and ensures that the chromatin is folded into higher-order three-dimensional structures (Allan et al., 1986, Bednar et al., 2017, Fyodorov et al., 2018). Furthermore, H1 bound to DNA presents an additional obstacle, both of which make it more difficult for binding proteins such as transcription factors to interact with the DNA (Laybourn and Kadonaga, 1991). H1 is accumulated in silenced chromatin domains and is associated with various silencing marks (Fyodorov et al., 2018). These include hypoacetylation of core histones (Reczek et al., 1982, Schröter et al., 1981). H1 is thought to negatively regulate HATs (histone acetyltransferases) and to enhance activity of one of the human histone deacetylases, SIRT1 (Herrera et al., 2000, Vaquero et al., 2004). Another important silencing marker is the methylation of H3K27, again linked to H1 (Martin and Zhang, 2005). In addition, H1 can hinder HMTs (histone methyltransferases) from binding histones, which further accelerates chromatin silencing (Fyodorov et al., 2018, Yang et al., 2013). H1 has also been found to be crucial for genetic stability as it regulates important parts of the DNA damage response and repair factors (Thorslund et al., 2015). These functions emphasize that mutations in the genes encoding for H1 can have significant consequences. In B-cell lymphomas, *HIST1H1B-E* mutations are quite common and act as driver mutations (Yusufova et al., 2021). Consequently, when function of the protein is impaired, the chromatin loosens its highly folded structure, changing from a compact to a relaxed state. This results in a variety of epigenetic changes such as loss of

silencing markers such as methylated H3K27. Subsequently, genes that are normally silenced at early stages of development are upregulated (Yusufova et al., 2021). In studies using mice with loss of the H1e allele, increased fitness and self-renewal in GC B-cells was noted (Yusufova et al., 2021, Zhang et al., 2012). With other genetic alterations, DLBCLs were mimicked in mice, and an expansion of monoclonal B-cells was observed. In conclusion, H1 is an important biochemical effector of chromatin structure and epigenetic programming, and mutations in the gene promote malignant transformation in lymph nodes by de-repression of important genes with stem cell properties (Yusufova et al., 2021).

In summary, genes participate in chromatin remodeling and transcriptional regulation appear to be essential in the pathogenesis of NMZL and contribute to the development of lymphoma in various ways.

4.3.3 NOTCH pathway mutated genes and their function

The NOTCH pathway is a highly conserved pathway that links cell membrane signaling to transcriptional regulation. Mutations in proteins of this signaling cascade are found in many different types of cancer, whereby the mutations can have a wide variety of effects and impair virtually all hallmarks of cancer (Aster et al., 2017). In our study of NMZL, we found several mutations in genes associated with this pathway. These include the genes *SPEN, NOTCH2* and *CREBBP*. First, a brief overview of this pathway is described in order to understand the role of the gene mutations. Via cell-cell contacts, the NOTCH pathway enables cells to respond to signals from neighboring cells by means of controlled proteolysis with the expression of certain genes (Kopan and Ilagan, 2009). First condition for this to happen is contact of one of the NOTCH receptors with an appropriate ligand of a neighboring cell. NOTCH receptors are transmembrane proteins, of which there are 4 different ones in mammals; NOTCH 1-4, each encoded by a different gene. Five ligands for these receptors are currently known; 3 from the delta family (Dll1, Dll3, Dll4) and 2 from the serrate giant family (Jag 1&2) (Aster et al., 2017). Usually, the NOTCH receptor is maintained in an inactivated state by the juxtamembrane NOTCH regulatory region (NRR) (Gordon et al., 2007). However,

when it binds one of its ligands, this inhibition of NRR is abolished. As a result, the receptor is cleaved by 2 enzymes, first by an ADAM metalloprotease and then by a gamma secretase, releasing the NOTCH intracellular domain (NICD) (Brou et al., 2000, Mumm et al., 2000, Schroeter et al., 1998). This domain then translocases to the nucleus and, together with DNA binding factor RBPJ (also known as CSL) and coactivators, forms the NOTCH transcription complex (NTC), which binds to NOTCH regulatory elements and ultimately initiates transcription of various NOTCH target genes. Termination of the NOTCH signal is achieved through phosphorylation of the PEST domain, a subunit of the intracellular region of the NOTCH receptor, ultimately leading to degradation of NICD (Aster et al., 2017, Kopan and Ilagan, 2009). However, this whole cascade can have wide-ranging consequences. On the one hand, this is achieved by different signal strength (Gama-Norton et al., 2015) and signal dynamics (Nandagopal et al., 2018). On the other hand, in addition to the well-studied canonical core pathway, a non-canonical pathway is suspected which additionally regulates NICD. Thus, interaction with downstream regulators and NICD presumably leads to communication between the NOTCH pathway and others such as the Wnt, TGFß and hypoxia-dependent pathway (Aster et al., 2017, Blokzijl et al., 2003, Gustafsson et al., 2005, Jin et al., 2009). Generally, the NOTCH pathway is more complex than at first glance due to a wide variety of variations and interactions. Overall, NOTCH signaling generally regulates cell proliferation, cell death and differentiation programs in adult tissue, including lymphocyte development (Kopan and Ilagan, 2009, Tanigaki et al., 2003). NOTCH ligands are physiologically expressed in bone marrow (BM) on the surface of developing B-cells and BM stromal cells (Bertrand et al., 2000, Tokoyoda et al., 2004). Furthermore, the NOTCH pathway is crucial for maturation of MZ B-cells and development of B1-cells (Saito et al., 2003, Tanigaki et al., 2002, Witt et al., 2003). In addition, NOTCH signaling promotes the activity of the BCR pathway and co-stimulatory signals and thus contributes to B-cell activation and terminal differentiation (Santos et al., 2007, Thomas et al., 2007). Knowing these various functions of NOTCH signaling in lymphocytes, it is obvious that aberrations of it can lead to the development of hematological malignancies (Arruga et al., 2018,

McCarter et al., 2018). In T-ALL, the role of activating *NOTCH* mutations is particularly well understood since occurring in approximately 50% of all T-ALL (Weng et al., 2004). However, *NOTCH* associated mutations also present an issue in many B-cell malignancies, for example in CLL, FL, DLBCL and also MZL. In the latter, NOTCH pathway is known to be one of the most frequently mutated (Arruga et al., 2018). In SMZL, *NOTCH* related mutations are even the most frequent; in total in 30-40% of all SMZL (Spina et al., 2016). Of the 4 NOTCH receptors, NOTCH2 is of particular interest in the emerge of MZL since it is considered to be the master regulator of MZ B-cell differentiation. In our study, we detected mutations in 2 of 29 cases (7%), whereas in other studies those were found with a frequency of 4% and 20%. NOTCH2 is specifically expressed on mature peripheral B- cells (Saito et al., 2003). In this context, it is essential for the maturation of MZ B-cells. Upon knockout of *NOTCH2* in murine B-cells, no MZ B-cells were able to develop, whereas all other B-cell lineages remained unaffected (Saito et al., 2003, Tanigaki et al., 2002). Moreover, *NOTCH2* plays a key role in the development of B1-cells (Witt et al., 2003). NOTCH receptors generally consist of an extracellular and an intracellular domain. Part of the latter forms the C terminal degron domain, more precisely the PEST domain. Phosphorylation of that domain leads to proteasomal receptor degradation and therefore terminates NOTCH signaling (Aster et al., 2017, Kopan and Ilagan, 2009). Depending on the cancer type, different mutation patterns of NOTCH receptors exist. In B-cell lymphomas, the affected domain is mostly PEST. Mutations in it leads to increased stability of the domain and thus to reduced degradation of the receptor (Aster et al., 2017, Rossi et al., 2012b, Spina and Rossi, 2017). This ultimately results in increased NOTCH2 activity and therefore increased signaling for MZ differentiation.

SPEN, also known as SHARP or MINT, also affects the NOTCH signaling cascade and its gene was mutated in 2 of 29 cases (7%) in our study. In comparable studies, mutations were detected in 8-11% (Pillonel et al., 2018, Spina et al., 2016). However, mutations are also present in SMZL. In a study with 117 SMZL cases they could be identified in 5% of the cases (Rossi et al., 2012b). SPEN is known to suppress NOTCH signaling by forming a high affinity complex

with RBPJ, inhibiting its function (Kuroda et al., 2003, Li et al., 2005, VanderWielen et al., 2011, Yuan et al., 2019). RBPJ, as described above, is a DNA-binding factor that forms the NTC with NICD and other proteins when NOTCH signaling is activated. That ultimately results in the transcription of NOTCH target genes (Aster et al., 2017, Kopan and Ilagan, 2009). Deficiency of RBPJ in B cells has been shown to lead to an almost complete loss of MZ cells and an increase of follicular B-cells, demonstrating that activation of NOTCH increases MZ B cell and decreases follicular B-cell differentiation (Tanigaki et al., 2002). In a mouse model with SPEN-deficient B cells, it was observed that the B-cells differentiated mainly into MZ cells, suggesting that SPEN inhibits the activity of RBPJ. Thus, physiologically, functional SPEN inhibits the differentiation of B lymphocytes into MZ B cells (Kuroda et al., 2003). In a large study with SMZL, the *SPEN* mutations were characterized in more detail and found to be mainly inactivating mutations affecting the SPOC domain, which is important for interaction of SPEN with proteins (Rossi et al., 2012b). However, this on/off model is still somewhat more complicated. SPEN or the SPEN/RBPJ complex additionally interacts with the corepressor NCor and the coactivator KMT2D. These two compete for the SPOC binding domain of SPEN and a balance is created in which NCor binding tends to steer the balance towards chromatin repression, while KMT2D binding steers the balance towards chromatin activation. Deducting from this model, *SPEN* mutations disturb this balance and thus lead to dysregulation of NOTCH target genes (Oswald et al., 2016). Concluding, the exact mechanisms of the function of SPEN as a NOTCH signaling repressor and thus as a SMZL/NMZL tumor suppressor need to be investigated in more detail.

When *CREBBP*, encoding an acetyltransferase that is involved in chromatin remodeling, which has been discussed previously, is mutated, it can also affect the NOTCH pathway. In DLBCL, *CREBBP/EP300* mutations are typically associated with a poorer prognosis (Juskevicius et al., 2017). These were investigated in more detail in a study, and it was discovered that mutations in the *CREBBP/EP300* gene are able to activate the NOTCH pathway (Huang et al.,

2021). This is accomplished by inhibition of FBXW7, an important repressor of this pathway (Huang et al., 2021, Yeh et al., 2018).

4.3.4 NF-KB pathway mutated genes and their function

Genes affecting the NF-KB pathway were less affected in our study than those of chromatin remodeling and the NOTCH pathway. This is also consistent with other studies (Pillonel et al., 2018, Spina et al., 2016). In our study, the most frequent mutated NF-KB pathway genes were *BCL10* with 7% (2 of 29) and *MYD88*, which affects the pathway via kinases (Deguine and Barton, 2014), with 14% (4/29). In comparable research, *BCL10* was mutated in 4% and 11% (Pillonel et al., 2018, Spina et al., 2016). *MYD88* mutations, which are typically found in LPL, have been detected with a frequency of 4-9% (Pillonel et al., 2018, Spina et al., 2016, van den Brand et al., 2017). However, in one of these studies, cases with the LPL typical L265P *MYD88* mutation were excluded beforehand (Pillonel et al., 2018). Strikingly in the comparative studies, *TNFAIP3* was one of the most frequent NF-KB related mutated genes in NMZL with a frequency of 12-50% (Ganapathi et al., 2016, Pillonel et al., 2018, Spina et al., 2016, van den Brand et al., 2017). On the contrary, we identified a mutation in only one of our NMZL cases. TNFAIP3 is a protein that negatively regulates the NF-KB pathway (Wertz et al., 2004) and leads to impaired B-cell maturation in the mouse model when deleted (Chu et al., 2011). In marginal zone lymphomas, it is most commonly mutated in EMZL (Pillonel et al., 2018). Multiple important processes in the body, including cell maturation, stress and immune response and cell survival depend on NF-KB signaling. Thus, when dysregulated, the pathway can be engaged in oncogenesis (van den Brand et al., 2017). In B cells, the NF-KB signaling physiologically serves the maturation and maintenance of MZ B-cells (Allman and Pillai, 2008). Overactive NF-KB signaling has been observed in a range of tumor types, making it a desirable therapy target (Karin, 2009). Related genes are also affected in many lymphomas, including DLBCL, SMZL and EMZL (Compagno et al., 2009, Du, 2011, Rossi et al., 2011). A canonical and a non-canonical pathway are distinguished. The canonical pathway is activated by cytokines, growth factors and tyrosine kinases. Hereby, signals from various receptors are involved, including the BCR, tumor necrosis factor receptor (TNFR), IL-1 receptor (IL1R)

and the toll like receptor (TLR). All of them ultimately activate the inhibitor of kappaB kinase (IKK) complex (Liu et al., 2017). NF-KB is usually located in the cytoplasm, bound to inhibitors and is thus inactive. The activated IKK complex phosphorylates those NF-KB inhibitors (NFKBIs), which are then degraded in the proteasome. As a result, the nuclear localization signal on the NF-KB dimers is exposed and they translocate into the nucleus and bind to DNA. As transcription factors, they regulate the expression of various genes (Dolcet et al., 2005, Spina and Rossi, 2017, van den Brand et al., 2017). One important target are apoptosis genes, through which NF-KB can inhibit cell death. On the one hand, this is achieved through increased expression of apoptosis inhibitors (IAPs), which inhibit the extrinsic and intrinsic cell death pathway directly via caspases (Deveraux et al., 1998, Wang et al., 1998). Furthermore, the expression of some genes of the BCL2 family, which inhibit important proapoptotic proteins, is increased (Dolcet et al., 2005, Lee et al., 1999). In addition, NF-KB affects proliferation by increasing the expression of genes encoding cell cycle cyclins, cell adhesion molecules and COX-2 (Dolcet et al., 2005, Guttridge et al., 1999).

BCL10, mutated in 2 cases in our study, is crucial for activation of NF-KB transcription factors via T- and B-cell receptor pathway. Once an antigen binds to a B-cell receptor, a cascade is initiated in which the tyrosine residues of CD79A and CD79B are phosphorylated. This leads to the activation of several other kinases, which finally phosphorylate CARD11. CARD11 changes its conformation allowing BCL10 and MALT1 to bind. These 3 proteins form the CBM complex, which links upstream BCR signaling to the NK-KB pathway. The complex then interacts with various regulators, including TRAFs, ultimately activating the IKK complex through a chain of phosphorylation and ubiquitination, and initiating NK-KB signaling as described above (Lucas et al., 2001, Ruland and Hartjes, 2019, Sommer et al., 2005, van den Brand et al., 2017, Zhou et al., 2004). BCL10 is thus an important part of this cascade. It has been shown that overexpression of BCL10 can lead to abnormal maturation and functioning of B lymphocytes through constitutive activation of NF-KB signaling (Li et al., 2009). In MALT lymphomas, BCL10 is frequently affected by one of the typical translocations. Hereby, BCL10 is moved under the control of an IgH enhancer,

which has effects on the NF-KB pathway (Bertoni et al., 2018, Thome, 2004), and thus contributes to antigen-independent tumor progression (Ruland and Hartjes, 2019, Xue et al., 2003). In experiments with transgenic mice showing aberrant human BCL10 expression, it was observed that both the canonical and the noncanonical NF-KB pathway were constitutively activated in the B-cells. The gene expression pattern showed that BAFF (B-cell activating factor) was overexpressed (Li et al., 2009). BAFF is able to activate the pathway via both pathways and furthermore enhances survival and expansion of the MZ B-cell lineage (Enzler et al., 2006, Thien et al., 2004). Therefore, it provides a positive feedback loop of aberrant BCL10 signaling. In fact, a significant increase in the MZ B-cell population was observed in the animals. Some of the mice, but not all developed lymphomas. This demonstrates that although altered BCL10 expression contributes to the development of lymphoma, it is not sufficient on its own and that other genetic aberrations are required for cancer to arise (Li et al., 2009).

14% (4/29) of our cohort showed mutations in *MYD88*, a gene encoding for the eponymous protein which also impacts the NF-KB pathway. It functions as an adapter protein in the signaling of TLR and IL-1/IL18 receptors, activating NF-KB transcription factors (Medzhitov et al., 1998). Therefore, like BCL10, it is indirectly involved in physiological MZ B-cell differentiation in healthy organisms (Wang et al., 2014). By regulating and promoting the production of pro- and anti-inflammatory cytokines, it is considered a key element in inflammatory signaling (Deguine and Barton, 2014, Oda and Kitano, 2006). The protein is composed of 3 domains: the toll IL-1R (TIR) domain, the death domain (DD) and the intermediate domain (INT) (Burns et al., 1998, Medzhitov et al., 1998, Muzio et al., 1997). These each fulfill different functions. The c-terminal TIR domain interacts with the intracellular TIR domain of TLR and is therefore crucial for further signal transduction (Rossi, 2014). Thereby, the n-terminal DD domain is able to oligomerize with the respective DDs of threonine kinases IRAK 1-4. Together, these form a multimeric complex, also called myddosome, which is then able to amplify and expatiate the signal (Motshwene et al., 2009). This ultimately initiates NF-KB signaling, controlling the respective target genes.

Additionally, some studies have shown that MYD88 can interact TIR independently with downstream receptors, including the INF-γ receptor and members of the TNF receptor family (He et al., 2010, Sun and Ding, 2006). Dysfunctional or lack of MYD88 in this cascade causes impaired expression of certain genes, which leads to a loss of MZ B-cells in the organism (Wang et al., 2014). In contrast, overexpression of MYD88 leads to gain of function of the protein, resulting in accordingly opposing effects, which is relevant for the genesis of many lymphomas (Ngo et al., 2011, Spina and Rossi, 2017). In LPL, approximately 90% of cases carry the L265P *MYD88* mutation, which is located in the TIR domain and leads to persistent NF-KB and STAT3 activation (Wang and Lin, 2020). Rarely, somatic *MYD88* mutations are also identified in SMZL, NMZL and CLL (Swerdlow et al., 2016, Martinez-Lopez et al., 2015). They are mostly located in the TIR domain, more specifically in the beta-beta loop, and led to a change of the MYD88 structure. As a result, IRAK1 & 4 were recruited spontaneously, leading to uncontrolled formation of the myddosome complex und thus constitutive NF-KB activation (Spina and Rossi, 2017). *MYD88* is able to serve as an oncological driver mutation in various lymphomas (Kraan et al., 2013). Since mutations of *MYD88* occur much more frequently in LPL, but sometimes also in NMZL, differentiating between these two entities in the lymph node remains challenging and requires other factors such as clinical presentation, morphology and immunohistochemistry to allow a diagnosis.

4.4 Genetic landscape of t(14;18) negative FL compared to NMZL

Prior to genetic analysis, FL was entertained as a differential diagnosis in 17 of 45 samples; finally, 6 cases were classified as t(14;18) negative FLs. These FLs that do not carry the chromosomal t(14;18)(q32;q21) translocation, account for about 10-15% of FLs (Laurent et al., 2023). The differential diagnosis between NMZL and *BCL2*-neg FL can be cumbersome, and many times genetic analysis is performed and needed to resolve the problem. In our 6 cases, we detected mutations in 13 of the total 81 genes examined. The most frequently mutated gene among them was *STAT6*, which was mutated in 4/6 cases. The presence of *STAT6* mutation supports the diagnosis of *BCL2*-negative FL that although not

specific is very characteristic. In contrast, we could not find any in the 29 NMZL cases. In addition, we identified *KMT2D* and *CREBBP* mutations in 3 cases each, which, in comparison, were found in 7 and 3 of the NMZL cases, respectively. *TNFRSF14* mutations were demonstrated in 2 cases, while one of those could be detected in only one NMZL case. Nevertheless, the presence of *KMT2D* variants does not help in the differential diagnosis, whereas the presence of *CREBBP* and *TNFRSF14* variants supports the diagnosis of FL but does not exclude the possibility of NMZL. Mutations in *EZH2, CD79B, MYC, JAK3, TNFAIP3, SOCS1, BIRC3, TP53* and *SPEN* could be found in one case each.

The findings in our study are in perfect agreement to what was reported by Nann et al in a series of *BCL2*-negative FL(Nann et al., 2020). As in our cohort, *STAT6* mutations were the most frequent (57% of the cases), which in comparison can only be observed in 11-12% of the conventional FL cases according to the literature (Okosun et al., 2014, Yildiz et al., 2015). Similar to our findings, *CREBBP* mutations were the second most frequent (49%), followed by *KMT2D* aberrations (27%). Striking was the frequent simultaneous presence of *STAT6* with *CREBBP* mutations, which is characteristic of the *BCL2*-neg FL confirming further this diagnosis (Nann et al., 2020, Yildiz et al., 2015, Zamò et al., 2018, Salmeron-Villalobos et al., 2022). While mutant inactivated *CREBBP* supports lymphoma development through epigenetic modifications in GC B-cells, mutant *STAT6* provides additional survival-promoting signals via the JAK-STAT pathway (Erdogan et al., 2022, Zhang et al., 2017). In our study, two of the four *STAT6* mutated cases showed an additional *CREBBP* mutation. Furthermore, in the work of Nann et. al. *TNFRSF14* mutations were detected in 39% and *EZH2* mutations in 18% of the cases. In summary, the genetic landscape we were able to identify in the few cases is very similar to that of this study (Nann et al., 2020). In 2009, Katzenberger et. al. already described a subgroup of follicular lymphomas with a diffuse growth pattern and 1p36 chromosomal deletion that lacked the classic t(14;18) translocation. These were also distinctive in being immunohistochemically CD23 positive and often showed a loss of CD10 (Katzenberger et al., 2009). In further studies this subgroup of lymphomas was investigated concerning it´s mutational landscape. All of them detected *STAT6*

as the most frequent mutation in about 82% of the cases, followed by other already mentioned mutations of *CREBBP, KMT2D* (Siddiqi et al., 2016, Zamò et al., 2018). Since *STAT6* mutations are substantially less common in conventional FLs, they may be particularly important to determine a diagnosis (Morin et al., 2011, Pasqualucci et al., 2014). In 2022, this subgroup of FL was proposed as a provisional entity by the ICC (Campo et al., 2022), while the 5th WHO classification of hematologic neoplasms did not recognize it as such (Alaggio et al., 2022). Of our six cases, four could also fit well into the above mentioned subgroup, as they showed a distinct CD23 positivity in immunohistochemistry, in addition, to the typical mutation spectrum as they all carried *STAT6* mutations, whereas it is unclear if a typical 1p36 chromosomal deletion is present. In the following, the role of the mutated genes will be discussed. The function and effect of mutations of *CREBBP* and *KMT2D* have already been explained above. Signal transducer and activator of transcription 6 (*STAT6*), the key gene in this context, encodes for STAT6, which is part of a family of 7 transcription factors (Erdogan et al., 2022). Physiologically, it modulates key biological processes including the differentiation of Th2 cells and the proliferation and maturation of B cells via gene expression (Kaplan et al., 1996, Schindler et al., 2007). It accomplishes this via the JAK STAT pathway, a crucial signal transduction pathway for a variety of autoimmune diseases and malignancies (O'Shea and Plenge, 2012, O'Shea et al., 2015). The canonical pathway is activated when a ligand, in the case of STAT6 mainly being the cytokines IL-4 and IL-13, binds to a receptor on the cell surface. As a result of the following receptor dimerization, JAK is transphosphorylated. This in turn allows STAT to bind to its docking site, which is then also phosphorylated. Subsequently, STAT dissociates and forms homo- or heterodimers. These translocate to the nucleus where they bind DNA promoters and affect gene expression (Hu et al., 2021b, Erdogan et al., 2022). Significant processes affected include hematopoiesis, tissue repair, apoptosis, inflammation and immune fitness (Owen et al., 2019). In addition, a non-canonical pathway, which is much more complicated, exists. This pathway is responsible for maintaining the stability of heterochromatin (Li, 2008, Shi et al., 2006). Thus, it is comprehensible that a disordered function can contribute to tumor

development due to instability of heterochromatin (Shi et al., 2008). Moreover, the JAK/STAT pathway is able to crosstalk to other central pathways at various levels, including the NF-KB, TGFß, NOTCH and MAPK pathways (Hu et al., 2021b). In hematologic neoplasms, *STAT6* mutations typically result in a gain of function of the respective protein; for instance, approximately 80% of all classical Hodgkin lymphomas carry such a mutation (Guiter et al., 2004, Skinnider et al., 2002).

HVEM/TNFRSF14, on the other hand, physiologically functions as a tumor suppressor and is encoded by *TNFRSF14* or *HVEM*, another frequently altered gene in t(14;18) - FL. Loss of its function can lead to autonomous activation of B cells (Boice et al., 2016).

Therefore, translocation-negative FLs are a challenging diagnosis since the typical translocation is lacking. Moreover, it is particularly difficult to distinguish these FLs from other small B-cell lymphomas such as NMZL (van den Brand et al., 2016). As no *STAT6* mutations were found in our cohort of NMZL, our study confirm that *STAT6* mutations may be the most important factor in the differentiation to NMZL. *KMT2D* and *CREBBP* mutations should be considered with caution because, although they are more common in FL, they are also among the most frequent mutations in NMZL. Mutations in *TNFRSF14 / HVEM* should steer the diagnosis more towards FL, as they are very rarely seen in NMZL. Overall, mutation analysis seems to contribute to establish a diagnosis.

4.5 Genetic landscape of CLL compared to NMZL

Before NGS analysis, CLL as a differential diagnosis was considered in 4 cases. After histological and mutational evaluation, 5 cases have been classified as CLL. Immunohistochemically, the neoplastic cells lacked the classical strong CD23 expression. CD5 was also negative in the tumor cells.

In total, we detected 10 mutations in the 81 genes examined in these 5 cases. The most frequently mutated gene was *ATM* in 3 samples. Mutations in *MYD88, CXCR4, BRAF, TP53, BIRC3, NLRP14, NOTCH1*, and *KRAS*, were found in only

one case each. However, since the number of cases is only five, the results are only moderately representative. *ATM, TP53, BIRC3, NOTCH1* and *MYD88* are known mutations in CLL, which is why these will be discussed in more detail below.

ATM was the most frequent mutated gene in the CLL group which was not detected in any of the 29 NMZL cases. It is considered a tumor suppressor, which is why its deletion or inactivation contributes to tumorigenesis. In 10% of CLL patients, the *ATM* gene is affected by deletions of the short arm of chromosome 11 (Bosch and Dalla-Favera, 2019). It has been demonstrated that these monoallelic *ATM* deletions lead to an advantage of survival of the affected cells, which are therefore able to proliferate. Subsequently, clones with a second hit in the remaining allele of *ATM* expand preferably (Landau et al., 2015). Thus, about 1/3 of patients with a 11p deletion hold a mutation in the second *ATM* allele. Taken together, deletions of 11q and *ATM* mutations occur in 9-18% of all CLL patients at primary diagnosis (Bosch and Dalla-Favera, 2019, Fabbri and Dalla-Favera, 2016). Physiologically, ATM serves as an upstream regulator of TP53 and therefore has tumor suppressive effects (Banin et al., 1998, Siliciano et al., 1997). It belongs to the PIKK family and consists of 3 functional domains which are obligatory for its functionality. In response to DNA double-strand breaks, the protein manages to activate specific signaling cascades. On the one hand, this leads to the assembly of a complex of proteins which subsequently recognize the DNA damage, enable relaxation of the surrounding chromatin and ultimately repair the damaged strands (Goodarzi et al., 2008, Stankovic and Skowronska, 2014). On the other hand, ATM interacts with cell cycle regulators and initiates cell cycle arrest and apoptosis via activation of TP53 (Barlow et al., 1997).

TP53 itself, also a tumor suppressor, was mutated once in both the NMZL group and the CLL group in our study. In CLLs, *TP53* is frequently affected in the context of 17p13 deletions. In 90% of cases with this deletion, a missense mutation in the remaining *TP53* gene is also present and in 65% of cases with a *TP53* mutation, a deletion of this region can be found (Bosch and Dalla-Favera, 2019, Catherwood et al., 2019). This indicates that biallelic inactivation is presumably required to have an impact on tumor development (Landau et al., 2015).

Furthermore, it is of importance that in treatment naïve patients, *TP53* mutations are present in only about 10% whereas they can be identified in up to 25-50% of treatment-resistant patients. This suggests that the mutation is acquired during the course of the disease and provides for certain resistance mechanisms that cause chemoresistance (Catherwood et al., 2019, Gonzalez et al., 2011). Physiologically, p53 encoded by the *TP53* gene is a DNA-binding protein that affects transcription and thus regulates cellular proliferation. Upon DNA damage or activation of oncogenes, it is reflexively upregulated and p53 levels in the affected cells increase (Peller and Rotter, 2003). As mentioned above, this process is preceded by ATM. In the presence of genotoxic stress, ATM phosphorylates p53 and thus initiates cell cycle arrest via CDKN1A and induces apoptosis through members of the BCL2 family (Barlow et al., 1997, Burns and El-Deiry, 2003, Clarke et al., 1993). Aberrations in one or both tumor suppressors thus support the development and progression of CLL through increased genomic instability. Especially *TP53* mutations are associated with advanced disease and a short survival time (Döhner et al., 1995, Rossi et al., 2009, Zenz et al., 2008).

NOTCH1 was mutated in 1 of our 5 CLL cases. According to literature, it is one of the most frequently mutated genes in primary diagnosis of CLL in 4-20% of cases (Bosch and Dalla-Favera, 2019). It serves as a transmembrane receptor and initiates a signaling cascade which leads to activation of several genes involved in survival, proliferation and metabolism, including the oncoprotein MYC (Guruharsha et al., 2012).

BIRC3 and *MYD88* mutations, each of which were present in one of our CLL cases, are known to be mutated in approximately 2-4% of all CLLs (Bosch and Dalla-Favera, 2019). Both ultimately cause constitutive NF-KB activation. *BIRC3* mutations in CLL lead to loss of the C terminal RING finger domain (Rossi et al., 2012a) whereas *MYD88* is mostly affected by the typical L265P mutations that have already be mentioned above (Wang and Lin, 2020).

Interpreting these results, mutational analysis of certain genes using NGS could be helpful in differentiating CLL from NMZL in unclear cases. In this context, *ATM*

mutations seem to be of great importance and should lead the diagnosis in direction of CLL since they could only be identified in CLL cases and have not been found in NMZL.

4.6 Conclusions and Outlook

The main objective of this work was to characterize the genetic landscape of NMZL, a rather rare entity. Because of its rarity, the number of cases in previous studies has often been relatively small. An additional aspect of this project was to investigate whether genetic analysis using NGS is helpful to differentiate NMZLs from other small B-cell lymphomas, since the diagnosis of NMZL is still considered a diagnosis of exclusion. Discussed differential diagnoses in our project were t(14;18) negative FLs, atypical CLLs with atypical mutational or immunohistochemical profiles and LPLs. For this purpose, we performed NGS on a collective of a total of 45 samples using a customized panel. Concerning patient characteristics such as age at diagnosis and gender distribution the collective seems to be appropriately representative. The spectrum of affected genes and pathways was rather heterogeneous. Nevertheless, we observed that numerous altered genes are engaged in processes of epigenetic regulation and chromatin remodeling. In addition, pathways such as NF-KB and NOTCH, which physiologically play an important role in the regulation of B-cell homeostasis, were frequently affected by mutations.

These results are consistent with comparable studies in many aspects, but not in all. Some previous studies identified accumulated mutations exclusive to NMZL, which in our study were only detected in individual cases. In the work of Spina et al, these were *PTPRD* mutations, which occurred in 20% of the cases. To examine this in our collective, we performed mutation analyses for this gene in a group of cases but identified only one case with this aberration. Moreover, Pillonel et al described *BRAF* mutations in 16% of NMZL cases in their study whereas a *BRAF* mutation was present in one case in our study.

However, the results of our study demonstrate that some mutations in fact are useful in differentiating NMZL from FL and atypical CLL. Of particular importance

are *KLF2* mutations, which may serve well to differentiate NMZL from other non-marginal zone lymphomas such as FL or CLL. On the other hand, *STAT6* mutations should guide the diagnosis towards FL in cases that are difficult to assess, as they are almost never observed in NMZL. Concerning immunohistochemical evaluation, markers have been suggested to help differentiate these two entities, namely IRTA1 and MNDA. Previous studies have described a much stronger positivity of these markers in MZL compared to FL (Wang and Cook, 2019). In subsequent experiments, it would be interesting to stain the cases we have assigned to the NMZL and FL groups with those markers and evaluate if the results match the genetic ones.

In cases with CLL as a differential diagnosis, the detection of *ATM* mutations could be important, in addition to the histopathological evaluation. These mutations occur more frequently in CLL and have not yet been detected in NMZL.

In summary, the results of the project have helped to provide a better insight into the histology and genetic background of NMZL compared to other lymphomas. Nevertheless, many questions have been left unanswered and need to be clarified in additional studies and experiments. For instance, in a few cases we were not able to detect gene mutations with the 78 analyzed genes. It is possible that other mutated genes that have not yet been documented could be involved in the pathogenesis of NMZL. Furthermore, neither alterations in splicing variants nor introns and deviations in copy number have been investigated in this study. These issues could be addressed in further studies such as whole genome analyses and microarray analyses. In cases without mutations, other possible pathogenetic mechanisms such as acetylation and methylation patterns need to be discussed. In addition to further genetic studies, a shift to functional assays would also be valuable to gain a better insight into the pathogenesis of NMZL. Furthermore, the analysis of clinical data could be of interest. It could be explored whether certain mutations have an impact on the course of the disease and whether specific alterations in genes such as *TP53* have led to therapy resistance in the collective. In the future, mutation analysis could also open the possibility of personalized therapy for patients depending on their mutation status. Thus, therapy approaches for some of the genes are already being tested. Commonly

mutated genes in NMZL are *CREBBP* and *KMT2D*, which result in reduced acetylation and methylation activity of the respective proteins. The negative effects of this reduced activity could be counteracted by restoring the physiological acetylation and methylation patterns of the affected DNA (Pasqualucci et al., 2011). Therefore, so-called histone deacetylase inhibitors (HDACIs) have been developed, which prevent the removal of these acetyl groups (Finnin et al., 1999, Singh et al., 2010). Analogously, there are H3K4 demethylase inhibitors, which may be able to reverse the effects of *KMT2D* mutant cells (Ortega-Molina et al., 2015). Such targeted therapies may represent the future of treatment for NMZL patients. However, more research is still necessary, each of which, including this one, provides a better insight into the NMZL entity.

5 Summary (English)

Nodal Marginal Zone Lymphomas (NMZL), along with Splenic Marginal Zone Lymphoma (SMZL), Extranodal Marginal Zone Lymphoma (EMZL) and primary cutaneous Marginal Zone Lymphoma (PCMZL), belong to the group of marginal zone lymphomas, which are mature small B-cell lymphomas. MZL account for approximately 6% of all lymphoid neoplasms. NMZL, as the rarest entity in this group, thus corresponds to only 1.5-1.8% of all lymphoid neoplasms. The diagnosis of this lymphoma presents a constant challenge in clinical practice. There are usually several differential diagnoses, including *BCL2* negative follicular lymphoma, chronic lymphocytic leukemia and lymphoplasmacytic lymphoma. NMZL frequently is a diagnosis of exclusion. Accurate histopathologic, immunophenotypic, and genetic analysis is essential. To date, no specific treatment exists for this type of lymphoma, which is why the therapeutic principles of other, more common indolent B-cell lymphomas are being adopted. Histologically, the growth pattern and morphology of the malignant cells is heterogeneous. In addition, the immunophenotype is rather unspecific, which makes a reliable diagnosis difficult. Mutation analysis may be an important pillar of diagnosis. In the past, some studies on the genetic background have been performed, but their validity is often limited by the low number of cases. The main objective of this thesis was to gain a more detailed insight into the genetic background of this entity by analyzing a large number of NMZL cases. For this purpose, all cases with differential diagnosis of NMZL from 2010 to 2023 were histologically evaluated and DNA integrity was assessed using PCR, and subsequently subjected to NGS. Five cases had to be excluded from mutation analysis due to poor quality, with a final cohort of 44 cases. After obtaining the mutation analysis, these cases were again subjected to histopathological evaluation and then divided into 3 groups: NMZL, t(14;18) negative FL, and CLL with atypical immunohistochemical profiles. The former comprised 29 cases, which were subdivided into 3 histological subgroups: 22 cases corresponded to the classic presentation of NMZL, 4 were CD5 positive, and 3 could be assigned to the splenic subtype. Overall, *KLF2* was the most frequently mutated gene. Physiologically, this factor is crucial for the development

of B cells and is usually associated with a loss-of-function mutation in lymphomas. Since this mutation occurs frequently in MZL and rather rarely in other small B-cell lymphomas, its occurrence could facilitate the diagnosis of NMZL. Furthermore, it can be assumed that aberrations in chromatin remodeling and epigenetic regulation play a particularly important role in the development of NMZL, since genes involved in these processes were mutated most frequently, including *KMT2D* and *TBL1XR1*. Moreover, we observed that NF-KB and NOTCH signaling pathways, which are essential for normal B-cell development and maturation, were often affected by mutations. These results seem to be in close agreement with comparable studies. Overall, the mutational pattern is very similar to that of SMZL, which is why other aspects are more relevant to distinguish NMZL from SMZL. However, for the differential diagnoses with FL and CLL, mutation analysis is of value as demonstrated in this study. In summary, we identified *STAT6* mutations in *BCL2*-negative FLs and *ATM* mutations in CLL, each of which were not observed in the group of NMZL. Nevertheless, the number of cases was too small to draw a substantiated conclusion. Because of the size of the panel we were unable to identify mutations in all cases.

Our study demonstrates that not a single mutation is exclusive to any disease; however, the mutational profile was very helpful to increase the accuracy in the diagnosis.

In the future, this could help to achieve the overall goal of providing NMZL patients with a targeted therapy tailored to their specific mutation profile.

6 Zusammenfassung (Deutsch)

Nodale Marginalzonenlymphome (NMZL) gehören mit splenischen Marginalzonenlymphomen (SMZL), extranodalen Marginalzonenlymphomen (EMZL) und primär kutanen Marginalzonenlymphomen (PCMZL) zu der Gruppe der Marginalzonenlymphome, die den reifen kleinzelligen B-Zell Lymphomen angehören. MZL etwa 6% aller lymphoiden Neoplasien aus. Das NMZL als seltenste Entität dieser Gruppe entspricht damit nur 1,5-1,8% aller lymphoiden Neoplasien. Die Diagnose dieses Lymphoms stellt immer wieder eine Herausforderung im klinischen Alltag dar. Meist stehen viele Differentialdiagnosen im Raum, darunter das *BCL2* negative follikuläre Lymphom und die chronisch lymphatische Leukämie. Das NMZL ist oft nur eine Ausschlussdiagnose. Umso wichtiger ist also eine genaue histopathologische, immunophänotypische und genetische Analyse. Bisher existiert keine spezielle Therapie für diese Art der Lymphome, weshalb die Therapieprinzipien anderer, häufigerer indolenter B Zell Lymphome übernommen werden. Histologisch gestaltet sich das Wachstumsmuster und die Morphologie der malignen Zellen heterogen. Dazu kommt, dass der Immunophänotyp recht unspezifisch ist, was eine sicherer Diagnosestellung erschwert. Die Mutationsanalyse stellt einen wichtigen Pfeiler der Diagnosefindung dar. In der Vergangenheit wurden schon einige Studien zum genetischen Hintergrund durchgeführt, deren Aussagekraft jedoch oft durch die niedrige Zahl an Fällen eingeschränkt ist. Das Hauptziel dieser Arbeit war die Analyse einer großen Zahl von NMZL Fällen um einen detaillierteren Einblick in den genetischen Hintergrund dieser Entität zu erlangen. Dafür wurden alle Fälle mit der Differentialdiagnose NMZL von 2010 bis 2023 histologisch evaluiert und die DNA Integrität mittels PCR überprüft. Anschließend führten wir Next Generation Sequencing mit den Proben durch. Fünf Fälle mussten aufgrund von mangelnder Qualität von der Mutationsanalyse ausgeschlossen werden mit einem finalen Kollektiv von 44 Fällen. Nach der Mutationsanalyse wurden diese Fälle erneut einer histopathologischen Evaluation unterzogen und anschließend in 3 Gruppen eingeteilt: NMZL, t(14;18) negative FL und CLL mit atypischem immunhistochemischem Profil. Erstere umfasst 29 Fälle, wobei diese wiederum in 3 histologische Untergruppen

unterteilt wurde: 22 Fälle entsprachen dem klassischen Bild eines NMZL, 4 waren CD5 positiv und 3 konnten dem splenischen Subtyp zugeordnet werden. Insgesamt war KLF2 das am häufigsten mutierte Gen. Dieser ist physiologisch wichtig für die Entwicklung von B-Zellen und geht in Lymphomen meist mit einer loss of function Mutation einher. Da diese Mutation gehäuft in MZL und eher selten in anderen kleinzelligen B Zell Lymphomen vorkommt, könnte das Auftreten dieser die Diagnosestellung NMZL vereinfachen. Des Weiteren lässt sich vermuten, dass Aberrationen im Chromatin Remodelling und der epigenetischen Regulation eine besonders wichtige Rolle für die Entstehung von NMZL spielen, da Gene die an die diesen Vorgängen beteiligt sind am häufigsten mutiert waren, darunter *KMT2D* und *TBL1XR1*. Zudem war zu beobachten, dass die Signalwege NF-KB und NOTCH, die im gesunden Organismus essenteil für die Entwicklung und Reifung von B Zellen sind, oft von Mutationen betroffen waren. Diese Ergebnisse scheinen gut mit vergleichbaren Studien übereinzustimmen. Insgesamt ähnelt das Mutationsmuster sehr dem von SMZL, weshalb zur Unterscheidung von diesem eher andere Aspekte eine Rolle spielen. Für die Unterscheidung zweier weiterer wichtiger Differenzialdiagnosen, FL und CLL, zu NMZL haben die Mutationsanalysen laut unserer Ergebnisse einen wichtigen Stellenwert. So konnten wir in *BCL2* negativen FLs gehäuft *STAT6* Mutationen und in CLL *ATM* Mutationen identifizieren, die jeweils nicht in der Gruppe von NMZL zu beobachten waren. Um eine fundierte Aussage zu treffen war hier jedoch die Anzahl der Fälle zu niedrig. Aufgrund der Größe des Panels konnten wir nicht in allen Fällen Mutationen identifizieren.

Mit unserer Studie konnten wir demonstrieren, dass keine einzelne Mutation exklusiv einer einzigen Entität zuzuordnen ist, jedoch ist die Kenntnis des Mutationsprofils sehr hilfreich in der Präzision der Diagnosestellung.

In Zukunft könnte damit das übergeordnete Ziel erreicht werden, NMZL Patienten eine zielgerichtete, auf das jeweilige Mutationsprofil zugeschnittene Therapie zu bieten.

7 References

ALAGGIO, R., AMADOR, C., ANAGNOSTOPOULOS, I., ATTYGALLE, A. D., ARAUJO, I. B. O., BERTI, E., BHAGAT, G., BORGES, A. M., BOYER, D., CALAMINICI, M., CHADBURN, A., CHAN, J. K. C., CHEUK, W., CHNG, W. J., CHOI, J. K., CHUANG, S. S., COUPLAND, S. E., CZADER, M., DAVE, S. S., DE JONG, D., DU, M. Q., ELENITOBA-JOHNSON, K. S., FERRY, J., GEYER, J., GRATZINGER, D., GUITART, J., GUJRAL, S., HARRIS, M., HARRISON, C. J., HARTMANN, S., HOCHHAUS, A., JANSEN, P. M., KARUBE, K., KEMPF, W., KHOURY, J., KIMURA, H., KLAPPER, W., KOVACH, A. E., KUMAR, S., LAZAR, A. J., LAZZI, S., LEONCINI, L., LEUNG, N., LEVENTAKI, V., LI, X. Q., LIM, M. S., LIU, W. P., LOUISSAINT, A., JR., MARCOGLIESE, A., MEDEIROS, L. J., MICHAL, M., MIRANDA, R. N., MITTELDORF, C., MONTES-MORENO, S., MORICE, W., NARDI, V., NARESH, K. N., NATKUNAM, Y., NG, S. B., OSCHLIES, I., OTT, G., PARRENS, M., PULITZER, M., RAJKUMAR, S. V., RAWSTRON, A. C., RECH, K., ROSENWALD, A., SAID, J., SARKOZY, C., SAYED, S., SAYGIN, C., SCHUH, A., SEWELL, W., SIEBERT, R., SOHANI, A. R., TOOZE, R., TRAVERSE-GLEHEN, A., VEGA, F., VERGIER, B., WECHALEKAR, A. D., WOOD, B., XERRI, L. & XIAO, W. 2022. The 5th edition of the World Health Organization Classification of Haematolymphoid Tumours: Lymphoid Neoplasms. *Leukemia,* 36**,** 1720-1748.

ALLAN, J., MITCHELL, T., HARBORNE, N., BOHM, L. & CRANE-ROBINSON, C. 1986. Roles of H1 domains in determining higher order chromatin structure and H1 location. *J Mol Biol,* 187**,** 591-601.

ALLMAN, D. & PILLAI, S. 2008. Peripheral B cell subsets. *Curr Opin Immunol,* 20**,** 149-57.

ANDERSON, L. A., PFEIFFER, R., WARREN, J. L., LANDGREN, O., GADALLA, S., BERNDT, S. I., RICKER, W., PARSONS, R., WHEELER, W. & ENGELS, E. A. 2008. Hematopoietic malignancies associated with viral and alcoholic hepatitis. *Cancer Epidemiol Biomarkers Prev,* 17**,** 3069-75.

ANGELOPOULOU, M. K., KALPADAKIS, C., PANGALIS, G. A., KYRTSONIS, M. C. & VASSILAKOPOULOS, T. P. 2014. Nodal marginal zone lymphoma. *Leuk Lymphoma,* 55**,** 1240-50.

ARCAINI, L., LUCIONI, M., BOVERI, E. & PAULLI, M. 2009. Nodal marginal zone lymphoma: current knowledge and future directions of an heterogeneous disease. *Eur J Haematol,* 83**,** 165-74.

ARCAINI, L., PAULLI, M., BURCHERI, S., ROSSI, A., SPINA, M., PASSAMONTI, F., LUCIONI, M., MOTTA, T., CANZONIERI, V., MONTANARI, M., BONOLDI, E., GALLAMINI, A., UZIEL, L., CRUGNOLA, M., RAMPONI, A., MONTANARI, F., PASCUTTO, C., MORRA, E. & LAZZARINO, M. 2007. Primary nodal marginal zone B-cell lymphoma: clinical features and prognostic assessment of a rare disease. *Br J Haematol,* 136**,** 301-4.

ARMAND, M., BESSON, C., HERMINE, O. & DAVI, F. 2017. Hepatitis C virus - Associated marginal zone lymphoma. *Best Pract Res Clin Haematol,* 30**,** 41-49.

ARRUGA, F., VAISITTI, T. & DEAGLIO, S. 2018. The NOTCH Pathway and Its Mutations in Mature B Cell Malignancies. *Front Oncol,* 8**,** 550.

ASTER, J. C., PEAR, W. S. & BLACKLOW, S. C. 2017. The Varied Roles of Notch in Cancer. *Annu Rev Pathol,* 12**,** 245-275.

BANIN, S., MOYAL, L., SHIEH, S., TAYA, Y., ANDERSON, C. W., CHESSA, L., SMORODINSKY, N. I., PRIVES, C., REISS, Y., SHILOH, Y. & ZIV, Y. 1998. Enhanced phosphorylation of p53 by ATM in response to DNA damage. *Science,* 281**,** 1674-7.

BARLOW, C., BROWN, K. D., DENG, C. X., TAGLE, D. A. & WYNSHAW-BORIS, A. 1997. Atm selectively regulates distinct p53-dependent cell-cycle checkpoint and apoptotic pathways. *Nat Genet,* 17**,** 453-6.

BEDNAR, J., GARCIA-SAEZ, I., BOOPATHI, R., CUTTER, A. R., PAPAI, G., REYMER, A., SYED, S. H., LONE, I. N., TONCHEV, O., CRUCIFIX, C., MENONI, H., PAPIN, C., SKOUFIAS, D. A., KURUMIZAKA, H., LAVERY, R., HAMICHE, A., HAYES, J. J., SCHULTZ, P., ANGELOV, D., PETOSA, C. & DIMITROV, S. 2017. Structure and Dynamics of a 197 bp Nucleosome in Complex with Linker Histone H1. *Mol Cell,* 66**,** 384-397.e8.

BERGER, F., FELMAN, P., THIEBLEMONT, C., PRADIER, T., BASEGGIO, L., BRYON, P. A., SALLES, G., CALLET-BAUCHU, E. & COIFFIER, B. 2000. Non-MALT marginal zone B-cell lymphomas: a description of clinical presentation and outcome in 124 patients. *Blood,* 95**,** 1950-6.

BERGER, F., TRAVERSE-GLEHEN, A., FELMAN, P., CALLET-BAUCHU, E., BASEGGIO, L., GAZZO, S., THIEBLEMONT, C., FFRENCH, M., MAGAUD, J. P., SALLES, G. & COIFFER, B. 2005. Clinicopathologic features of Waldenstrom's macroglobulinemia and marginal zone lymphoma: are they distinct or the same entity? *Clin Lymphoma,* 5**,** 220-4.

BERTONI, F., CONCONI, A., LUMINARI, S., REALINI, C., ROGGERO, E., BALDINI, L., CAROBBIO, S., CAVALLI, F., NERI, A. & ZUCCA, E. 2000. Lack of CD95/FAS gene somatic mutations in extranodal, nodal and splenic marginal zone B cell lymphomas. *Leukemia,* 14**,** 446-8.

BERTONI, F., ROSSI, D. & ZUCCA, E. 2018. Recent advances in understanding the biology of marginal zone lymphoma. *F1000Res,* 7**,** 406.

BERTRAND, F. E., ECKFELDT, C. E., LYSHOLM, A. S. & LEBIEN, T. W. 2000. Notch-1 and Notch-2 exhibit unique patterns of expression in human B-lineage cells. *Leukemia,* 14**,** 2095-102.

BHATTACHARYA, D., CHEAH, M. T., FRANCO, C. B., HOSEN, N., PIN, C. L., SHA, W. C. & WEISSMAN, I. L. 2007. Transcriptional profiling of antigen-dependent murine B cell differentiation and memory formation. *J Immunol,* 179**,** 6808-19.

BLOKZIJL, A., DAHLQVIST, C., REISSMANN, E., FALK, A., MOLINER, A., LENDAHL, U. & IBÁÑEZ, C. F. 2003. Cross-talk between the Notch and TGF-beta signaling pathways mediated by interaction of the Notch intracellular domain with Smad3. *J Cell Biol,* 163**,** 723-8.

BOICE, M., SALLOUM, D., MOURCIN, F., SANGHVI, V., AMIN, R., ORICCHIO, E., JIANG, M., MOTTOK, A., DENIS-LAGACHE, N., CIRIELLO, G., TAM,

W., TERUYA-FELDSTEIN, J., DE STANCHINA, E., CHAN, W. C., MALEK, S. N., ENNISHI, D., BRENTJENS, R. J., GASCOYNE, R. D., COGNÉ, M., TARTE, K. & WENDEL, H. G. 2016. Loss of the HVEM Tumor Suppressor in Lymphoma and Restoration by Modified CAR-T Cells. *Cell,* 167**,** 405-418.e13.

BONATO, M., PITTALUGA, S., TIERENS, A., CRIEL, A., VERHOEF, G., WLODARSKA, I., VANUTYSEL, L., MICHAUX, L., VANDEKERCKHOVE, P., VAN DEN BERGHE, H. & DE WOLF-PEETERS, C. 1998. Lymph node histology in typical and atypical chronic lymphocytic leukemia. *Am J Surg Pathol,* 22**,** 49-56.

BONFIGLIO, F., BRUSCAGGIN, A., GUIDETTI, F., TERZI DI BERGAMO, L., FADERL, M., SPINA, V., CONDOLUCI, A., BONOMINI, L., FORESTIERI, G., KOCH, R., PIFFARETTI, D., PINI, K., PIROSA, M. C., CITTONE, M. G., ARRIBAS, A., LUCIONI, M., GHILARDI, G., WU, W., ARCAINI, L., BAPTISTA, M. J., BASTIDAS, G., BEA, S., BOLDORINI, R., BROCCOLI, A., BUEHLER, M. M., CANZONIERI, V., CASCIONE, L., CERIANI, L., COGLIATTI, S., CORRADINI, P., DERENZINI, E., DEVIZZI, L., DIETRICH, S., ELIA, A. R., FACCHETTI, F., GAIDANO, G., GARCIA, J. F., GERBER, B., GHIA, P., GOMES DA SILVA, M., GRITTI, G., GUIDETTI, A., HITZ, F., INGHIRAMI, G., LADETTO, M., LOPEZ-GUILLERMO, A., LUCCHINI, E., MAIORANA, A., MARASCA, R., MATUTES, E., MEIGNIN, V., MERLI, M., MOCCIA, A., MOLLEJO, M., MONTALBAN, C., NOVAK, U., OSCIER, D. G., PASSAMONTI, F., PIAZZA, F., PIZZOLITTO, S., RAMBALDI, A., SABATTINI, E., SALLES, G., SANTAMBROGIO, E., SCARFÒ, L., STATHIS, A., STÜSSI, G., GEYER, J. T., TAPIA, G., TARELLA, C., THIEBLEMONT, C., TOUSSEYN, T., TUCCI, A., VANINI, G., VISCO, C., VITOLO, U., WALEWSKA, R., ZAJA, F., ZENZ, T., ZINZANI, P. L., KHIABANIAN, H., CALCINOTTO, A., BERTONI, F., BHAGAT, G., CAMPO, E., DE LEVAL, L., DIRNHOFER, S., PILERI, S. A., PIRIS, M. A., TRAVERSE-GLEHEN, A., TZANKOV, A., PAULLI, M., PONZONI, M., MAZZUCCHELLI, L., CAVALLI, F., ZUCCA, E. & ROSSI, D. 2022. Genetic and phenotypic attributes of splenic marginal zone lymphoma. *Blood,* 139**,** 732-747.

BOSCH, F. & DALLA-FAVERA, R. 2019. Chronic lymphocytic leukaemia: from genetics to treatment. *Nat Rev Clin Oncol,* 16**,** 684-701.

BOUVARD, V., BAAN, R., STRAIF, K., GROSSE, Y., SECRETAN, B., EL GHISSASSI, F., BENBRAHIM-TALLAA, L., GUHA, N., FREEMAN, C., GALICHET, L. & COGLIANO, V. 2009. A review of human carcinogens--Part B: biological agents. *Lancet Oncol,* 10**,** 321-2.

BRACCI, P. M., BENAVENTE, Y., TURNER, J. J., PALTIEL, O., SLAGER, S. L., VAJDIC, C. M., NORMAN, A. D., CERHAN, J. R., CHIU, B. C., BECKER, N., COCCO, P., DOGAN, A., NIETERS, A., HOLLY, E. A., KANE, E. V., SMEDBY, K. E., MAYNADIÉ, M., SPINELLI, J. J., ROMAN, E., GLIMELIUS, B., WANG, S. S., SAMPSON, J. N., MORTON, L. M. & DE SANJOSÉ, S. 2014. Medical history, lifestyle, family history, and occupational risk factors for marginal zone lymphoma: the InterLymph Non-Hodgkin Lymphoma Subtypes Project. *J Natl Cancer Inst Monogr,* 2014**,** 52-65.

BROU, C., LOGEAT, F., GUPTA, N., BESSIA, C., LEBAIL, O., DOEDENS, J. R., CUMANO, A., ROUX, P., BLACK, R. A. & ISRAËL, A. 2000. A novel proteolytic cleavage involved in Notch signaling: the role of the disintegrin-metalloprotease TACE. *Mol Cell,* 5**,** 207-16.

BUCKLEY, A. F., KUO, C. T. & LEIDEN, J. M. 2001. Transcription factor LKLF is sufficient to program T cell quiescence via a c-Myc-dependent pathway. *Nat Immunol,* 2**,** 698-704.

BURNS, K., MARTINON, F., ESSLINGER, C., PAHL, H., SCHNEIDER, P., BODMER, J. L., DI MARCO, F., FRENCH, L. & TSCHOPP, J. 1998. MyD88, an adapter protein involved in interleukin-1 signaling. *J Biol Chem,* 273**,** 12203-9.

BURNS, T. F. & EL-DEIRY, W. S. 2003. Microarray analysis of p53 target gene expression patterns in the spleen and thymus in response to ionizing radiation. *Cancer Biol Ther,* 2**,** 431-43.

CAMACHO, F. I., ALGARA, P., MOLLEJO, M., GARCÍA, J. F., MONTALBÁN, C., MARTÍNEZ, N., SÁNCHEZ-BEATO, M. & PIRIS, M. A. 2003. Nodal marginal zone lymphoma: a heterogeneous tumor: a comprehensive analysis of a series of 27 cases. *Am J Surg Pathol,* 27**,** 762-71.

CAMPO, E., JAFFE, E. S., COOK, J. R., QUINTANILLA-MARTINEZ, L., SWERDLOW, S. H., ANDERSON, K. C., BROUSSET, P., CERRONI, L., DE LEVAL, L., DIRNHOFER, S., DOGAN, A., FELDMAN, A. L., FEND, F., FRIEDBERG, J. W., GAULARD, P., GHIA, P., HORWITZ, S. M., KING, R. L., SALLES, G., SAN-MIGUEL, J., SEYMOUR, J. F., TREON, S. P., VOSE, J. M., ZUCCA, E., ADVANI, R., ANSELL, S., AU, W. Y., BARRIONUEVO, C., BERGSAGEL, L., CHAN, W. C., COHEN, J. I., D'AMORE, F., DAVIES, A., FALINI, B., GHOBRIAL, I. M., GOODLAD, J. R., GRIBBEN, J. G., HSI, E. D., KAHL, B. S., KIM, W. S., KUMAR, S., LACASCE, A. S., LAURENT, C., LENZ, G., LEONARD, J. P., LINK, M. P., LOPEZ-GUILLERMO, A., MATEOS, M. V., MACINTYRE, E., MELNICK, A. M., MORSCHHAUSER, F., NAKAMURA, S., NARBAITZ, M., PAVLOVSKY, A., PILERI, S. A., PIRIS, M., PRO, B., RAJKUMAR, V., ROSEN, S. T., SANDER, B., SEHN, L., SHIPP, M. A., SMITH, S. M., STAUDT, L. M., THIEBLEMONT, C., TOUSSEYN, T., WILSON, W. H., YOSHINO, T., ZINZANI, P. L., DREYLING, M., SCOTT, D. W., WINTER, J. N. & ZELENETZ, A. D. 2022. The International Consensus Classification of Mature Lymphoid Neoplasms: a report from the Clinical Advisory Committee. *Blood,* 140**,** 1229-1253.

CAMPO, E., MIQUEL, R., KRENACS, L., SORBARA, L., RAFFELD, M. & JAFFE, E. S. 1999. Primary nodal marginal zone lymphomas of splenic and MALT type. *Am J Surg Pathol,* 23**,** 59-68.

CARBONE, A., ROULLAND, S., GLOGHINI, A., YOUNES, A., VON KEUDELL, G., LÓPEZ-GUILLERMO, A. & FITZGIBBON, J. 2019. Follicular lymphoma. *Nat Rev Dis Primers,* 5**,** 83.

CATHERWOOD, M. A., GONZALEZ, D., DONALDSON, D., CLIFFORD, R., MILLS, K. & THORNTON, P. 2019. Relevance of TP53 for CLL diagnostics. *J Clin Pathol,* 72**,** 343-346.

CERHAN, J. R. & HABERMANN, T. M. 2021. Epidemiology of Marginal Zone Lymphoma. *Ann Lymphoma,* 5.

CHAPUY, B., STEWART, C., DUNFORD, A. J., KIM, J., KAMBUROV, A., REDD, R. A., LAWRENCE, M. S., ROEMER, M. G. M., LI, A. J., ZIEPERT, M., STAIGER, A. M., WALA, J. A., DUCAR, M. D., LESHCHINER, I., RHEINBAY, E., TAYLOR-WEINER, A., COUGHLIN, C. A., HESS, J. M., PEDAMALLU, C. S., LIVITZ, D., ROSEBROCK, D., ROSENBERG, M., TRACY, A. A., HORN, H., VAN HUMMELEN, P., FELDMAN, A. L., LINK, B. K., NOVAK, A. J., CERHAN, J. R., HABERMANN, T. M., SIEBERT, R., ROSENWALD, A., THORNER, A. R., MEYERSON, M. L., GOLUB, T. R., BEROUKHIM, R., WULF, G. G., OTT, G., RODIG, S. J., MONTI, S., NEUBERG, D. S., LOEFFLER, M., PFREUNDSCHUH, M., TRÜMPER, L., GETZ, G. & SHIPP, M. A. 2018. Molecular subtypes of diffuse large B cell lymphoma are associated with distinct pathogenic mechanisms and outcomes. *Nat Med,* 24**,** 679-690.

CHEAH, C. Y., ZUCCA, E., ROSSI, D. & HABERMANN, T. M. 2022. Marginal zone lymphoma: present status and future perspectives. *Haematologica,* 107**,** 35-43.

CHESON, B. D., FISHER, R. I., BARRINGTON, S. F., CAVALLI, F., SCHWARTZ, L. H., ZUCCA, E. & LISTER, T. A. 2014. Recommendations for initial evaluation, staging, and response assessment of Hodgkin and non-Hodgkin lymphoma: the Lugano classification. *J Clin Oncol,* 32**,** 3059-68.

CHU, Y., VAHL, J. C., KUMAR, D., HEGER, K., BERTOSSI, A., WÓJTOWICZ, E., SOBERON, V., SCHENTEN, D., MACK, B., REUTELSHÖFER, M., BEYAERT, R., AMANN, K., VAN LOO, G. & SCHMIDT-SUPPRIAN, M. 2011. B cells lacking the tumor suppressor TNFAIP3/A20 display impaired differentiation and hyperactivation and cause inflammation and autoimmunity in aged mice. *Blood,* 117**,** 2227-36.

CLARKE, A. R., PURDIE, C. A., HARRISON, D. J., MORRIS, R. G., BIRD, C. C., HOOPER, M. L. & WYLLIE, A. H. 1993. Thymocyte apoptosis induced by p53-dependent and independent pathways. *Nature,* 362**,** 849-52.

CLIPSON, A., WANG, M., DE LEVAL, L., ASHTON-KEY, M., WOTHERSPOON, A., VASSILIOU, G., BOLLI, N., GROVE, C., MOODY, S., ESCUDERO-IBARZ, L., GUNDEM, G., BRUGGER, K., XUE, X., MI, E., BENCH, A., SCOTT, M., LIU, H., FOLLOWS, G., ROBLES, E. F., MARTINEZ-CLIMENT, J. A., OSCIER, D., WATKINS, A. J. & DU, M. Q. 2015. KLF2 mutation is the most frequent somatic change in splenic marginal zone lymphoma and identifies a subset with distinct genotype. *Leukemia,* 29**,** 1177-85.

COMPAGNO, M., LIM, W. K., GRUNN, A., NANDULA, S. V., BRAHMACHARY, M., SHEN, Q., BERTONI, F., PONZONI, M., SCANDURRA, M., CALIFANO, A., BHAGAT, G., CHADBURN, A., DALLA-FAVERA, R. & PASQUALUCCI, L. 2009. Mutations of multiple genes cause deregulation of NF-kappaB in diffuse large B-cell lymphoma. *Nature,* 459**,** 717-21.

CRIEL, A., MICHAUX, L. & DE WOLF-PEETERS, C. 1999. The concept of typical and atypical chronic lymphocytic leukaemia. *Leuk Lymphoma,* 33**,** 33-45.

DAL MASO, L. & FRANCESCHI, S. 2006. Hepatitis C virus and risk of lymphoma and other lymphoid neoplasms: a meta-analysis of epidemiologic studies. *Cancer Epidemiol Biomarkers Prev,* 15**,** 2078-85.

DAVIES, H., BIGNELL, G. R., COX, C., STEPHENS, P., EDKINS, S., CLEGG, S., TEAGUE, J., WOFFENDIN, H., GARNETT, M. J., BOTTOMLEY, W., DAVIS, N., DICKS, E., EWING, R., FLOYD, Y., GRAY, K., HALL, S., HAWES, R., HUGHES, J., KOSMIDOU, V., MENZIES, A., MOULD, C., PARKER, A., STEVENS, C., WATT, S., HOOPER, S., WILSON, R., JAYATILAKE, H., GUSTERSON, B. A., COOPER, C., SHIPLEY, J., HARGRAVE, D., PRITCHARD-JONES, K., MAITLAND, N., CHENEVIX-TRENCH, G., RIGGINS, G. J., BIGNER, D. D., PALMIERI, G., COSSU, A., FLANAGAN, A., NICHOLSON, A., HO, J. W., LEUNG, S. Y., YUEN, S. T., WEBER, B. L., SEIGLER, H. F., DARROW, T. L., PATERSON, H., MARAIS, R., MARSHALL, C. J., WOOSTER, R., STRATTON, M. R. & FUTREAL, P. A. 2002. Mutations of the BRAF gene in human cancer. *Nature,* 417**,** 949-54.

DE VOS, S., GOY, A., DAKHIL, S. R., SALEH, M. N., MCLAUGHLIN, P., BELT, R., FLOWERS, C. R., KNAPP, M., HART, L., PATEL-DONNELLY, D., GLENN, M., GREGORY, S. A., HOLLADAY, C., ZHANG, T. & BORAL, A. L. 2009. Multicenter randomized phase II study of weekly or twice-weekly bortezomib plus rituximab in patients with relapsed or refractory follicular or marginal-zone B-cell lymphoma. *J Clin Oncol,* 27**,** 5023-30.

DEGUINE, J. & BARTON, G. M. 2014. MyD88: a central player in innate immune signaling. *F1000Prime Rep,* 6**,** 97.

DEVERAUX, Q. L., ROY, N., STENNICKE, H. R., VAN ARSDALE, T., ZHOU, Q., SRINIVASULA, S. M., ALNEMRI, E. S., SALVESEN, G. S. & REED, J. C. 1998. IAPs block apoptotic events induced by caspase-8 and cytochrome c by direct inhibition of distinct caspases. *Embo j,* 17**,** 2215-23.

DHAR, S. S. & LEE, M. G. 2021. Cancer-epigenetic function of the histone methyltransferase KMT2D and therapeutic opportunities for the treatment of KMT2D-deficient tumors. *Oncotarget,* 12**,** 1296-1308.

DI NAPOLI, A., ATTARBASCHI, A. & OSCHLIES, I. 2022. Paediatric nodal marginal zone lymphoma. *In:* ALAGGIO, R. (ed.) *WHO Classification of Tumours Editorial Board. Haematolymphoid Tumours.* 5 ed. Lyon (France): International Agency for Research on Cancer.

DI SANTO, J. P. 2001. Lung Krüpple-like factor: a quintessential player in T cell quiescence. *Nat Immunol,* 2**,** 667-8.

DING, H., ZHAO, J., ZHANG, Y., YU, J., LIU, M., LI, X., XU, L., LIN, M., LIU, C., HE, Z., CHEN, S. & JIANG, H. 2019. Systematic Analysis of Drug Vulnerabilities Conferred by Tumor Suppressor Loss. *Cell Rep,* 27**,** 3331-3344.e6.

DÖHNER, H., FISCHER, K., BENTZ, M., HANSEN, K., BENNER, A., CABOT, G., DIEHL, D., SCHLENK, R., COY, J., STILGENBAUER, S., VOLKMANN, M., GALLE, P. R., POUSTKA, A., HUNSTEIN, W. & LICHTER, P. 1995. p53 gene deletion predicts for poor survival and non-response to therapy with purine analogs in chronic B-cell leukemias. *Blood,* 85**,** 1580-9.

DOLCET, X., LLOBET, D., PALLARES, J. & MATIAS-GUIU, X. 2005. NF-kB in development and progression of human cancer. *Virchows Arch,* 446**,** 475-82.

DU, M. Q. 2011. MALT lymphoma: many roads lead to nuclear factor-κb activation. *Histopathology,* 58**,** 26-38.
DUTTA, R., TIU, B. & SAKAMOTO, K. M. 2016. CBP/p300 acetyltransferase activity in hematologic malignancies. *Mol Genet Metab,* 119**,** 37-43.
DUTTO, I., SCALERA, C. & PROSPERI, E. 2018. CREBBP and p300 lysine acetyl transferases in the DNA damage response. *Cell Mol Life Sci,* 75**,** 1325-1338.
DYHDALO, K. S., LANIGAN, C., TUBBS, R. R. & COOK, J. R. 2013. Immunoarchitectural patterns of germinal center antigens including LMO2 assist in the differential diagnosis of marginal zone lymphoma vs follicular lymphoma. *Am J Clin Pathol,* 140**,** 149-54.
ENZLER, T., BONIZZI, G., SILVERMAN, G. J., OTERO, D. C., WIDHOPF, G. F., ANZELON-MILLS, A., RICKERT, R. C. & KARIN, M. 2006. Alternative and classical NF-kappa B signaling retain autoreactive B cells in the splenic marginal zone and result in lupus-like disease. *Immunity,* 25**,** 403-15.
ERDOGAN, F., RADU, T. B., ORLOVA, A., QADREE, A. K., DE ARAUJO, E. D., ISRAELIAN, J., VALENT, P., MUSTJOKI, S. M., HERLING, M., MORIGGL, R. & GUNNING, P. T. 2022. JAK-STAT core cancer pathway: An integrative cancer interactome analysis. *J Cell Mol Med,* 26**,** 2049-2062.
FABBRI, G. & DALLA-FAVERA, R. 2016. The molecular pathogenesis of chronic lymphocytic leukaemia. *Nat Rev Cancer,* 16**,** 145-62.
FALINI, B., AGOSTINELLI, C., BIGERNA, B., PUCCIARINI, A., PACINI, R., TABARRINI, A., FALCINELLI, F., PICCIOLI, M., PAULLI, M., GAMBACORTA, M., PONZONI, M., TIACCI, E., ASCANI, S., MARTELLI, M. P., DALLA FAVERA, R., STEIN, H. & PILERI, S. A. 2012. IRTA1 is selectively expressed in nodal and extranodal marginal zone lymphomas. *Histopathology,* 61**,** 930-41.
FERRY, J. 2022. Introduction to Marginal zone lymphoma. *In:* FERRY, J. & COUPLAND, S. E. (eds.) *WHO Classification of Tumours Editorial Board. Haematolymphoid Tumours.* 5 ed. Lyon (France): International Agency for Research on Cancer.
FINNIN, M. S., DONIGIAN, J. R., COHEN, A., RICHON, V. M., RIFKIND, R. A., MARKS, P. A., BRESLOW, R. & PAVLETICH, N. P. 1999. Structures of a histone deacetylase homologue bound to the TSA and SAHA inhibitors. *Nature,* 401**,** 188-93.
FYODOROV, D. V., ZHOU, B. R., SKOULTCHI, A. I. & BAI, Y. 2018. Emerging roles of linker histones in regulating chromatin structure and function. *Nat Rev Mol Cell Biol,* 19**,** 192-206.
GAMA-NORTON, L., FERRANDO, E., RUIZ-HERGUIDO, C., LIU, Z., GUIU, J., ISLAM, A. B., LEE, S. U., YAN, M., GUIDOS, C. J., LÓPEZ-BIGAS, N., MAEDA, T., ESPINOSA, L., KOPAN, R. & BIGAS, A. 2015. Notch signal strength controls cell fate in the haemogenic endothelium. *Nat Commun,* 6**,** 8510.
GANAPATHI, K. A., JOBANPUTRA, V., IWAMOTO, F., JAIN, P., CHEN, J., CASCIONE, L., NAHUM, O., LEVY, B., XIE, Y., KHATTAR, P., HOEHN, D., BERTONI, F., MURTY, V. V., PITTALUGA, S., JAFFE, E. S., ALOBEID, B., MANSUKHANI, M. M. & BHAGAT, G. 2016. The genetic

landscape of dural marginal zone lymphomas. *Oncotarget,* 7**,** 43052-43061.
GARCIA-CARPIZO, V., RUIZ-LLORENTE, S., SARMENTERO, J., GRAÑA-CASTRO, O., PISANO, D. G. & BARRERO, M. J. 2018. CREBBP/EP300 bromodomains are critical to sustain the GATA1/MYC regulatory axis in proliferation. *Epigenetics Chromatin,* 11**,** 30.
GHISLETTI, S., HUANG, W., JEPSEN, K., BENNER, C., HARDIMAN, G., ROSENFELD, M. G. & GLASS, C. K. 2009. Cooperative NCoR/SMRT interactions establish a corepressor-based strategy for integration of inflammatory and anti-inflammatory signaling pathways. *Genes Dev,* 23**,** 681-93.
GITELSON, E., AL-SALEEM, T., ROBU, V., MILLENSON, M. M. & SMITH, M. R. 2010. Pediatric nodal marginal zone lymphoma may develop in the adult population. *Leuk Lymphoma,* 51**,** 89-94.
GLASER, S. L. & JARRETT, R. F. 1996. The epidemiology of Hodgkin's disease. *Baillieres Clin Haematol,* 9**,** 401-16.
GLYNNE, R., GHANDOUR, G., RAYNER, J., MACK, D. H. & GOODNOW, C. C. 2000. B-lymphocyte quiescence, tolerance and activation as viewed by global gene expression profiling on microarrays. *Immunol Rev,* 176**,** 216-46.
GONZALEZ, D., MARTINEZ, P., WADE, R., HOCKLEY, S., OSCIER, D., MATUTES, E., DEARDEN, C. E., RICHARDS, S. M., CATOVSKY, D. & MORGAN, G. J. 2011. Mutational status of the TP53 gene as a predictor of response and survival in patients with chronic lymphocytic leukemia: results from the LRF CLL4 trial. *J Clin Oncol,* 29**,** 2223-9.
GOODARZI, A. A., NOON, A. T., DECKBAR, D., ZIV, Y., SHILOH, Y., LÖBRICH, M. & JEGGO, P. A. 2008. ATM signaling facilitates repair of DNA double-strand breaks associated with heterochromatin. *Mol Cell,* 31**,** 167-77.
GORDON, W. R., VARDAR-ULU, D., HISTEN, G., SANCHEZ-IRIZARRY, C., ASTER, J. C. & BLACKLOW, S. C. 2007. Structural basis for autoinhibition of Notch. *Nat Struct Mol Biol,* 14**,** 295-300.
GUITER, C., DUSANTER-FOURT, I., COPIE-BERGMAN, C., BOULLAND, M. L., LE GOUVELLO, S., GAULARD, P., LEROY, K. & CASTELLANO, F. 2004. Constitutive STAT6 activation in primary mediastinal large B-cell lymphoma. *Blood,* 104**,** 543-9.
GURUHARSHA, K. G., KANKEL, M. W. & ARTAVANIS-TSAKONAS, S. 2012. The Notch signalling system: recent insights into the complexity of a conserved pathway. *Nat Rev Genet,* 13**,** 654-66.
GUSTAFSSON, M. V., ZHENG, X., PEREIRA, T., GRADIN, K., JIN, S., LUNDKVIST, J., RUAS, J. L., POELLINGER, L., LENDAHL, U. & BONDESSON, M. 2005. Hypoxia requires notch signaling to maintain the undifferentiated cell state. *Dev Cell,* 9**,** 617-28.
GUTTRIDGE, D. C., ALBANESE, C., REUTHER, J. Y., PESTELL, R. G. & BALDWIN, A. S., JR. 1999. NF-kappaB controls cell growth and differentiation through transcriptional regulation of cyclin D1. *Mol Cell Biol,* 19**,** 5785-99.
HART, G. T., HOGQUIST, K. A. & JAMESON, S. C. 2012. Krüppel-like factors in lymphocyte biology. *J Immunol,* 188**,** 521-6.

HART, G. T., WANG, X., HOGQUIST, K. A. & JAMESON, S. C. 2011. Krüppel-like factor 2 (KLF2) regulates B-cell reactivity, subset differentiation, and trafficking molecule expression. *Proc Natl Acad Sci U S A,* 108**,** 716-21.

HATZI, K., JIANG, Y., HUANG, C., GARRETT-BAKELMAN, F., GEARHART, M. D., GIANNOPOULOU, E. G., ZUMBO, P., KIROUAC, K., BHASKARA, S., POLO, J. M., KORMAKSSON, M., MACKERELL, A. D., JR., XUE, F., MASON, C. E., HIEBERT, S. W., PRIVE, G. G., CERCHIETTI, L., BARDWELL, V. J., ELEMENTO, O. & MELNICK, A. 2013. A hybrid mechanism of action for BCL6 in B cells defined by formation of functionally distinct complexes at enhancers and promoters. *Cell Rep,* 4**,** 578-88.

HE, B., SANTAMARIA, R., XU, W., COLS, M., CHEN, K., PUGA, I., SHAN, M., XIONG, H., BUSSEL, J. B., CHIU, A., PUEL, A., REICHENBACH, J., MARODI, L., DÖFFINGER, R., VASCONCELOS, J., ISSEKUTZ, A., KRAUSE, J., DAVIES, G., LI, X., GRIMBACHER, B., PLEBANI, A., MEFFRE, E., PICARD, C., CUNNINGHAM-RUNDLES, C., CASANOVA, J. L. & CERUTTI, A. 2010. The transmembrane activator TACI triggers immunoglobulin class switching by activating B cells through the adaptor MyD88. *Nat Immunol,* 11**,** 836-45.

HEATHER, J. M. & CHAIN, B. 2016. The sequence of sequencers: The history of sequencing DNA. *Genomics,* 107**,** 1-8.

HEILGEIST, A., MCCLANAHAN, F., HO, A. D. & WITZENS-HARIG, M. 2013. Prognostic value of the Follicular Lymphoma International Prognostic Index score in marginal zone lymphoma: an analysis of clinical presentation and outcome in 144 patients. *Cancer,* 119**,** 99-106.

HELMING, K. C., WANG, X. & ROBERTS, C. W. M. 2014. Vulnerabilities of mutant SWI/SNF complexes in cancer. *Cancer Cell,* 26**,** 309-317.

HERRERA, J. E., WEST, K. L., SCHILTZ, R. L., NAKATANI, Y. & BUSTIN, M. 2000. Histone H1 is a specific repressor of core histone acetylation in chromatin. *Mol Cell Biol,* 20**,** 523-9.

HOEK, K. L., GORDY, L. E., COLLINS, P. L., PAREKH, V. V., AUNE, T. M., JOYCE, S., THOMAS, J. W., VAN KAER, L. & SEBZDA, E. 2010. Follicular B cell trafficking within the spleen actively restricts humoral immune responses. *Immunity,* 33**,** 254-65.

HOFFMANN, M., KLETTER, K., BECHERER, A., JÄGER, U., CHOTT, A. & RADERER, M. 2003. 18F-fluorodeoxyglucose positron emission tomography (18F-FDG-PET) for staging and follow-up of marginal zone B-cell lymphoma. *Oncology,* 64**,** 336-40.

HÖPKEN, U. E. 2017. Targeting HDAC3 in CREBBP-Mutant Lymphomas Counterstrikes Unopposed Enhancer Deacetylation of B-cell Signaling and Immune Response Genes. *Cancer Discov,* 7**,** 14-16.

HU, T., CHITNIS, N., MONOS, D. & DINH, A. 2021a. Next-generation sequencing technologies: An overview. *Hum Immunol,* 82**,** 801-811.

HU, X., LI, J., FU, M., ZHAO, X. & WANG, W. 2021b. The JAK/STAT signaling pathway: from bench to clinic. *Signal Transduct Target Ther,* 6**,** 402.

HUANG, Y. H., CAI, K., XU, P. P., WANG, L., HUANG, C. X., FANG, Y., CHENG, S., SUN, X. J., LIU, F., HUANG, J. Y., JI, M. M. & ZHAO, W. L. 2021. CREBBP/EP300 mutations promoted tumor progression in diffuse large

B-cell lymphoma through altering tumor-associated macrophage polarization via FBXW7-NOTCH-CCL2/CSF1 axis. *Signal Transduct Target Ther,* 6**,** 10.

JASO, J. M., YIN, C. C., WANG, S. A., MIRANDA, R. N., JABCUGA, C. E., CHEN, L. & MEDEIROS, L. J. 2013. Clinicopathologic features of CD5-positive nodal marginal zone lymphoma. *Am J Clin Pathol,* 140**,** 693-700.

JIANG, T., CHEN, X., SU, C., REN, S. & ZHOU, C. 2020. Pan-cancer analysis of ARID1A Alterations as Biomarkers for Immunotherapy Outcomes. *J Cancer,* 11**,** 776-780.

JIANG, Y., ORTEGA-MOLINA, A., GENG, H., YING, H. Y., HATZI, K., PARSA, S., MCNALLY, D., WANG, L., DOANE, A. S., AGIRRE, X., TEATER, M., MEYDAN, C., LI, Z., POLOWAY, D., WANG, S., ENNISHI, D., SCOTT, D. W., STENGEL, K. R., KRANZ, J. E., HOLSON, E., SHARMA, S., YOUNG, J. W., CHU, C. S., ROEDER, R. G., SHAKNOVICH, R., HIEBERT, S. W., GASCOYNE, R. D., TAM, W., ELEMENTO, O., WENDEL, H. G. & MELNICK, A. M. 2017. CREBBP Inactivation Promotes the Development of HDAC3-Dependent Lymphomas. *Cancer Discov,* 7**,** 38-53.

JIN, Y. H., KIM, H., KI, H., YANG, I., YANG, N., LEE, K. Y., KIM, N., PARK, H. S. & KIM, K. 2009. Beta-catenin modulates the level and transcriptional activity of Notch1/NICD through its direct interaction. *Biochim Biophys Acta,* 1793**,** 290-9.

JUNG, H., YOO, H. Y., LEE, S. H., SHIN, S., KIM, S. C., LEE, S., JOUNG, J. G., NAM, J. Y., RYU, D., YUN, J. W., CHOI, J. K., GHOSH, A., KIM, K. K., KIM, S. J., KIM, W. S., PARK, W. Y. & KO, Y. H. 2017. The mutational landscape of ocular marginal zone lymphoma identifies frequent alterations in TNFAIP3 followed by mutations in TBL1XR1 and CREBBP. *Oncotarget,* 8**,** 17038-17049.

JUSKEVICIUS, D., JUCKER, D., KLINGBIEL, D., MAMOT, C., DIRNHOFER, S. & TZANKOV, A. 2017. Mutations of CREBBP and SOCS1 are independent prognostic factors in diffuse large B cell lymphoma: mutational analysis of the SAKK 38/07 prospective clinical trial cohort. *J Hematol Oncol,* 10**,** 70.

KACZYNSKI, J., COOK, T. & URRUTIA, R. 2003. Sp1- and Krüppel-like transcription factors. *Genome Biol,* 4**,** 206.

KANELLIS, G., RONCADOR, G., ARRIBAS, A., MOLLEJO, M., MONTES-MORENO, S., MAESTRE, L., CAMPOS-MARTIN, Y., RÍOS GONZALEZ, J. L., MARTINEZ-TORRECUADRADA, J. L., SANCHEZ-VERDE, L., PAJARES, R., CIGUDOSA, J. C., MARTIN, M. C. & PIRIS, M. A. 2009. Identification of MNDA as a new marker for nodal marginal zone lymphoma. *Leukemia,* 23**,** 1847-57.

KAPLAN, M. H., SCHINDLER, U., SMILEY, S. T. & GRUSBY, M. J. 1996. Stat6 is required for mediating responses to IL-4 and for development of Th2 cells. *Immunity,* 4**,** 313-9.

KARIN, M. 2009. NF-kappaB as a critical link between inflammation and cancer. *Cold Spring Harb Perspect Biol,* 1**,** a000141.

KATZENBERGER, T., KALLA, J., LEICH, E., STÖCKLEIN, H., HARTMANN, E., BARNICKEL, S., WESSENDORF, S., OTT, M. M., MÜLLER-HERMELINK, H. K., ROSENWALD, A. & OTT, G. 2009. A distinctive

subtype of t(14;18)-negative nodal follicular non-Hodgkin lymphoma characterized by a predominantly diffuse growth pattern and deletions in the chromosomal region 1p36. *Blood,* 113**,** 1053-61.

KHALIL, M. O., MORTON, L. M., DEVESA, S. S., CHECK, D. P., CURTIS, R. E., WEISENBURGER, D. D. & DORES, G. M. 2014. Incidence of marginal zone lymphoma in the United States, 2001-2009 with a focus on primary anatomic site. *Br J Haematol,* 165**,** 67-77.

KNAUF, W., ABENHARDT, W., KOENIGSMANN, M., MAINTZ, C., SANDNER, R., ZAHN, M. O., SCHNELL, R., TECH, S., KAISER-OSTERHUES, A., HOUET, L. & MARSCHNER, N. 2021. Rare lymphomas in routine practice - Treatment and outcome in marginal zone lymphoma in the prospective German Tumour Registry Lymphatic Neoplasms. *Hematol Oncol,* 39**,** 313-325.

KOJIMA, M., INAGAKI, H., MOTOORI, T., ITOH, H., SHIMIZU, K., TAMAKI, Y., MURASE, T. & NAKAMURA, S. 2007. Clinical implications of nodal marginal zone B-cell lymphoma among Japanese: study of 65 cases. *Cancer Sci,* 98**,** 44-9.

KOPAN, R. & ILAGAN, M. X. 2009. The canonical Notch signaling pathway: unfolding the activation mechanism. *Cell,* 137**,** 216-33.

KRAAN, W., HORLINGS, H. M., VAN KEIMPEMA, M., SCHILDER-TOL, E. J., OUD, M. E., SCHEEPSTRA, C., KLUIN, P. M., KERSTEN, M. J., SPAARGAREN, M. & PALS, S. T. 2013. High prevalence of oncogenic MYD88 and CD79B mutations in diffuse large B-cell lymphomas presenting at immune-privileged sites. *Blood Cancer J,* 3**,** e139.

KUNG, A. L., REBEL, V. I., BRONSON, R. T., CH'NG, L. E., SIEFF, C. A., LIVINGSTON, D. M. & YAO, T. P. 2000. Gene dose-dependent control of hematopoiesis and hematologic tumor suppression by CBP. *Genes Dev,* 14**,** 272-7.

KUO, C. T., VESELITS, M. L. & LEIDEN, J. M. 1997. LKLF: A transcriptional regulator of single-positive T cell quiescence and survival. *Science,* 277**,** 1986-90.

KURODA, K., HAN, H., TANI, S., TANIGAKI, K., TUN, T., FURUKAWA, T., TANIGUCHI, Y., KUROOKA, H., HAMADA, Y., TOYOKUNI, S. & HONJO, T. 2003. Regulation of marginal zone B cell development by MINT, a suppressor of Notch/RBP-J signaling pathway. *Immunity,* 18**,** 301-12.

LANDAU, D. A., TAUSCH, E., TAYLOR-WEINER, A. N., STEWART, C., REITER, J. G., BAHLO, J., KLUTH, S., BOZIC, I., LAWRENCE, M., BÖTTCHER, S., CARTER, S. L., CIBULSKIS, K., MERTENS, D., SOUGNEZ, C. L., ROSENBERG, M., HESS, J. M., EDELMANN, J., KLESS, S., KNEBA, M., RITGEN, M., FINK, A., FISCHER, K., GABRIEL, S., LANDER, E. S., NOWAK, M. A., DÖHNER, H., HALLEK, M., NEUBERG, D., GETZ, G., STILGENBAUER, S. & WU, C. J. 2015. Mutations driving CLL and their evolution in progression and relapse. *Nature,* 526**,** 525-30.

LAURENT, C., COOK, J. R., YOSHINO, T., QUINTANILLA-MARTINEZ, L. & JAFFE, E. S. 2023. Follicular lymphoma and marginal zone lymphoma: how many diseases? *Virchows Arch,* 482**,** 149-162.

LAYBOURN, P. J. & KADONAGA, J. T. 1991. Role of nucleosomal cores and histone H1 in regulation of transcription by RNA polymerase II. *Science,* 254**,** 238-45.

LEE, J. U., HOSOTANI, R., WADA, M., DOI, R., KOSIBA, T., FUJIMOTO, K., MIYAMOTO, Y., TSUJI, S., NAKAJIMA, S., NISHIMURA, Y. & IMAMURA, M. 1999. Role of Bcl-2 family proteins (Bax, Bcl-2 and Bcl-X) on cellular susceptibility to radiation in pancreatic cancer cells. *Eur J Cancer,* 35**,** 1374-80.

LEICH, E., HOSTER, E., WARTENBERG, M., UNTERHALT, M., SIEBERT, R., KOCH, K., KLAPPER, W., ENGELHARD, M., PUPPE, B., HORN, H., STAIGER, A. M., STUHLMANN-LAEISZ, C., BERND, H. W., FELLER, A. C., HUMMEL, M., LENZE, D., STEIN, H., HARTMANN, S., HANSMANN, M. L., MÖLLER, P., HIDDEMANN, W., DREYLING, M., OTT, G. & ROSENWALD, A. 2016. Similar clinical features in follicular lymphomas with and without breaks in the BCL2 locus. *Leukemia,* 30**,** 854-60.

LENNERT, K. 1978. *Malignant lymphomas other than Hodgkin´s disease,* New York, Springer Verlag.

LI, J., LI, J., YANG, X., QIN, H., ZHOU, P., LIANG, Y. & HAN, H. 2005. The C terminus of MINT forms homodimers and abrogates MINT-mediated transcriptional repression. *Biochim Biophys Acta,* 1729**,** 50-6.

LI, J., WANG, J., WANG, J., NAWAZ, Z., LIU, J. M., QIN, J. & WONG, J. 2000. Both corepressor proteins SMRT and N-CoR exist in large protein complexes containing HDAC3. *Embo j,* 19**,** 4342-50.

LI, J. Y., DANIELS, G., WANG, J. & ZHANG, X. 2015. TBL1XR1 in physiological and pathological states. *Am J Clin Exp Urol,* 3**,** 13-23.

LI, W. X. 2008. Canonical and non-canonical JAK-STAT signaling. *Trends Cell Biol,* 18**,** 545-51.

LI, Z., WANG, H., XUE, L., SHIN, D. M., ROOPENIAN, D., XU, W., QI, C. F., SANGSTER, M. Y., ORIHUELA, C. J., TUOMANEN, E., REHG, J. E., CUI, X., ZHANG, Q., MORSE, H. C., 3RD & MORRIS, S. W. 2009. Emu-BCL10 mice exhibit constitutive activation of both canonical and noncanonical NF-kappaB pathways generating marginal zone (MZ) B-cell expansion as a precursor to splenic MZ lymphoma. *Blood,* 114**,** 4158-68.

LING, D. C., VARGO, J. A., BALASUBRAMANI, G. K. & BERIWAL, S. 2016. Underutilization of radiation therapy in early-stage marginal zone lymphoma negatively impacts overall survival. *Pract Radiat Oncol,* 6**,** e97-e105.

LIU, L., LI, Y., LI, S., HU, N., HE, Y., PONG, R., LIN, D., LU, L. & LAW, M. 2012. Comparison of next-generation sequencing systems. *J Biomed Biotechnol,* 2012**,** 251364.

LIU, T., ZHANG, L., JOO, D. & SUN, S. C. 2017. NF-κB signaling in inflammation. *Signal Transduct Target Ther,* 2**,** 17023-.

LUCAS, P. C., YONEZUMI, M., INOHARA, N., MCALLISTER-LUCAS, L. M., ABAZEED, M. E., CHEN, F. F., YAMAOKA, S., SETO, M. & NUNEZ, G. 2001. Bcl10 and MALT1, independent targets of chromosomal translocation in malt lymphoma, cooperate in a novel NF-kappa B signaling pathway. *J Biol Chem,* 276**,** 19012-9.

MARTIN, C. & ZHANG, Y. 2005. The diverse functions of histone lysine methylation. *Nat Rev Mol Cell Biol,* 6**,** 838-49.
MARTINEZ-LOPEZ, A., CURIEL-OLMO, S., MOLLEJO, M., CERECEDA, L., MARTINEZ, N., MONTES-MORENO, S., ALMARAZ, C., REVERT, J. B. & PIRIS, M. A. 2015. MYD88 (L265P) somatic mutation in marginal zone B-cell lymphoma. *Am J Surg Pathol,* 39**,** 644-51.
MATHUR, R. 2018. ARID1A loss in cancer: Towards a mechanistic understanding. *Pharmacol Ther,* 190**,** 15-23.
MATUTES, E., OSCIER, D., GARCIA-MARCO, J., ELLIS, J., COPPLESTONE, A., GILLINGHAM, R., HAMBLIN, T., LENS, D., SWANSBURY, G. J. & CATOVSKY, D. 1996. Trisomy 12 defines a group of CLL with atypical morphology: correlation between cytogenetic, clinical and laboratory features in 544 patients. *Br J Haematol,* 92**,** 382-8.
MCCARTER, A. C., WANG, Q. & CHIANG, M. 2018. Notch in Leukemia. *Adv Exp Med Biol,* 1066**,** 355-394.
MEDZHITOV, R., PRESTON-HURLBURT, P., KOPP, E., STADLEN, A., CHEN, C., GHOSH, S. & JANEWAY, C. A., JR. 1998. MyD88 is an adaptor protein in the hToll/IL-1 receptor family signaling pathways. *Mol Cell,* 2**,** 253-8.
MENTER, T., GASSER, A., JUSKEVICIUS, D., DIRNHOFER, S. & TZANKOV, A. 2015. Diagnostic Utility of the Germinal Center-associated Markers GCET1, HGAL, and LMO2 in Hematolymphoid Neoplasms. *Appl Immunohistochem Mol Morphol,* 23**,** 491-8.
MOLINA, T. J., LIN, P., SWERDLOW, S. H. & COOK, J. R. 2011. Marginal zone lymphomas with plasmacytic differentiation and related disorders. *Am J Clin Pathol,* 136**,** 211-25.
MOODY, S., ESCUDERO-IBARZ, L., WANG, M., CLIPSON, A., OCHOA RUIZ, E., DUNN-WALTERS, D., XUE, X., ZENG, N., ROBSON, A., CHUANG, S. S., COGLIATTI, S., LIU, H., GOODLAD, J., ASHTON-KEY, M., RADERER, M., BI, Y. & DU, M. Q. 2017. Significant association between TNFAIP3 inactivation and biased immunoglobulin heavy chain variable region 4-34 usage in mucosa-associated lymphoid tissue lymphoma. *J Pathol,* 243**,** 3-8.
MORIN, R. D., MENDEZ-LAGO, M., MUNGALL, A. J., GOYA, R., MUNGALL, K. L., CORBETT, R. D., JOHNSON, N. A., SEVERSON, T. M., CHIU, R., FIELD, M., JACKMAN, S., KRZYWINSKI, M., SCOTT, D. W., TRINH, D. L., TAMURA-WELLS, J., LI, S., FIRME, M. R., ROGIC, S., GRIFFITH, M., CHAN, S., YAKOVENKO, O., MEYER, I. M., ZHAO, E. Y., SMAILUS, D., MOKSA, M., CHITTARANJAN, S., RIMSZA, L., BROOKS-WILSON, A., SPINELLI, J. J., BEN-NERIAH, S., MEISSNER, B., WOOLCOCK, B., BOYLE, M., MCDONALD, H., TAM, A., ZHAO, Y., DELANEY, A., ZENG, T., TSE, K., BUTTERFIELD, Y., BIROL, I., HOLT, R., SCHEIN, J., HORSMAN, D. E., MOORE, R., JONES, S. J., CONNORS, J. M., HIRST, M., GASCOYNE, R. D. & MARRA, M. A. 2011. Frequent mutation of histone-modifying genes in non-Hodgkin lymphoma. *Nature,* 476**,** 298-303.
MOTSHWENE, P. G., MONCRIEFFE, M. C., GROSSMANN, J. G., KAO, C., AYALURU, M., SANDERCOCK, A. M., ROBINSON, C. V., LATZ, E. & GAY, N. J. 2009. An oligomeric signaling platform formed by the Toll-like

receptor signal transducers MyD88 and IRAK-4. *J Biol Chem,* 284**,** 25404-11.
MUGNAINI, E. N. & GHOSH, N. 2016. Lymphoma. *Prim Care,* 43**,** 661-675.
MULLEN, J., KATO, S., SICKLICK, J. K. & KURZROCK, R. 2021. Targeting ARID1A mutations in cancer. *Cancer Treat Rev,* 100**,** 102287.
MUMM, J. S., SCHROETER, E. H., SAXENA, M. T., GRIESEMER, A., TIAN, X., PAN, D. J., RAY, W. J. & KOPAN, R. 2000. A ligand-induced extracellular cleavage regulates gamma-secretase-like proteolytic activation of Notch1. *Mol Cell,* 5**,** 197-206.
MUZIO, M., NI, J., FENG, P. & DIXIT, V. M. 1997. IRAK (Pelle) family member IRAK-2 and MyD88 as proximal mediators of IL-1 signaling. *Science,* 278**,** 1612-5.
NAGL, N. G., JR., PATSIALOU, A., HAINES, D. S., DALLAS, P. B., BECK, G. R., JR. & MORAN, E. 2005. The p270 (ARID1A/SMARCF1) subunit of mammalian SWI/SNF-related complexes is essential for normal cell cycle arrest. *Cancer Res,* 65**,** 9236-44.
NAGL, N. G., JR., WANG, X., PATSIALOU, A., VAN SCOY, M. & MORAN, E. 2007. Distinct mammalian SWI/SNF chromatin remodeling complexes with opposing roles in cell-cycle control. *Embo j,* 26**,** 752-63.
NANDAGOPAL, N., SANTAT, L. A., LEBON, L., SPRINZAK, D., BRONNER, M. E. & ELOWITZ, M. B. 2018. Dynamic Ligand Discrimination in the Notch Signaling Pathway. *Cell,* 172**,** 869-880.e19.
NANN, D., RAMIS-ZALDIVAR, J. E., MÜLLER, I., GONZALEZ-FARRE, B., SCHMIDT, J., EGAN, C., SALMERON-VILLALOBOS, J., CLOT, G., MATTERN, S., OTTO, F., MANKEL, B., COLOMER, D., BALAGUÉ, O., SZABLEWSKI, V., LOME-MALDONADO, C., LEONCINI, L., DOJCINOV, S., CHOTT, A., COPIE-BERGMAN, C., BONZHEIM, I., FEND, F., JAFFE, E. S., CAMPO, E., SALAVERRIA, I. & QUINTANILLA-MARTINEZ, L. 2020. Follicular lymphoma t(14;18)-negative is genetically a heterogeneous disease. *Blood Adv,* 4**,** 5652-5665.
NARESH, K., FERRY, J., ROSSI, A., GEDDIE, W. R., WU, C. J., RAWSTRON, A. C., EICHHORST, B., AKINOLA, N. O., YANG, S., CHIATTONE, C., BURGER, J. A., CHIORAZZI, N., STAMATOPOULOS, K., ROSENQUIST, R., RAI, K. R., STILGENBAUER, S., VARGHESE, A. & SLAGER, S. L. 2022. Chronic lymphocytic leukaemia/small lymphocytic lymphoma. *In:* SCHUH, A. (ed.) *WHO Classification of Tumours Editorial Board. Haematolymphoid Tumours.* 5 ed. Lyon (France): International Agency for Research on Cancer.
NATHWANI, B. N., ANDERSON, J. R., ARMITAGE, J. O., CAVALLI, F., DIEBOLD, J., DRACHENBERG, M. R., HARRIS, N. L., MACLENNAN, K. A., MÜLLER-HERMELINK, H. K., ULLRICH, F. A. & WEISENBURGER, D. D. 1999. Clinical significance of follicular lymphoma with monocytoid B cells. Non-Hodgkin's Lymphoma Classification Project. *Hum Pathol,* 30**,** 263-8.
NATKUNAM, Y., ROSSI, A., ATTARBASCHI, A., DI NAPOLI, A., NARESH, K. & SHIGEO OHGAMI, R. 2022. Nodal marginal zone lymphoma. *In:* FERRY, J. (ed.) *WHO Classification of Tumours Editorial Board. Haematolymphoid*

Tumours. 5 ed. Lyon (France): International Agency for Research on Cancer.

NATKUNAM, Y., ZHAO, S., MASON, D. Y., CHEN, J., TAIDI, B., JONES, M., HAMMER, A. S., HAMILTON DUTOIT, S., LOSSOS, I. S. & LEVY, R. 2007. The oncoprotein LMO2 is expressed in normal germinal-center B cells and in human B-cell lymphomas. *Blood,* 109**,** 1636-42.

NGO, V. N., YOUNG, R. M., SCHMITZ, R., JHAVAR, S., XIAO, W., LIM, K. H., KOHLHAMMER, H., XU, W., YANG, Y., ZHAO, H., SHAFFER, A. L., ROMESSER, P., WRIGHT, G., POWELL, J., ROSENWALD, A., MULLER-HERMELINK, H. K., OTT, G., GASCOYNE, R. D., CONNORS, J. M., RIMSZA, L. M., CAMPO, E., JAFFE, E. S., DELABIE, J., SMELAND, E. B., FISHER, R. I., BRAZIEL, R. M., TUBBS, R. R., COOK, J. R., WEISENBURGER, D. D., CHAN, W. C. & STAUDT, L. M. 2011. Oncogenically active MYD88 mutations in human lymphoma. *Nature,* 470**,** 115-9.

O'SHEA, J. J. & PLENGE, R. 2012. JAK and STAT signaling molecules in immunoregulation and immune-mediated disease. *Immunity,* 36**,** 542-50.

O'SHEA, J. J., SCHWARTZ, D. M., VILLARINO, A. V., GADINA, M., MCINNES, I. B. & LAURENCE, A. 2015. The JAK-STAT pathway: impact on human disease and therapeutic intervention. *Annu Rev Med,* 66**,** 311-28.

ODA, K. & KITANO, H. 2006. A comprehensive map of the toll-like receptor signaling network. *Mol Syst Biol,* 2**,** 2006.0015.

OGIWARA, H., SASAKI, M., MITACHI, T., OIKE, T., HIGUCHI, S., TOMINAGA, Y. & KOHNO, T. 2016. Targeting p300 Addiction in CBP-Deficient Cancers Causes Synthetic Lethality by Apoptotic Cell Death due to Abrogation of MYC Expression. *Cancer Discov,* 6**,** 430-45.

OH, S. Y., RYOO, B. Y., KIM, W. S., KIM, K., LEE, J., KIM, H. J., KWON, J. M., LEE, H. R., KO, Y. H., OH, S. J., PARK, K. W., KIM, H. J., KWON, H. C., NAM, E., KIM, J. H., PARK, Y. H., LEE, S. S., KIM, H. Y. & PARK, K. 2006. Nodal marginal zone B-cell lymphoma: Analysis of 36 cases. Clinical presentation and treatment outcomes of nodal marginal zone B-cell lymphoma. *Ann Hematol,* 85**,** 781-6.

OKOSUN, J., BÖDÖR, C., WANG, J., ARAF, S., YANG, C. Y., PAN, C., BOLLER, S., CITTARO, D., BOZEK, M., IQBAL, S., MATTHEWS, J., WRENCH, D., MARZEC, J., TAWANA, K., POPOV, N., O'RIAIN, C., O'SHEA, D., CARLOTTI, E., DAVIES, A., LAWRIE, C. H., MATOLCSY, A., CALAMINICI, M., NORTON, A., BYERS, R. J., MEIN, C., STUPKA, E., LISTER, T. A., LENZ, G., MONTOTO, S., GRIBBEN, J. G., FAN, Y., GROSSCHEDL, R., CHELALA, C. & FITZGIBBON, J. 2014. Integrated genomic analysis identifies recurrent mutations and evolution patterns driving the initiation and progression of follicular lymphoma. *Nat Genet,* 46**,** 176-181.

OLSZEWSKI, A. J. & CASTILLO, J. J. 2013. Survival of patients with marginal zone lymphoma: analysis of the Surveillance, Epidemiology, and End Results database. *Cancer,* 119**,** 629-38.

ORTEGA-MOLINA, A., BOSS, I. W., CANELA, A., PAN, H., JIANG, Y., ZHAO, C., JIANG, M., HU, D., AGIRRE, X., NIESVIZKY, I., LEE, J. E., CHEN, H. T., ENNISHI, D., SCOTT, D. W., MOTTOK, A., HOTHER, C., LIU, S.,

CAO, X. J., TAM, W., SHAKNOVICH, R., GARCIA, B. A., GASCOYNE, R. D., GE, K., SHILATIFARD, A., ELEMENTO, O., NUSSENZWEIG, A., MELNICK, A. M. & WENDEL, H. G. 2015. The histone lysine methyltransferase KMT2D sustains a gene expression program that represses B cell lymphoma development. *Nat Med,* 21**,** 1199-208.

OSWALD, F., RODRIGUEZ, P., GIAIMO, B. D., ANTONELLO, Z. A., MIRA, L., MITTLER, G., THIEL, V. N., COLLINS, K. J., TABAJA, N., CIZELSKY, W., ROTHE, M., KÜHL, S. J., KÜHL, M., FERRANTE, F., HEIN, K., KOVALL, R. A., DOMINGUEZ, M. & BORGGREFE, T. 2016. A phospho-dependent mechanism involving NCoR and KMT2D controls a permissive chromatin state at Notch target genes. *Nucleic Acids Res,* 44**,** 4703-20.

OTT, G., KATZENBERGER, T., LOHR, A., KINDELBERGER, S., RÜDIGER, T., WILHELM, M., KALLA, J., ROSENWALD, A., MÜLLER, J. G., OTT, M. M. & MÜLLER-HERMELINK, H. K. 2002. Cytomorphologic, immunohistochemical, and cytogenetic profiles of follicular lymphoma: 2 types of follicular lymphoma grade 3. *Blood,* 99**,** 3806-12.

OWEN, K. L., BROCKWELL, N. K. & PARKER, B. S. 2019. JAK-STAT Signaling: A Double-Edged Sword of Immune Regulation and Cancer Progression. *Cancers (Basel),* 11.

PASQUALUCCI, L., DOMINGUEZ-SOLA, D., CHIARENZA, A., FABBRI, G., GRUNN, A., TRIFONOV, V., KASPER, L. H., LERACH, S., TANG, H., MA, J., ROSSI, D., CHADBURN, A., MURTY, V. V., MULLIGHAN, C. G., GAIDANO, G., RABADAN, R., BRINDLE, P. K. & DALLA-FAVERA, R. 2011. Inactivating mutations of acetyltransferase genes in B-cell lymphoma. *Nature,* 471**,** 189-95.

PASQUALUCCI, L., KHIABANIAN, H., FANGAZIO, M., VASISHTHA, M., MESSINA, M., HOLMES, A. B., OUILLETTE, P., TRIFONOV, V., ROSSI, D., TABBÒ, F., PONZONI, M., CHADBURN, A., MURTY, V. V., BHAGAT, G., GAIDANO, G., INGHIRAMI, G., MALEK, S. N., RABADAN, R. & DALLA-FAVERA, R. 2014. Genetics of follicular lymphoma transformation. *Cell Rep,* 6**,** 130-40.

PEARSON, R., FLEETWOOD, J., EATON, S., CROSSLEY, M. & BAO, S. 2008. Krüppel-like transcription factors: a functional family. *Int J Biochem Cell Biol,* 40**,** 1996-2001.

PELLER, S. & ROTTER, V. 2003. TP53 in hematological cancer: low incidence of mutations with significant clinical relevance. *Hum Mutat,* 21**,** 277-84.

PERRY, A. M., DIEBOLD, J., NATHWANI, B. N., MACLENNAN, K. A., MÜLLER-HERMELINK, H. K., BAST, M., BOILESEN, E., ARMITAGE, J. O. & WEISENBURGER, D. D. 2016. Non-Hodgkin lymphoma in the developing world: review of 4539 cases from the International Non-Hodgkin Lymphoma Classification Project. *Haematologica,* 101**,** 1244-1250.

PILLONEL, V., JUSKEVICIUS, D., NG, C. K. Y., BODMER, A., ZETTL, A., JUCKER, D., DIRNHOFER, S. & TZANKOV, A. 2018. High-throughput sequencing of nodal marginal zone lymphomas identifies recurrent BRAF mutations. *Leukemia,* 32**,** 2412-2426.

PIVA, R., DEAGLIO, S., FAMÀ, R., BUONINCONTRI, R., SCARFÒ, I., BRUSCAGGIN, A., MEREU, E., SERRA, S., SPINA, V., BRUSA, D., GARAFFO, G., MONTI, S., DAL BO, M., MARASCA, R., ARCAINI, L.,

NERI, A., GATTEI, V., PAULLI, M., TIACCI, E., BERTONI, F., PILERI, S. A., FOÀ, R., INGHIRAMI, G., GAIDANO, G. & ROSSI, D. 2015. The Krüppel-like factor 2 transcription factor gene is recurrently mutated in splenic marginal zone lymphoma. *Leukemia,* 29**,** 503-7.

PRAY, B. A., YOUSSEF, Y. & ALINARI, L. 2022. TBL1X: At the crossroads of transcriptional and posttranscriptional regulation. *Exp Hematol,* 116**,** 18-25.

QUINTANILLA-MARTINEZ, L., SANDER, B., CHAN, J. K., XERRI, L., OTT, G., CAMPO, E. & SWERDLOW, S. H. 2016. Indolent lymphomas in the pediatric population: follicular lymphoma, IRF4/MUM1+ lymphoma, nodal marginal zone lymphoma and chronic lymphocytic leukemia. *Virchows Arch,* 468**,** 141-57.

RECZEK, P. R., WEISSMAN, D., HÜVÖS, P. E. & FASMAN, G. D. 1982. Sodium butyrate induced structural changes in HeLa cell chromatin. *Biochemistry,* 21**,** 993-1002.

RIZZO, K. A., STREUBEL, B., PITTALUGA, S., CHOTT, A., XI, L., RAFFELD, M. & JAFFE, E. S. 2010. Marginal zone lymphomas in children and the young adult population; characterization of genetic aberrations by FISH and RT-PCR. *Mod Pathol,* 23**,** 866-73.

ROSSI, D. 2014. Role of MYD88 in lymphoplasmacytic lymphoma diagnosis and pathogenesis. *Hematology Am Soc Hematol Educ Program,* 2014**,** 113-8.

ROSSI, D., BERTONI, F. & ZUCCA, E. 2022. Marginal-Zone Lymphomas. *N Engl J Med,* 386**,** 568-581.

ROSSI, D., CERRI, M., DEAMBROGI, C., SOZZI, E., CRESTA, S., RASI, S., DE PAOLI, L., SPINA, V., GATTEI, V., CAPELLO, D., FORCONI, F., LAURIA, F. & GAIDANO, G. 2009. The prognostic value of TP53 mutations in chronic lymphocytic leukemia is independent of Del17p13: implications for overall survival and chemorefractoriness. *Clin Cancer Res,* 15**,** 995-1004.

ROSSI, D., DEAGLIO, S., DOMINGUEZ-SOLA, D., RASI, S., VAISITTI, T., AGOSTINELLI, C., SPINA, V., BRUSCAGGIN, A., MONTI, S., CERRI, M., CRESTA, S., FANGAZIO, M., ARCAINI, L., LUCIONI, M., MARASCA, R., THIEBLEMONT, C., CAPELLO, D., FACCHETTI, F., KWEE, I., PILERI, S. A., FOÀ, R., BERTONI, F., DALLA-FAVERA, R., PASQUALUCCI, L. & GAIDANO, G. 2011. Alteration of BIRC3 and multiple other NF-κB pathway genes in splenic marginal zone lymphoma. *Blood,* 118**,** 4930-4.

ROSSI, D., FANGAZIO, M., RASI, S., VAISITTI, T., MONTI, S., CRESTA, S., CHIARETTI, S., DEL GIUDICE, I., FABBRI, G., BRUSCAGGIN, A., SPINA, V., DEAMBROGI, C., MARINELLI, M., FAMÀ, R., GRECO, M., DANIELE, G., FORCONI, F., GATTEI, V., BERTONI, F., DEAGLIO, S., PASQUALUCCI, L., GUARINI, A., DALLA-FAVERA, R., FOÀ, R. & GAIDANO, G. 2012a. Disruption of BIRC3 associates with fludarabine chemorefractoriness in TP53 wild-type chronic lymphocytic leukemia. *Blood,* 119**,** 2854-62.

ROSSI, D., TRIFONOV, V., FANGAZIO, M., BRUSCAGGIN, A., RASI, S., SPINA, V., MONTI, S., VAISITTI, T., ARRUGA, F., FAMÀ, R., CIARDULLO, C., GRECO, M., CRESTA, S., PIRANDA, D., HOLMES, A., FABBRI, G., MESSINA, M., RINALDI, A., WANG, J., AGOSTINELLI, C., PICCALUGA, P. P., LUCIONI, M., TABBÒ, F., SERRA, R.,

FRANCESCHETTI, S., DEAMBROGI, C., DANIELE, G., GATTEI, V., MARASCA, R., FACCHETTI, F., ARCAINI, L., INGHIRAMI, G., BERTONI, F., PILERI, S. A., DEAGLIO, S., FOÀ, R., DALLA-FAVERA, R., PASQUALUCCI, L., RABADAN, R. & GAIDANO, G. 2012b. The coding genome of splenic marginal zone lymphoma: activation of NOTCH2 and other pathways regulating marginal zone development. *J Exp Med,* 209**,** 1537-51.

ROWLEY, J. D. 1988. Chromosome studies in the non-Hodgkin's lymphomas: the role of the 14;18 translocation. *J Clin Oncol,* 6**,** 919-25.

RULAND, J. & HARTJES, L. 2019. CARD-BCL-10-MALT1 signalling in protective and pathological immunity. *Nat Rev Immunol,* 19**,** 118-134.

RUMMEL, M., KAISER, U., BALSER, C., STAUCH, M., BRUGGER, W., WELSLAU, M., NIEDERLE, N., LOSEM, C., BOECK, H. P., WEIDMANN, E., VON GRUENHAGEN, U., MUELLER, L., SANDHERR, M., HAHN, L., VERESHCHAGINA, J., KAUFF, F., BLAU, W., HINKE, A. & BARTH, J. 2016. Bendamustine plus rituximab versus fludarabine plus rituximab for patients with relapsed indolent and mantle-cell lymphomas: a multicentre, randomised, open-label, non-inferiority phase 3 trial. *Lancet Oncol,* 17**,** 57-66.

SAITO, T., CHIBA, S., ICHIKAWA, M., KUNISATO, A., ASAI, T., SHIMIZU, K., YAMAGUCHI, T., YAMAMOTO, G., SEO, S., KUMANO, K., NAKAGAMI-YAMAGUCHI, E., HAMADA, Y., AIZAWA, S. & HIRAI, H. 2003. Notch2 is preferentially expressed in mature B cells and indispensable for marginal zone B lineage development. *Immunity,* 18**,** 675-85.

SALAMA, M. E., LOSSOS, I. S., WARNKE, R. A. & NATKUNAM, Y. 2009. Immunoarchitectural patterns in nodal marginal zone B-cell lymphoma: a study of 51 cases. *Am J Clin Pathol,* 132**,** 39-49.

SALMERON-VILLALOBOS, J., EGAN, C., BORGMANN, V., MÜLLER, I., GONZALEZ-FARRE, B., RAMIS-ZALDIVAR, J. E., NANN, D., BALAGUÉ, O., LÓPEZ-GUERRA, M., COLOMER, D., OSCHLIES, I., KLAPPER, W., GLASER, S., KO, Y. H., BONZHEIM, I., SIEBERT, R., FEND, F., PITTALUGA, S., CAMPO, E., SALAVERRIA, I., JAFFE, E. S. & QUINTANILLA-MARTINEZ, L. 2022. A unifying hypothesis for PNMZL and PTFL: morphological variants with a common molecular profile. *Blood Adv,* 6**,** 4661-4674.

SANGER, F., NICKLEN, S. & COULSON, A. R. 1977. DNA sequencing with chain-terminating inhibitors. *Proc Natl Acad Sci U S A,* 74**,** 5463-7.

SANTOS, M. A., SARMENTO, L. M., REBELO, M., DOCE, A. A., MAILLARD, I., DUMORTIER, A., NEVES, H., RADTKE, F., PEAR, W. S., PARREIRA, L. & DEMENGEOT, J. 2007. Notch1 engagement by Delta-like-1 promotes differentiation of B lymphocytes to antibody-secreting cells. *Proc Natl Acad Sci U S A,* 104**,** 15454-9.

SCHINDLER, C., LEVY, D. E. & DECKER, T. 2007. JAK-STAT signaling: from interferons to cytokines. *J Biol Chem,* 282**,** 20059-63.

SCHMITZ, R., WRIGHT, G. W., HUANG, D. W., JOHNSON, C. A., PHELAN, J. D., WANG, J. Q., ROULLAND, S., KASBEKAR, M., YOUNG, R. M., SHAFFER, A. L., HODSON, D. J., XIAO, W., YU, X., YANG, Y., ZHAO, H., XU, W., LIU, X., ZHOU, B., DU, W., CHAN, W. C., JAFFE, E. S.,

GASCOYNE, R. D., CONNORS, J. M., CAMPO, E., LOPEZ-GUILLERMO, A., ROSENWALD, A., OTT, G., DELABIE, J., RIMSZA, L. M., TAY KUANG WEI, K., ZELENETZ, A. D., LEONARD, J. P., BARTLETT, N. L., TRAN, B., SHETTY, J., ZHAO, Y., SOPPET, D. R., PITTALUGA, S., WILSON, W. H. & STAUDT, L. M. 2018. Genetics and Pathogenesis of Diffuse Large B-Cell Lymphoma. *N Engl J Med,* 378**,** 1396-1407.

SCHROETER, E. H., KISSLINGER, J. A. & KOPAN, R. 1998. Notch-1 signalling requires ligand-induced proteolytic release of intracellular domain. *Nature,* 393**,** 382-6.

SCHRÖTER, H., GÓMEZ-LIRA, M. M., PLANK, K. H. & BODE, J. 1981. The extent of histone acetylation induced by butyrate and the turnover of acetyl groups depend on the nature of the cell line. *Eur J Biochem,* 120**,** 21-8.

SCHUH, W., MEISTER, S., HERRMANN, K., BRADL, H. & JÄCK, H. M. 2008. Transcriptome analysis in primary B lymphoid precursors following induction of the pre-B cell receptor. *Mol Immunol,* 45**,** 362-75.

SHEN, J., PENG, Y., WEI, L., ZHANG, W., YANG, L., LAN, L., KAPOOR, P., JU, Z., MO, Q., SHIH IE, M., URAY, I. P., WU, X., BROWN, P. H., SHEN, X., MILLS, G. B. & PENG, G. 2015. ARID1A Deficiency Impairs the DNA Damage Checkpoint and Sensitizes Cells to PARP Inhibitors. *Cancer Discov,* 5**,** 752-67.

SHI, S., CALHOUN, H. C., XIA, F., LI, J., LE, L. & LI, W. X. 2006. JAK signaling globally counteracts heterochromatic gene silencing. *Nat Genet,* 38**,** 1071-6.

SHI, S., LARSON, K., GUO, D., LIM, S. J., DUTTA, P., YAN, S. J. & LI, W. X. 2008. Drosophila STAT is required for directly maintaining HP1 localization and heterochromatin stability. *Nat Cell Biol,* 10**,** 489-96.

SHILATIFARD, A. 2012. The COMPASS family of histone H3K4 methylases: mechanisms of regulation in development and disease pathogenesis. *Annu Rev Biochem,* 81**,** 65-95.

SIDDIQI, I. N., FRIEDMAN, J., BARRY-HOLSON, K. Q., MA, C., THODIMA, V., KANG, I., PADMANABHAN, R., DIAS, L. M., KELLY, K. R., BRYNES, R. K., KAMALAKARAN, S. & HOULDSWORTH, J. 2016. Characterization of a variant of t(14;18) negative nodal diffuse follicular lymphoma with CD23 expression, 1p36/TNFRSF14 abnormalities, and STAT6 mutations. *Mod Pathol,* 29**,** 570-81.

SIEGEL, R. L., MILLER, K. D., FUCHS, H. E. & JEMAL, A. 2021. Cancer Statistics, 2021. *CA Cancer J Clin,* 71**,** 7-33.

SILICIANO, J. D., CANMAN, C. E., TAYA, Y., SAKAGUCHI, K., APPELLA, E. & KASTAN, M. B. 1997. DNA damage induces phosphorylation of the amino terminus of p53. *Genes Dev,* 11**,** 3471-81.

SIMS, R. J., 3RD, NISHIOKA, K. & REINBERG, D. 2003. Histone lysine methylation: a signature for chromatin function. *Trends Genet,* 19**,** 629-39.

SINGH, B. N., ZHANG, G., HWA, Y. L., LI, J., DOWDY, S. C. & JIANG, S. W. 2010. Nonhistone protein acetylation as cancer therapy targets. *Expert Rev Anticancer Ther,* 10**,** 935-54.

SKINNIDER, B. F., ELIA, A. J., GASCOYNE, R. D., PATTERSON, B., TRUMPER, L., KAPP, U. & MAK, T. W. 2002. Signal transducer and

activator of transcription 6 is frequently activated in Hodgkin and Reed-Sternberg cells of Hodgkin lymphoma. *Blood,* 99**,** 618-26.
SOMMER, K., GUO, B., POMERANTZ, J. L., BANDARANAYAKE, A. D., MORENO-GARCÍA, M. E., OVECHKINA, Y. L. & RAWLINGS, D. J. 2005. Phosphorylation of the CARMA1 linker controls NF-kappaB activation. *Immunity,* 23**,** 561-74.
SOSMAN, J. A., KIM, K. B., SCHUCHTER, L., GONZALEZ, R., PAVLICK, A. C., WEBER, J. S., MCARTHUR, G. A., HUTSON, T. E., MOSCHOS, S. J., FLAHERTY, K. T., HERSEY, P., KEFFORD, R., LAWRENCE, D., PUZANOV, I., LEWIS, K. D., AMARAVADI, R. K., CHMIELOWSKI, B., LAWRENCE, H. J., SHYR, Y., YE, F., LI, J., NOLOP, K. B., LEE, R. J., JOE, A. K. & RIBAS, A. 2012. Survival in BRAF V600-mutant advanced melanoma treated with vemurafenib. *N Engl J Med,* 366**,** 707-14.
SPINA, V., KHIABANIAN, H., MESSINA, M., MONTI, S., CASCIONE, L., BRUSCAGGIN, A., SPACCAROTELLA, E., HOLMES, A. B., ARCAINI, L., LUCIONI, M., TABBÒ, F., ZAIRIS, S., DIOP, F., CERRI, M., CHIARETTI, S., MARASCA, R., PONZONI, M., DEAGLIO, S., RAMPONI, A., TIACCI, E., PASQUALUCCI, L., PAULLI, M., FALINI, B., INGHIRAMI, G., BERTONI, F., FOÀ, R., RABADAN, R., GAIDANO, G. & ROSSI, D. 2016. The genetics of nodal marginal zone lymphoma. *Blood,* 128**,** 1362-73.
SPINA, V. & ROSSI, D. 2016. NF-κB deregulation in splenic marginal zone lymphoma. *Semin Cancer Biol,* 39**,** 61-7.
SPINA, V. & ROSSI, D. 2017. Molecular pathogenesis of splenic and nodal marginal zone lymphoma. *Best Pract Res Clin Haematol,* 30**,** 5-12.
STANKOVIC, T. & SKOWRONSKA, A. 2014. The role of ATM mutations and 11q deletions in disease progression in chronic lymphocytic leukemia. *Leuk Lymphoma,* 55**,** 1227-39.
STONE, M. J. 2005. Thomas Hodgkin: medical immortal and uncompromising idealist. *Proc (Bayl Univ Med Cent),* 18**,** 368-75.
STRAHL, B. D., OHBA, R., COOK, R. G. & ALLIS, C. D. 1999. Methylation of histone H3 at lysine 4 is highly conserved and correlates with transcriptionally active nuclei in Tetrahymena. *Proc Natl Acad Sci U S A,* 96**,** 14967-72.
SUN, D. & DING, A. 2006. MyD88-mediated stabilization of interferon-gamma-induced cytokine and chemokine mRNA. *Nat Immunol,* 7**,** 375-81.
SURYO RAHMANTO, Y., JUNG, J. G., WU, R. C., KOBAYASHI, Y., HEAPHY, C. M., MEEKER, A. K., WANG, T. L. & SHIH IE, M. 2016. Inactivating ARID1A Tumor Suppressor Enhances TERT Transcription and Maintains Telomere Length in Cancer Cells. *J Biol Chem,* 291**,** 9690-9.
SWERDLOW, S., CAMPO, E., HARRIS, N. L., JAFFE, E. S., PILERI, S. A., STEIN, H. & THIELE, J. 2017. *WHO Classification of Tumours of Haematopoietic and Lymphoid Tissues (Revised 4th edition)*, IARC: Lyon.
SWERDLOW, S. H., KUZU, I., DOGAN, A., DIRNHOFER, S., CHAN, J. K., SANDER, B., OTT, G., XERRI, L., QUINTANILLA-MARTINEZ, L. & CAMPO, E. 2016. The many faces of small B cell lymphomas with plasmacytic differentiation and the contribution of MYD88 testing. *Virchows Arch,* 468**,** 259-75.

TADDESSE-HEATH, L., PITTALUGA, S., SORBARA, L., BUSSEY, M., RAFFELD, M. & JAFFE, E. S. 2003. Marginal zone B-cell lymphoma in children and young adults. *Am J Surg Pathol,* 27**,** 522-31.

TADMOR, T. & POLLIACK, A. 2017. Nodal marginal zone lymphoma: Clinical features, diagnosis, management and treatment. *Best Pract Res Clin Haematol,* 30**,** 92-98.

TANG, L., NOGALES, E. & CIFERRI, C. 2010. Structure and function of SWI/SNF chromatin remodeling complexes and mechanistic implications for transcription. *Prog Biophys Mol Biol,* 102**,** 122-8.

TANIGAKI, K., HAN, H., YAMAMOTO, N., TASHIRO, K., IKEGAWA, M., KURODA, K., SUZUKI, A., NAKANO, T. & HONJO, T. 2002. Notch-RBP-J signaling is involved in cell fate determination of marginal zone B cells. *Nat Immunol,* 3**,** 443-50.

TANIGAKI, K., KURODA, K., HAN, H. & HONJO, T. 2003. Regulation of B cell development by Notch/RBP-J signaling. *Semin Immunol,* 15**,** 113-9.

TERAS, L. R., DESANTIS, C. E., CERHAN, J. R., MORTON, L. M., JEMAL, A. & FLOWERS, C. R. 2016. 2016 US lymphoid malignancy statistics by World Health Organization subtypes. *CA Cancer J Clin,* 66**,** 443-459.

THIEBLEMONT, C., DAVI, F., NOGUERA, M. E. & BRIÈRE, J. 2011. Non-MALT marginal zone lymphoma. *Curr Opin Hematol,* 18**,** 273-9.

THIEN, M., PHAN, T. G., GARDAM, S., AMESBURY, M., BASTEN, A., MACKAY, F. & BRINK, R. 2004. Excess BAFF rescues self-reactive B cells from peripheral deletion and allows them to enter forbidden follicular and marginal zone niches. *Immunity,* 20**,** 785-98.

THOMAS, M., CALAMITO, M., SRIVASTAVA, B., MAILLARD, I., PEAR, W. S. & ALLMAN, D. 2007. Notch activity synergizes with B-cell-receptor and CD40 signaling to enhance B-cell activation. *Blood,* 109**,** 3342-50.

THOME, M. 2004. CARMA1, BCL-10 and MALT1 in lymphocyte development and activation. *Nat Rev Immunol,* 4**,** 348-59.

THORSLUND, T., RIPPLINGER, A., HOFFMANN, S., WILD, T., UCKELMANN, M., VILLUMSEN, B., NARITA, T., SIXMA, T. K., CHOUDHARY, C., BEKKER-JENSEN, S. & MAILAND, N. 2015. Histone H1 couples initiation and amplification of ubiquitin signalling after DNA damage. *Nature,* 527**,** 389-93.

TIACCI, E., PARK, J. H., DE CAROLIS, L., CHUNG, S. S., BROCCOLI, A., SCOTT, S., ZAJA, F., DEVLIN, S., PULSONI, A., CHUNG, Y. R., CIMMINIELLO, M., KIM, E., ROSSI, D., STONE, R. M., MOTTA, G., SAVEN, A., VARETTONI, M., ALTMAN, J. K., ANASTASIA, A., GREVER, M. R., AMBROSETTI, A., RAI, K. R., FRATICELLI, V., LACOUTURE, M. E., CARELLA, A. M., LEVINE, R. L., LEONI, P., RAMBALDI, A., FALZETTI, F., ASCANI, S., CAPPONI, M., MARTELLI, M. P., PARK, C. Y., PILERI, S. A., ROSEN, N., FOÀ, R., BERGER, M. F., ZINZANI, P. L., ABDEL-WAHAB, O., FALINI, B. & TALLMAN, M. S. 2015. Targeting Mutant BRAF in Relapsed or Refractory Hairy-Cell Leukemia. *N Engl J Med,* 373**,** 1733-47.

TIACCI, E., PETTIROSSI, V., SCHIAVONI, G. & FALINI, B. 2017. Genomics of Hairy Cell Leukemia. *J Clin Oncol,* 35**,** 1002-1010.

TOKOYODA, K., EGAWA, T., SUGIYAMA, T., CHOI, B. I. & NAGASAWA, T. 2004. Cellular niches controlling B lymphocyte behavior within bone marrow during development. *Immunity,* 20**,** 707-18.

TRAVERSE-GLEHEN, A., FELMAN, P., CALLET-BAUCHU, E., GAZZO, S., BASEGGIO, L., BRYON, P. A., THIEBLEMONT, C., COIFFIER, B., SALLES, G. & BERGER, F. 2006. A clinicopathological study of nodal marginal zone B-cell lymphoma. A report on 21 cases. *Histopathology,* 48**,** 162-73.

TUCKER, T., MARRA, M. & FRIEDMAN, J. M. 2009. Massively parallel sequencing: the next big thing in genetic medicine. *Am J Hum Genet,* 85**,** 142-54.

VAN DEN BRAND, M., RIJNTJES, J., HEBEDA, K. M., MENTING, L., BREGITHA, C. V., STEVENS, W. B., VAN DER VELDEN, W. J., TOPS, B. B., VAN KRIEKEN, J. H. & GROENEN, P. J. 2017. Recurrent mutations in genes involved in nuclear factor-κB signalling in nodal marginal zone lymphoma-diagnostic and therapeutic implications. *Histopathology,* 70**,** 174-184.

VAN DEN BRAND, M., VAN DER VELDEN, W. J., DIETS, I. J., ECTOR, G. I., DE HAAN, A. F., STEVENS, W. B., HEBEDA, K. M., GROENEN, P. J. & VAN KRIEKEN, H. J. 2016. Clinical features of patients with nodal marginal zone lymphoma compared to follicular lymphoma: similar presentation, but differences in prognostic factors and rate of transformation. *Leuk Lymphoma,* 57**,** 1649-56.

VAN DEN BRAND, M. & VAN KRIEKEN, J. H. 2013. Recognizing nodal marginal zone lymphoma: recent advances and pitfalls. A systematic review. *Haematologica,* 98**,** 1003-13.

VAN DIJK, E. L., AUGER, H., JASZCZYSZYN, Y. & THERMES, C. 2014. Ten years of next-generation sequencing technology. *Trends Genet,* 30**,** 418-26.

VAN DONGEN, J. J., LANGERAK, A. W., BRÜGGEMANN, M., EVANS, P. A., HUMMEL, M., LAVENDER, F. L., DELABESSE, E., DAVI, F., SCHUURING, E., GARCÍA-SANZ, R., VAN KRIEKEN, J. H., DROESE, J., GONZÁLEZ, D., BASTARD, C., WHITE, H. E., SPAARGAREN, M., GONZÁLEZ, M., PARREIRA, A., SMITH, J. L., MORGAN, G. J., KNEBA, M. & MACINTYRE, E. A. 2003. Design and standardization of PCR primers and protocols for detection of clonal immunoglobulin and T-cell receptor gene recombinations in suspect lymphoproliferations: report of the BIOMED-2 Concerted Action BMH4-CT98-3936. *Leukemia,* 17**,** 2257-317.

VAN KRIEKEN, J. H. & LENNERT, K. 1990. Proliferation of marginal zone cells mimicking malignant lymphoma. *Pathol Res Pract,* 186**,** 397-9; discussion 400-2.

VANDERWIELEN, B. D., YUAN, Z., FRIEDMANN, D. R. & KOVALL, R. A. 2011. Transcriptional repression in the Notch pathway: thermodynamic characterization of CSL-MINT (Msx2-interacting nuclear target protein) complexes. *J Biol Chem,* 286**,** 14892-902.

VAQUERO, A., SCHER, M., LEE, D., ERDJUMENT-BROMAGE, H., TEMPST, P. & REINBERG, D. 2004. Human SirT1 interacts with histone H1 and promotes formation of facultative heterochromatin. *Mol Cell,* 16**,** 93-105.

VELA, V., JUSKEVICIUS, D., DIRNHOFER, S., MENTER, T. & TZANKOV, A. 2022. Mutational landscape of marginal zone B-cell lymphomas of various origin: organotypic alterations and diagnostic potential for assignment of organ origin. *Virchows Arch,* 480**,** 403-413.

VENTURUTTI, L., TEATER, M., ZHAI, A., CHADBURN, A., BABIKER, L., KIM, D., BÉGUELIN, W., LEE, T. C., KIM, Y., CHIN, C. R., YEWDELL, W. T., RAUGHT, B., PHILLIP, J. M., JIANG, Y., STAUDT, L. M., GREEN, M. R., CHAUDHURI, J., ELEMENTO, O., FARINHA, P., WENG, A. P., NISSEN, M. D., STEIDL, C., MORIN, R. D., SCOTT, D. W., PRIVÉ, G. G. & MELNICK, A. M. 2020. TBL1XR1 Mutations Drive Extranodal Lymphoma by Inducing a Pro-tumorigenic Memory Fate. *Cell,* 182**,** 297-316.e27.

WAJANT, H. 2002. The Fas signaling pathway: more than a paradigm. *Science,* 296**,** 1635-6.

WANG, C. Y., MAYO, M. W., KORNELUK, R. G., GOEDDEL, D. V. & BALDWIN, A. S., JR. 1998. NF-kappaB antiapoptosis: induction of TRAF1 and TRAF2 and c-IAP1 and c-IAP2 to suppress caspase-8 activation. *Science,* 281**,** 1680-3.

WANG, H. G., CAO, B., ZHANG, L. X., SONG, N., LI, H., ZHAO, W. Z., LI, Y. S., MA, S. M. & YIN, D. J. 2017. KLF2 inhibits cell growth via regulating HIF-1α/Notch-1 signal pathway in human colorectal cancer HCT116 cells. *Oncol Rep,* 38**,** 584-590.

WANG, J. Q., JEELALL, Y. S., BEUTLER, B., HORIKAWA, K. & GOODNOW, C. C. 2014. Consequences of the recurrent MYD88(L265P) somatic mutation for B cell tolerance. *J Exp Med,* 211**,** 413-26.

WANG, W. & LIN, P. 2020. Lymphoplasmacytic lymphoma and Waldenström macroglobulinaemia: clinicopathological features and differential diagnosis. *Pathology,* 52**,** 6-14.

WANG, Z. & COOK, J. R. 2019. IRTA1 and MNDA Expression in Marginal Zone Lymphoma: Utility in Differential Diagnosis and Implications for Classification. *Am J Clin Pathol,* 151**,** 337-343.

WATANABE, R., UI, A., KANNO, S., OGIWARA, H., NAGASE, T., KOHNO, T. & YASUI, A. 2014. SWI/SNF factors required for cellular resistance to DNA damage include ARID1A and ARID1B and show interdependent protein stability. *Cancer Res,* 74**,** 2465-75.

WENG, A. P., FERRANDO, A. A., LEE, W., MORRIS, J. P. T., SILVERMAN, L. B., SANCHEZ-IRIZARRY, C., BLACKLOW, S. C., LOOK, A. T. & ASTER, J. C. 2004. Activating mutations of NOTCH1 in human T cell acute lymphoblastic leukemia. *Science,* 306**,** 269-71.

WERTZ, I. E., O'ROURKE, K. M., ZHOU, H., EBY, M., ARAVIND, L., SESHAGIRI, S., WU, P., WIESMANN, C., BAKER, R., BOONE, D. L., MA, A., KOONIN, E. V. & DIXIT, V. M. 2004. De-ubiquitination and ubiquitin ligase domains of A20 downregulate NF-kappaB signalling. *Nature,* 430**,** 694-9.

WILSKER, D., PATSIALOU, A., ZUMBRUN, S. D., KIM, S., CHEN, Y., DALLAS, P. B. & MORAN, E. 2004. The DNA-binding properties of the ARID-

containing subunits of yeast and mammalian SWI/SNF complexes. *Nucleic Acids Res,* 32**,** 1345-53.
WINKELMANN, R., SANDROCK, L., KIRBERG, J., JÄCK, H. M. & SCHUH, W. 2014. KLF2--a negative regulator of pre-B cell clonal expansion and B cell activation. *PLoS One,* 9**,** e97953.
WINKELMANN, R., SANDROCK, L., PORSTNER, M., ROTH, E., MATHEWS, M., HOBEIKA, E., RETH, M., KAHN, M. L., SCHUH, W. & JÄCK, H. M. 2011. B cell homeostasis and plasma cell homing controlled by Krüppel-like factor 2. *Proc Natl Acad Sci U S A,* 108**,** 710-5.
WITT, C. M., WON, W. J., HUREZ, V. & KLUG, C. A. 2003. Notch2 haploinsufficiency results in diminished B1 B cells and a severe reduction in marginal zone B cells. *J Immunol,* 171**,** 2783-8.
WITZIG, T. E., WHITE, C. A., GORDON, L. I., WISEMAN, G. A., EMMANOUILIDES, C., MURRAY, J. L., LISTER, J. & MULTANI, P. S. 2003. Safety of yttrium-90 ibritumomab tiuxetan radioimmunotherapy for relapsed low-grade, follicular, or transformed non-hodgkin's lymphoma. *J Clin Oncol,* 21**,** 1263-70.
WOLFFE, A. P. 1997. Histone H1. *Int J Biochem Cell Biol,* 29**,** 1463-6.
XERRI, L., DIRNHOFER, S., QUINTANILLA-MARTINEZ, L., SANDER, B., CHAN, J. K., CAMPO, E., SWERDLOW, S. H. & OTT, G. 2016. The heterogeneity of follicular lymphomas: from early development to transformation. *Virchows Arch,* 468**,** 127-39.
XERRI, L., MEDEIROS, L. J., KLAPPER, W., LOUISSAINT, A., JR., WATANABE, T., KARUBE, K., MARAFIOTI, T., NADEL, B., FITZGIBBON, J., ARDESHNA, K. M., KRIDEL, R. & DAVIES, A. 2022. Follicular lymphoma. *In:* NARESH, K. (ed.) *WHO Classification of Tumours Editorial Board. Haematolymphoid Tumours.* 5 ed. Lyon (France): International Agency for Research on Cancer.
XUE, L., MORRIS, S. W., ORIHUELA, C., TUOMANEN, E., CUI, X., WEN, R. & WANG, D. 2003. Defective development and function of Bcl10-deficient follicular, marginal zone and B1 B cells. *Nat Immunol,* 4**,** 857-65.
YAN, H. T., SHINKA, T., KINOSHITA, K., SATO, Y., UMENO, M., CHEN, G., TSUJI, K., UNEMI, Y., YANG, X. J., IWAMOTO, T. & NAKAHORI, Y. 2005. Molecular analysis of TBL1Y, a Y-linked homologue of TBL1X related with X-linked late-onset sensorineural deafness. *J Hum Genet,* 50**,** 175-181.
YANG, S. M., KIM, B. J., NORWOOD TORO, L. & SKOULTCHI, A. I. 2013. H1 linker histone promotes epigenetic silencing by regulating both DNA methylation and histone H3 methylation. *Proc Natl Acad Sci U S A,* 110**,** 1708-13.
YEH, C. H., BELLON, M. & NICOT, C. 2018. FBXW7: a critical tumor suppressor of human cancers. *Mol Cancer,* 17**,** 115.
YILDIZ, M., LI, H., BERNARD, D., AMIN, N. A., OUILLETTE, P., JONES, S., SAIYA-CORK, K., PARKIN, B., JACOBI, K., SHEDDEN, K., WANG, S., CHANG, A. E., KAMINSKI, M. S. & MALEK, S. N. 2015. Activating STAT6 mutations in follicular lymphoma. *Blood,* 125**,** 668-79.
YOON, H. G., CHAN, D. W., HUANG, Z. Q., LI, J., FONDELL, J. D., QIN, J. & WONG, J. 2003. Purification and functional characterization of the human

N-CoR complex: the roles of HDAC3, TBL1 and TBLR1. *Embo j,* 22**,** 1336-46.

YUAN, Z., VANDERWIELEN, B. D., GIAIMO, B. D., PAN, L., COLLINS, C. E., TURKIEWICZ, A., HEIN, K., OSWALD, F., BORGGREFE, T. & KOVALL, R. A. 2019. Structural and Functional Studies of the RBPJ-SHARP Complex Reveal a Conserved Corepressor Binding Site. *Cell Rep,* 26**,** 845-854.e6.

YUSUFOVA, N., KLOETGEN, A., TEATER, M., OSUNSADE, A., CAMARILLO, J. M., CHIN, C. R., DOANE, A. S., VENTERS, B. J., PORTILLO-LEDESMA, S., CONWAY, J., PHILLIP, J. M., ELEMENTO, O., SCOTT, D. W., BÉGUELIN, W., LICHT, J. D., KELLEHER, N. L., STAUDT, L. M., SKOULTCHI, A. I., KEOGH, M. C., APOSTOLOU, E., MASON, C. E., IMIELINSKI, M., SCHLICK, T., DAVID, Y., TSIRIGOS, A., ALLIS, C. D., SOSHNEV, A. A., CESARMAN, E. & MELNICK, A. M. 2021. Histone H1 loss drives lymphoma by disrupting 3D chromatin architecture. *Nature,* 589**,** 299-305.

ZAMÒ, A., PISCHIMAROV, J., HORN, H., OTT, G., ROSENWALD, A. & LEICH, E. 2018. The exomic landscape of t(14;18)-negative diffuse follicular lymphoma with 1p36 deletion. *Br J Haematol,* 180**,** 391-394.

ZENZ, T., KRÖBER, A., SCHERER, K., HÄBE, S., BÜHLER, A., BENNER, A., DENZEL, T., WINKLER, D., EDELMANN, J., SCHWÄNEN, C., DÖHNER, H. & STILGENBAUER, S. 2008. Monoallelic TP53 inactivation is associated with poor prognosis in chronic lymphocytic leukemia: results from a detailed genetic characterization with long-term follow-up. *Blood,* 112**,** 3322-9.

ZHANG, F. L. & LI, D. Q. 2022. Targeting Chromatin-Remodeling Factors in Cancer Cells: Promising Molecules in Cancer Therapy. *Int J Mol Sci,* 23.

ZHANG, J., DOMINGUEZ-SOLA, D., HUSSEIN, S., LEE, J. E., HOLMES, A. B., BANSAL, M., VLASEVSKA, S., MO, T., TANG, H., BASSO, K., GE, K., DALLA-FAVERA, R. & PASQUALUCCI, L. 2015. Disruption of KMT2D perturbs germinal center B cell development and promotes lymphomagenesis. *Nat Med,* 21**,** 1190-8.

ZHANG, J., GRUBOR, V., LOVE, C. L., BANERJEE, A., RICHARDS, K. L., MIECZKOWSKI, P. A., DUNPHY, C., CHOI, W., AU, W. Y., SRIVASTAVA, G., LUGAR, P. L., RIZZIERI, D. A., LAGOO, A. S., BERNAL-MIZRACHI, L., MANN, K. P., FLOWERS, C., NARESH, K., EVENS, A., GORDON, L. I., CZADER, M., GILL, J. I., HSI, E. D., LIU, Q., FAN, A., WALSH, K., JIMA, D., SMITH, L. L., JOHNSON, A. J., BYRD, J. C., LUFTIG, M. A., NI, T., ZHU, J., CHADBURN, A., LEVY, S., DUNSON, D. & DAVE, S. S. 2013. Genetic heterogeneity of diffuse large B-cell lymphoma. *Proc Natl Acad Sci U S A,* 110**,** 1398-403.

ZHANG, J., VLASEVSKA, S., WELLS, V. A., NATARAJ, S., HOLMES, A. B., DUVAL, R., MEYER, S. N., MO, T., BASSO, K., BRINDLE, P. K., HUSSEIN, S., DALLA-FAVERA, R. & PASQUALUCCI, L. 2017. The CREBBP Acetyltransferase Is a Haploinsufficient Tumor Suppressor in B-cell Lymphoma. *Cancer Discov,* 7**,** 322-337.

ZHANG, Y., COOKE, M., PANJWANI, S., CAO, K., KRAUTH, B., HO, P. Y., MEDRZYCKI, M., BERHE, D. T., PAN, C., MCDEVITT, T. C. & FAN, Y.

2012. Histone h1 depletion impairs embryonic stem cell differentiation. *PLoS Genet,* 8**,** e1002691.
ZHANG, Y., YAO, C., JU, Z., JIAO, D., HU, D., QI, L., LIU, S., WU, X. & ZHAO, C. 2023. Krüppel-like factors in tumors: Key regulators and therapeutic avenues. *Front Oncol,* 13**,** 1080720.
ZHOU, H., WERTZ, I., O'ROURKE, K., ULTSCH, M., SESHAGIRI, S., EBY, M., XIAO, W. & DIXIT, V. M. 2004. Bcl10 activates the NF-kappaB pathway through ubiquitination of NEMO. *Nature,* 427**,** 167-71.
ZHU, Y., WANG, Z., LI, Y., PENG, H., LIU, J., ZHANG, J. & XIAO, X. 2023. The Role of CREBBP/EP300 and Its Therapeutic Implications in Hematological Malignancies. *Cancers (Basel),* 15.

8 Declaration of Authorship

Dieses Projekt wurde am Institut für Pathologie und Neuropathologie (Ärztlicher Direktor: **Herr Prof. Dr. Falko Fend**) unter Betreuung von **Frau Prof. Dr. Leticia Quintanilla Fend** durchgeführt. Des Weiteren erfolge die Betreuung durch **Vanessa Borgmann** und **Dr. Dominik Nann**.

Die Konzeption der Studie erfolgte durch **Frau Prof. Dr. Leticia Quintanilla Fend, Dr. Dominik Nann** und **Vanessa Borgmann**.

Sämtliche Versuche wurden, es sei denn anders angegeben, nach Einarbeitung durch **Esther Kohler, Franziska Mihalik** und **Rebecca Braun** von mir eigenständig durchgeführt.

Die immunhistochemischen Färbungen wurden von Mitarbeiter:innen des immunhistochemischen Labors der Pathologie durchgeführt.

Das Mikroskopieren und Auswerten der Schnitte erfolgte zusammen mit **Frau Prof. Dr. Leticia Quintanilla Fend** und **Dr. Dominik Nann.**

Die in der Arbeit gezeigten histologischen Bilder wurden von **Frau Prof. Dr. Leticia Quintanilla Fend** zu Verfügung gestellt.

Die FISH-Analysen zur Untersuchung möglicher Translokationen wurden im Rahmen der Diagnostik von **Barbara Mankel** durchgeführt.

Die Vorbereitung und Sequenzierung der Proben mit dem PMZL Panel (siehe 2.6.2) wurden von **Franziska Mihalik** und **Rebecca Braun** ausgeübt. Die Auswertung des PMZL Panels wurde von **Vanessa Borgmann** durchgeführt.

Ich versichere, das Manuskript selbständig (nach Anleitung/Korrektur von Frau Prof. Dr. Leticia Quintanilla de Fend, Dr. Dominik Nann und Vanessa Borgmann) verfasst zu haben und keine weiteren als die von mir angegebenen Quellen verwendet zu haben.

9 Acknoledgements

Ich möchte jedem und jeder danken, die mich bei dieser Arbeit unterstützt haben und an dem Prozess beteiligt waren.

In erster Linie gilt mein großer Dank Frau **Prof. Dr. Leticia Quintanilla Fend**, die das Projekt betreut hat. Sie stand mir während des gesamten Prozesses zur Seite und hatte immer ein offenes Ohr für Fragen und Anregungen. Ich schätze mich sehr glücklich, das Projekt unter ihrer Obhut gemacht haben zu dürfen und fühle mich geehrt, mit ihr zusammen gearbeitet zu haben dürfen.

Des Weiteren danke ich **Prof. Dr. Falko Fend** für die Gelegenheit, das Projekt am Institut für Pathologie und Neuropathologie durchzuführen. Seine Einschätzungen zu den schwierig zu beurteilenden Fällen ist nicht weg zu denken.

Mein besonderer Dank gilt außerdem **Vanessa Borgmann** und **Dr. Dominik Nann**. Zu ihnen konnte ich immer mit Fragen kommen, sie haben mir bei allen Unsicherheiten geholfen haben und standen auch bei viel Stress immer für ein Gespräch zur Verfügung. Ich habe mich exzellent betreut und immer gut aufgehoben gefühlt.

Danken möchte ich außerdem **Dr. Irina Bonzheim** für die Möglichkeit, die Experimente und Auswertungen in der Abteilung der Molekularpathologie gemacht haben zu dürfen.

Meinen Dank möchte ich außerdem aussprechen an **Esther Kohler, Franziska Mihalik** und **Rebecca Braun**, die mich geduldig in die Laborarbeiten eingearbeitet haben, mir alles gezeigt haben und auch später immer für Rückfragen zur Verfügung standen.

Zu guter Letzt möchte ich meinen Eltern, meiner Schwester Marlene, meinem Bruder Simon, meinen Großeltern und all meinen Freunden danken, die mich an schlechten sowie guten Tagen immer wieder motiviert haben und ohne deren Unterstützung die Arbeit nicht zustande gekommen wäre.